Electronic Supplementary Material (ESI) for Organic Chemistry Frontiers.

BODIPY-Amino Acid Conjugates – Tuning the Optical Response with a meso-Heteroatom

Marco Farinone, Joanna Cybińska and Miłosz Pawlicki

Table of contents:

1. General information

NMR Spectroscopy. ^{1}H NMR spectra were recorded on a high-field spectrometer (^{1}H 600.15 MHz and 500 MHz, ^{13}C 150 MHz and 125.75 MHz), equipped with a broadband inverse gradient probe head. Spectra were referenced to the residual solvent signal (chloroform-d, 7.26 ppm). Two dimensional NMR spectra were recorded with 2048 data points in the t2 domain and up to 1024 points in the t1 domain, with a 1s recovery delay. The experiments were performed at 300K if not specified. The estimation of activation energies relative to H(1) positions for compounds **6a**, **6b** and **6c** were calculated using the following equation:

$$\Delta G = aT[9.972 + \log\left(\frac{T}{\Delta v}\right)]$$

with *T* being the coalescence temperature experimentally observed, Δv the peak separation measured in slow exchange conditions and a = 4.575 x 10^{-3} for units of kcal/mol[1].

Mass Spectrometry. High resolution and Accurate Mass spectra were recorded on a Bruker apex ultra FTMS and a Bruker microTOF-Q spectrometers using the electrospray technique.

UV-Vis Spectroscopy. Electronic spectra were recorded on a Varian Carry-50 Bio spectrophotometer.

Fluorescence. Steady state fluorescence spectra were recorded with a JASCO FP-8600 Spectrofluorometer apparatus. Quantum yields were measured using cooled extended red Hamamatsu photomultiplier operating in range 200 – 1050 nm. Quantum yield measurements were performed by using an Edinburgh Instruments integrating sphere equipped with a small elliptical mirror and a baffle plate for beam steering and shielding against directly detected light. For the measurement, the integrating sphere replaces the standard sample holder inside the sample chamber. Calculations of quantum yields were made using the software provided by Edinburgh Instruments. The luminescence decay traces were registered by means of F-G05PM featuring a Hamamatsu H5773-04 detector. As excitation source picosecond pulsed light emitting diode EPLED-280 was used.

X-Ray Analysis. X-Ray quality crystals were prepared by slow evaporation of DCM (**6a**). Data were collected at 100K on an Xcalibur PX-k geometry diffractometer, with Mo (λ=0.7103) Kα radiation. Data were corrected for Lorentz and polarization effect. The structure was solved by direct methods with SHELXT (2015 release) and refined by full matrix least-squares method by using an iteration approach with SHELXL software with anisotropic thermal parameters for the non-H atoms. Hydrogen atoms have been Scattering factors were those incorporated in SHELXT.

Theoretical calculations. Geometry optimizations for all the derivatives were carried out with the Gaussian 09[2] software package within unconstrained C1 symmetry, with starting coordinates derived from semi-empirical calculations. Becke's three-parameter exchange functional with the gradient-corrected correlation formula of Lee, Yang and Parr (DFT-

1 K. D. Zimmer, R. Shoemaker, R. R. Ruminski, *Inorganica Chimica Acta*, 2006, **359**, 1478-1484.
2 Gaussian 09, Revision E.01; M. J. Frisch et al., Gaussian, Inc.: Wallingford CT, 2009.

B3LYP)[3] were used with the 6-31G(d,p) basis set. The polarizable continuum model of solvation was used (PCM, standard dichloromethane) for all optimizations.
The electronic spectra were simulated by means of time-dependent density functional theory (TD-DFT) using the Tamm-Dancoff approximation for 50 states and 6-31G(d,p) basis set for all the derivatives.
The electronic transitions and UV/Vis were analyzed by means of the GaussSum program. The transitions were convoluted by Gaussian curves with 2000 cm^{-1} half line width for all the derivatives.

2. Experimental section.

All solvents (MeOH, Ethyl Acetate, $CHCl_3$, *n*-hexane, toluene, acetone, water) if not indicated differently were used without purification. CH_2Cl_2 was distilled over CaH_2. Chloroform-*d* was prepared directly before using by passing through a basic alumina column. All reactions were performed under inert atmosphere.

2.1 Experimental procedures.

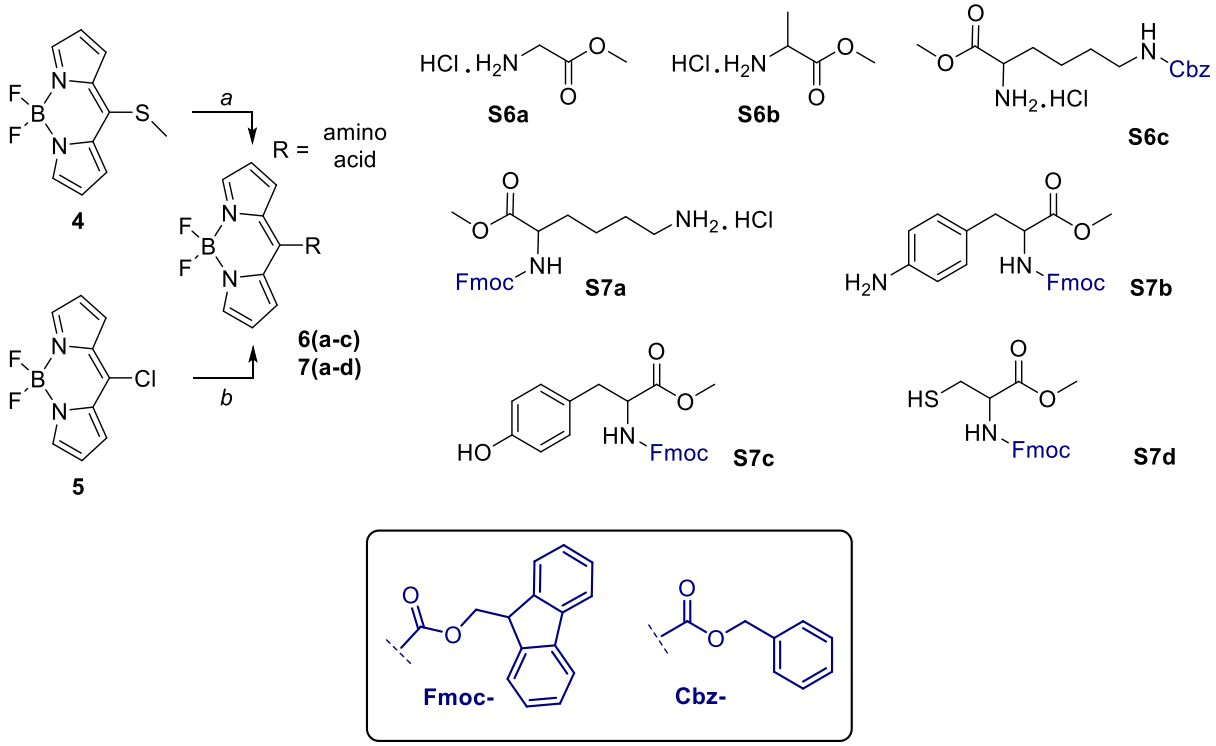

Scheme S1. Synthetic approach and precursor used in this work.

meso-methylthioBODIPY 4 was prepared according to Biellmann et al. procedure.[4]

3 a) C. T. Lee, W. T. Yang, R. G. Parr, *Phys. Rev. B*, 1988, **37**, 785-789. b) A. D. Becke, *Phys. Rev. A*, 1988, **38**, 3098-3100.
4 T. V. Goud, A. Tutar, J.-F. Biellmann, *Tetrahedron*, 2006, **62**, 5084-5091.

***meso*-chloroBODIPY 5** was prepared according to Dehaen et al. procedure.[5]

Protection of carboxylic groups through esterification was performed according to the procedures presented in literature.[6]

(*a*) General procedure for aminoacid-Bodipy hybrid systems using 4 as synthon.[4]

In a round bottom flask were placed *meso*-methylthioBODIPY (**4**) (0.3 mmol), the specific aminoacid (1.0 equivalent) and K_2CO_3. (2.0 equivalents) and the solids were purged with Argon. Dichloromethane was added (10 mL) to the flask and the reaction mixture was stirred at room temperature overnight. The crude mixture was evaporated to dryness under reduced pressure. The desired products were purified with column chromatography (CH_2Cl_2/ethyl acetate).

(*b*) General procedure for aminoacid-Bodipy hybrid systems using 5 as synthon.[5]

In a round bottom flask were placed *meso*-chloroBODIPY (**5**) (0.3 mmol), the specific aminoacid (1.0 equivalent) and K_2CO_3. (2.0 equivalents) and the solids were purged with Argon. Dichloromethane was added (10 mL) to the flask and the reaction mixture was stirred at room temperature overnight. The crude mixture was poured in diethyl ether (20 mL), washed with a saturated solution of Na_2CO_3 (3x10 mL) and the organic layer was dried with Na_2SO_4. The drying agent was filtered off and the solution evaporated to dryness under reduced pressure. The desired products were purified with column chromatography (CH_2Cl_2/ethyl acetate).

S6c protection on the amino side chain, starting from commercially available L-Lysine, was performed according to Baker et al. procedure.[7]

S7a was obtained starting from commercially available Fmoc-Lys(Boc)-OH, Boc protection was removed during the esterification reaction.

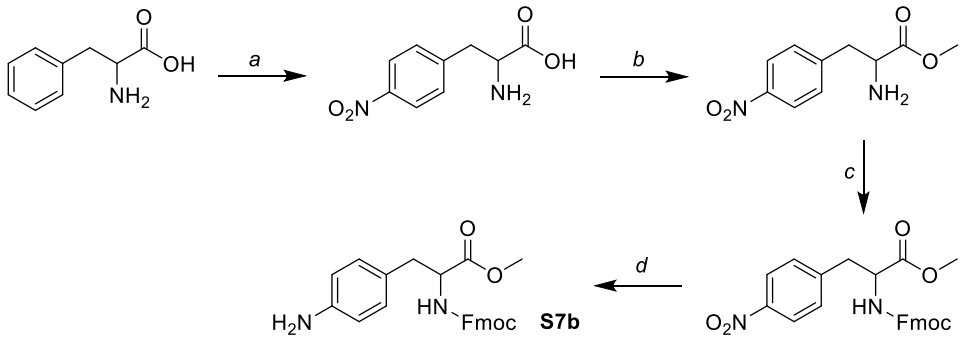

Scheme S2. Synthetic approach for the preparation of **S7b**. Conditions: *a*) HNO_3, H_2SO_4, 0°C-RT, 30 min;[8] *b*) $SOCl_2$, MeOH, -10°C-RT, 24 h;[6] *c*) Fmoc-OSu, TEA, H_2O, MeCN, 15 min;[6] *d*) 0.5M $SnCl_2$, DMF, RT, overnight.[9]

5 V. Leen, P. Yuan, L. Wang, N. Boens, W. Dehaen, *Org. Lett.*, 2012, **14**, 24, 6150-6153.

6 Houben-Weyl Methods of Organic Chemistry, 2004, Vol. **E 22a**.

7 Y. S. Casadio, D. H. Brown, T. V. Chirila, H.-B. Kreetz, M. V. Baker, *Biomacromolecules*, 2010, **11**, 11, 2949-2959.

8 F. Bergel, J. A. Stock, *J. Chem. Soc.*, 1954, 2409-2417.

9 T. Kersebohm, S. I. Kirin, N. Metzler-Nolte, *Bioorg. Med. Chem. Lett.*, 2006, **16**, 2964-2968.

S7b was obtained starting from commercially available L-Phenylalanine and following the approach presented in Scheme S2.

S7c was obtained starting from the commercially available Fmoc-Tyr(tBu)-OH, tBu protection was removed during the esterification reaction.

S7d was obtained starting from the commercially available Fmoc-Cys(Trt)-OH, Trt group was removed using the procedure presented by Campagne et al.[10]

GLYCINE BODIPY, 6a. The product was obtained in 71% (*a*) and 56% (*b*) yield as a yellow solid.

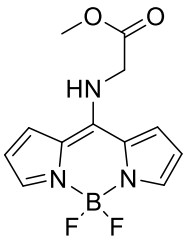

^{1}H NMR (600 MHz, 300K, $CDCl_3$) δ 7.63 (s, 2H), 7.27 (s, 1H), 7.06 (d, J = 4.0 Hz, 2H), 6.49 (s, 2H), 4.36 (d, J = 4.6 Hz, 2H), 3.95 (s, 3H). **^{13}C NMR (150 MHz, 220K, $CDCl_3$)** δ 168.5, 145.3, 135.9, 132.4, 123.9, 123.7, 121.7, 115.7, 115.5, 114.2, 54.0, 46.2., **HRMS (m/z)**: 302.08840 $[M+Na]^+$ (theor. calc. for 308.08829), **UV-Vis**: 317, 330, 411 nm, **Extinction**: $3.6235 \cdot 10^4$ $M^{-1}cm^{-1}$.

ALANINE BODIPY, 6b. The product was obtained in 64% (*a*) and 56% (*b*) yield as a yellow solid.

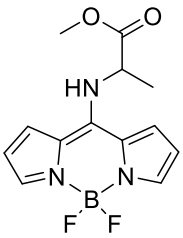

^{1}H NMR (600 MHz, CDCl3) δ 7.64 (s, 2H), 7.33 (d, J = 6.9 Hz, 1H), 7.10 (d, J = 4.0 Hz, 2H), 6.51 (s, 2H), 4.85 (p, J = 7.0 Hz, 1H), 3.91 (s, 3H), 1.73 (d, J = 6.9 Hz, 3H). **^{13}C NMR (150 MHz, 240K, $CDCl_3$)** δ = 172.2, 146.1, 136.3, 133.3, 124.7, 123.4, 121.1, 115.9, 115.8, 114.3, 54.1, 52.7, 17.9. **HRMS (m/z)**: 316.10398 $[M+Na]^+$ (theor. calc. for 316.10394), **UV-Vis**: 321, 330, 416 nm, **Extinction**: $3.6177 \cdot 10^4$ $M^{-1}cm^{-1}$.

a-LYSINE BODIPY, 6c. The product was obtained in 58% (*a*) and 68% (*b*) yield as a yellow solid

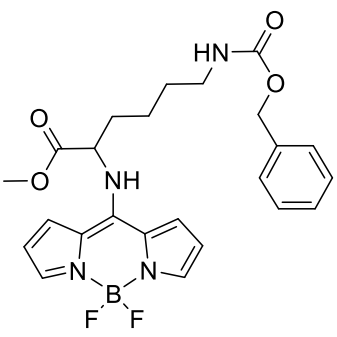

^{1}H NMR (500 MHz, 300K, $CDCl_3$) δ 7.63 (s, 2H), 7.42 (d, J = 7.4 Hz, 1H), 7.37 – 7.29 (m, 5H), 7.18 (s, 2H), 6.47 (s, 2H), 5.11 (d, J = 12.2 Hz, 1H), 5.04 (d, J = 12.2 Hz, 1H), 4.86 (m, 1H), 4.76 (m, 1H), 3.83 (s, 3H), 3.30 – 3.23 (m, 1H), 3.19 – 3.13 (m, 1H), 2.20 – 2.07 (m, 2H), 1.58 – 1.40 (m, 4H). **^{13}C NMR (150 MHz, 240K, $CDCl_3$)** δ 171.4, 157.4, 147.9, 136.0, 135.8, 133.2, 128.7, 128.6, 128.4, 128.1, 127.9, 124.9, 123.2, 121.8, 117.3, 115.6, 113.9, 67.2, 58.3, 53.7, 39.0, 30.7, 29.9, 22.4. **HRMS (m/z)**: 507.19634 $[M+Na]^+$ (theor. calc. for 507.19899), **UV-Vis**: 322, 333, 415 nm, **Extinction**: 3.3365 $\cdot 10^4$ $M^{-1}cm^{-1}$.

10 X. Moreau, J.-M. Campagne, *J. Org. Chem.*, 2003, **68**, 13, 5346-5350.

LYSINE BODIPY, 7a. The product was obtained in 86% (*a*) and 87% (*b*) yield as a green solid.

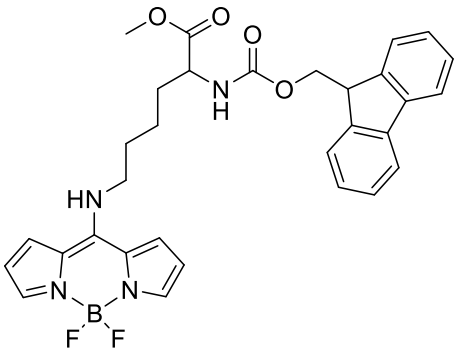

^{1}H NMR (600 MHz, $CDCl_3$) δ 7.75 (dd, J = 9.0, 8.3 Hz, 2H), 7.70 (s, 1H), 7.54 (dd, J = 18.4, 7.5 Hz, 2H), 7.43 (s, 1H), 7.40 (t, J = 7.5 Hz, 1H), 7.36 (t, J = 7.4 Hz, 1H), 7.31 – 7.27 (m, 2H), 7.15 (s, 1H), 7.11 (s, 1H), 7.07 (s, 1H), 6.51 (s, 1H), 6.13 (s, 1H), 5.55 (d, J = 7.9 Hz, 1H), 5.30 (s, 1H), 4.48 – 4.38 (m, 3H), 4.19 (t, J = 7.0 Hz, 1H), 3.80 (s, 3H), 3.67 (s, 1H), 3.59 (s, 1H), 1.99 (s, 1H), 1.91 (s, 1H), 1.83 (s, 1H), 1.74 (s, 1H), 1.59 (m, 2H), 1.53 (s, 1H). **^{13}C NMR (150 MHz, $CDCl_3$)** δ 172.7, 156.9, 148.9, 143.6, 141.5, 141.5, 135.6, 132.4, 128.0, 127.2, 127.2, 125.1, 125.1, 123.9, 120.3, 120.3, 115.8, 114.8, 113.6, 67.7, 53.6, 52.9, 52.8, 47.5, 47.2, 33.5, 27.4, 23.2. **HRMS (m/z)**: 595.2664 $[M+Na]^+$ (theor. calc. for 595.23040), **UV-Vis**: 301, 318, 328, 407 nm, **Extinction**: $3.2403 \cdot 10^4$ $M^{-1}cm^{-1}$.

***p*-aminoPHENYLALANINE BODIPY, 7b.** In this specific case, instead of using 1.0 equivalents of K_2CO_3, the amino acid was used in 2.0 equivalents. The product was obtained in 10% (*a*) and 92% (*b*) yield as a yellow solid.

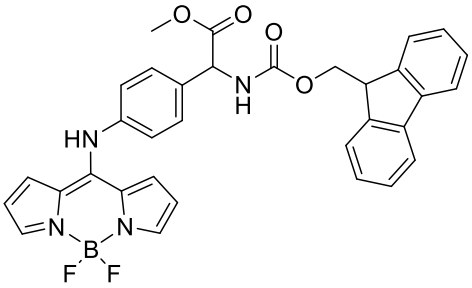

^{1}H NMR (600 MHz, 300K, CDCl3) δ 7.91 (s, 1H), 7.76 (d, J = 7.6 Hz, 2H), 7.58 (s, 2H), 7.55 (t, J = 7.5 Hz, 2H), 7.40 (t, J = 7.4 Hz, 2H), 7.30 (t, J = 6.5 Hz, 2H), 7.26 (d, J = 7.6 Hz, 2H), 7.22 (d, J = 7.9 Hz, 2H), 6.46 (s, 2H), 6.31 (dd, J = 4.0, 2.1 Hz, 2H), 5.35 (d, J = 8.0 Hz, 1H), 4.69 (dd, J = 13.4, 6.3 Hz, 1H), 4.46 (dd, J = 10.5, 7.1 Hz, 1H), 4.38 (dd, J = 10.5, 6.9 Hz, 1H), 4.19 (t, J = 6.7 Hz, 1H), 3.74 (s, 3H), 3.24 (dd, J = 13.6, 5.4 Hz, 1H), 3.09 (dd, J = 13.6, 6.4 Hz, 1H)., **^{13}C NMR (150 MHz, $CDCl_3$)** δ 171.7, 155.7, 147.8, 143.8, 143.8, 141.6, 141.5, 138.0, 136.6, 135.7, 131.5, 128.0, 127.8, 127.3, 127.2, 127.1, 125.8, 125.1, 125.1, 124.1, 120.6, 120.2, 120.2, 114.8, 67.1, 55.0, 52.7, 47.4, 38.5. **HRMS (m/z)**: 629.21086 $[M+Na]^+$ (theor. calc. for 629.21480), **UV-Vis**: 301, 325, 334, 419 nm, **Extinction**: $3.5359 \cdot 10^4$ $M^{-1}cm^{-1}$.

TYROSINE BODIPY, 7c. The product was obtained in 0% (*a*) and 63% (*b*) yield as a yellow solid.

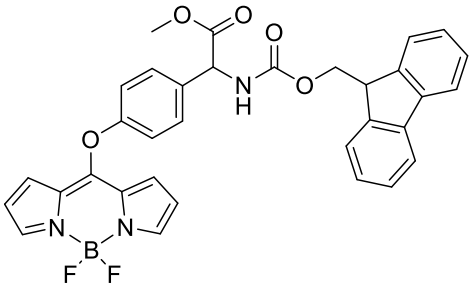

^{1}H NMR (600 MHz, CDCl3) δ 7.76 (d, J = 7.6 Hz, 2H), 7.74 (s, 2H), 7.56 (dd, J = 7.5, 0.8 Hz, 2H), 7.40 (td, J = 7.3, 2.0 Hz, 2H), 7.30 (m, 2H), 7.19 (d, J = 8.3 Hz, 2H), 7.15 (d, J = 8.4 Hz, 2H), 6.65 (d, J = 3.2 Hz, 2H), 6.39 (d, J = 2.5 Hz, 2H), 5.35 (d, J = 7.9 Hz, 1H), 4.69 (m, 1H), 4.48 (dd, J = 10.5, 7.1 Hz, 1H), 4.40 (dd, J = 10.5, 6.8 Hz, 1H), 4.20 (t, J = 6.7 Hz, 1H), 3.75 (s, 3H), 3.23 (dd, J = 13.7, 5.4 Hz, 1H), 3.10 (dd, J = 13.7, 6.2 Hz, 1H). **^{13}C NMR (150 MHz, $CDCl_3$)** δ 171.7, 159.5, 155.6, 154.9, 143.9, 143.8, 141.6, 141.5, 141.0, 135.3, 131.5, 127.9, 127.2, 126.9, 126.3, 125.1, 125.0, 120.3, 120.2, 120.2, 117.0, 67.0, 55.1, 52.6, 47.4, 38.2. **HRMS (m/z)**: 630.19443 $[M+Na]^+$ (theor. calc. for 630.19881), **UV-Vis**: 301, 456 nm, **Extinction**: $4.9054 \cdot 10^4$ $M^{-1}cm^{-1}$.

CYSTEINE BODIPY, 7d. The product was obtained in 22% (*a*) and 44% (*b*) yield as a deep red solid. **^{1}H NMR (600 MHz, CDCl3)** δ 7.85 (s, 2H), 7.77 (dd, J = 7.6, 2.8 Hz, 2H), 7.58 (t, J = 6.4 Hz, 2H), 7.43 (m, 1H), 7.42 – 7.39 (m, 2H), 7.32 (qd, J = 7.6, 1.1 Hz, 2H), 6.56 (d, J = 4.1 Hz, 2H), 5.65 (d, J = 6.5 Hz, 1H), 4.68 (m, 1H), 4.40 – 4.32 (m, 2H), 4.20 (t, J = 6.8 Hz, 1H), 3.92 (dd, J = 13.9, 4.0 Hz, 1H), 3.72 (dd, J = 13.9, 4.1 Hz, 1H), 3.61 (s, 3H). **^{13}C NMR (150 MHz, $CDCl_3$)** δ 169.7, 155.5, 147.8, 144.3, 143.9, 143.8, 141.5, 136.6, 129.9, 127.9, 127.3, 127.2, 125.3, 125.2, 120.2, 120.2, 118.90, 67.5, 54.7, 53.1, 47.2, 40.9. **HRMS (m/z)**: 570.14137 $[M+Na]^+$ (theor. calc. for 570.14409), **UV-Vis**: 380, 500, 519 nm**, Extinction**: $3.3718 \cdot 10^4$ $M^{-1}cm^{-1}$.

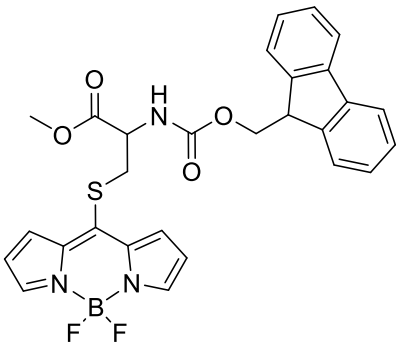

3. NMR spectra

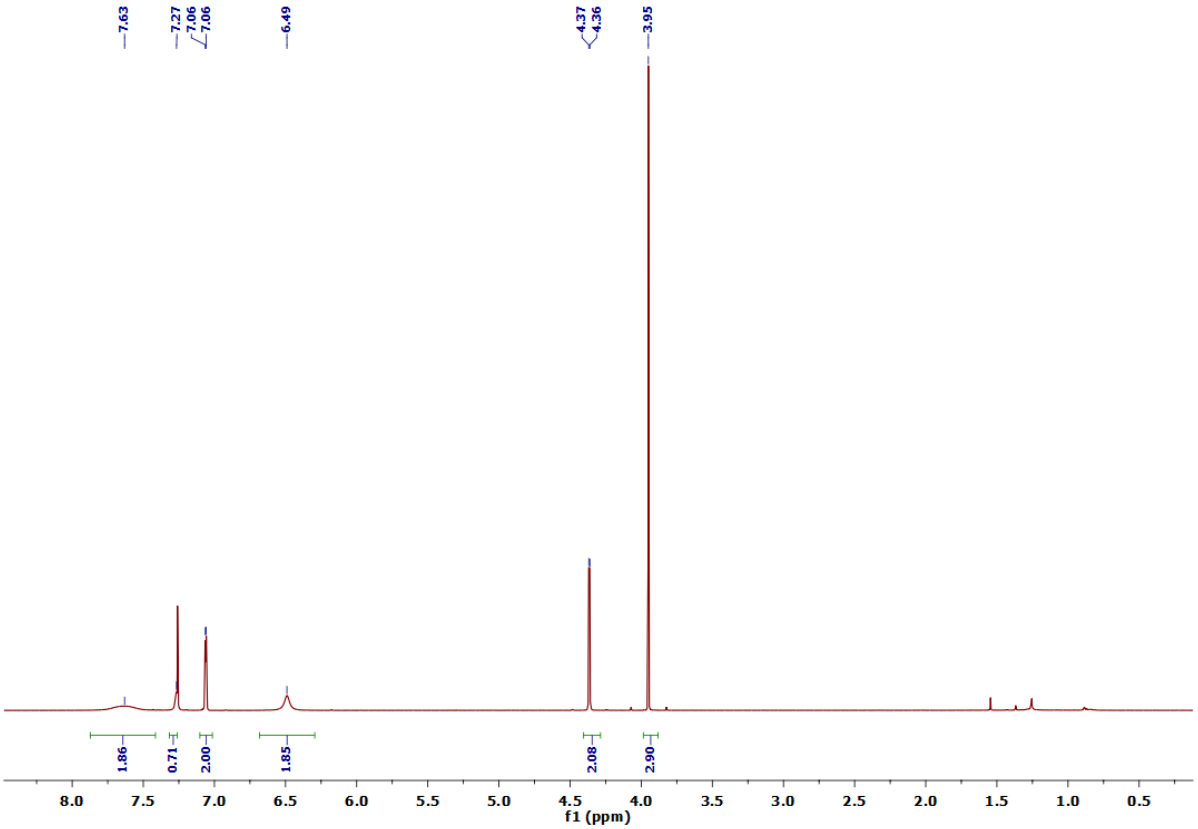

Figure S1. ^{1}H NMR spectrum of **6a** ($CDCl_3$, 300K, 600 MHz).

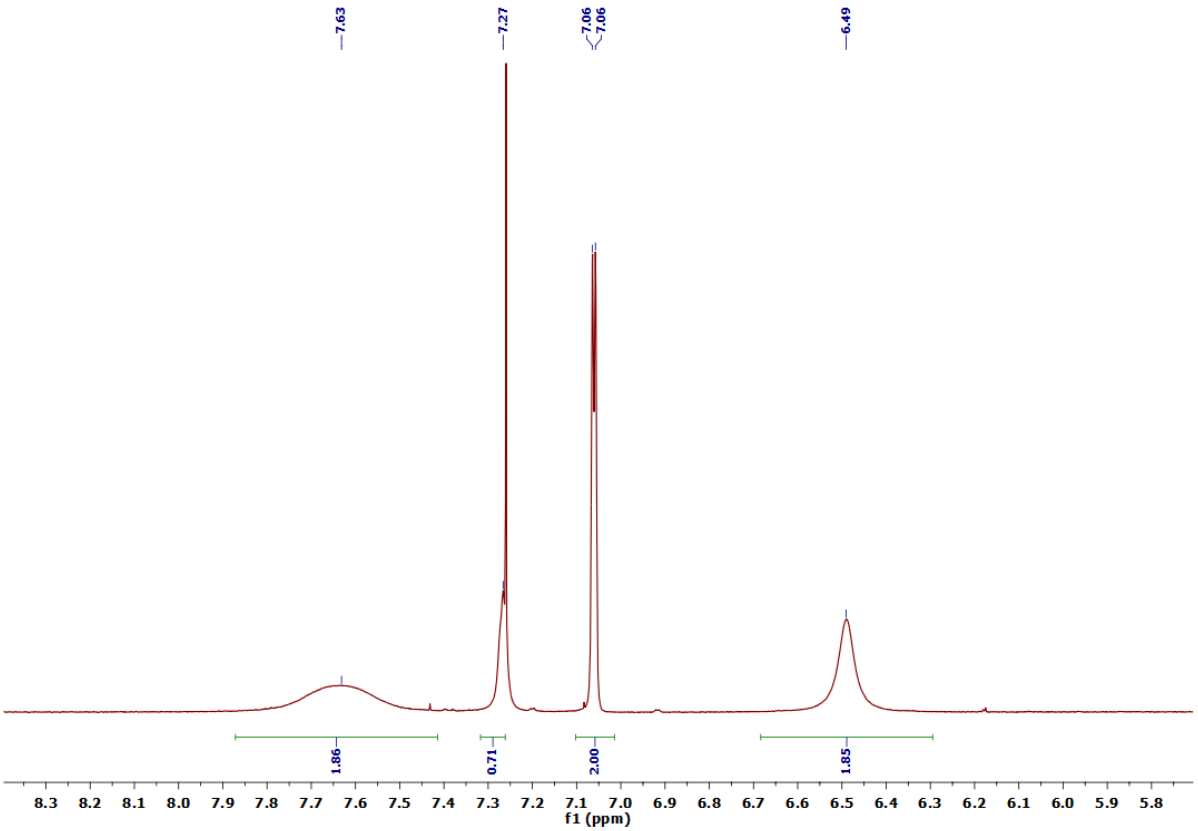

Figure S2. ^{1}H NMR spectrum (zoom, aromatic region) of **6a** ($CDCl_3$, 300K, 600 MHz).

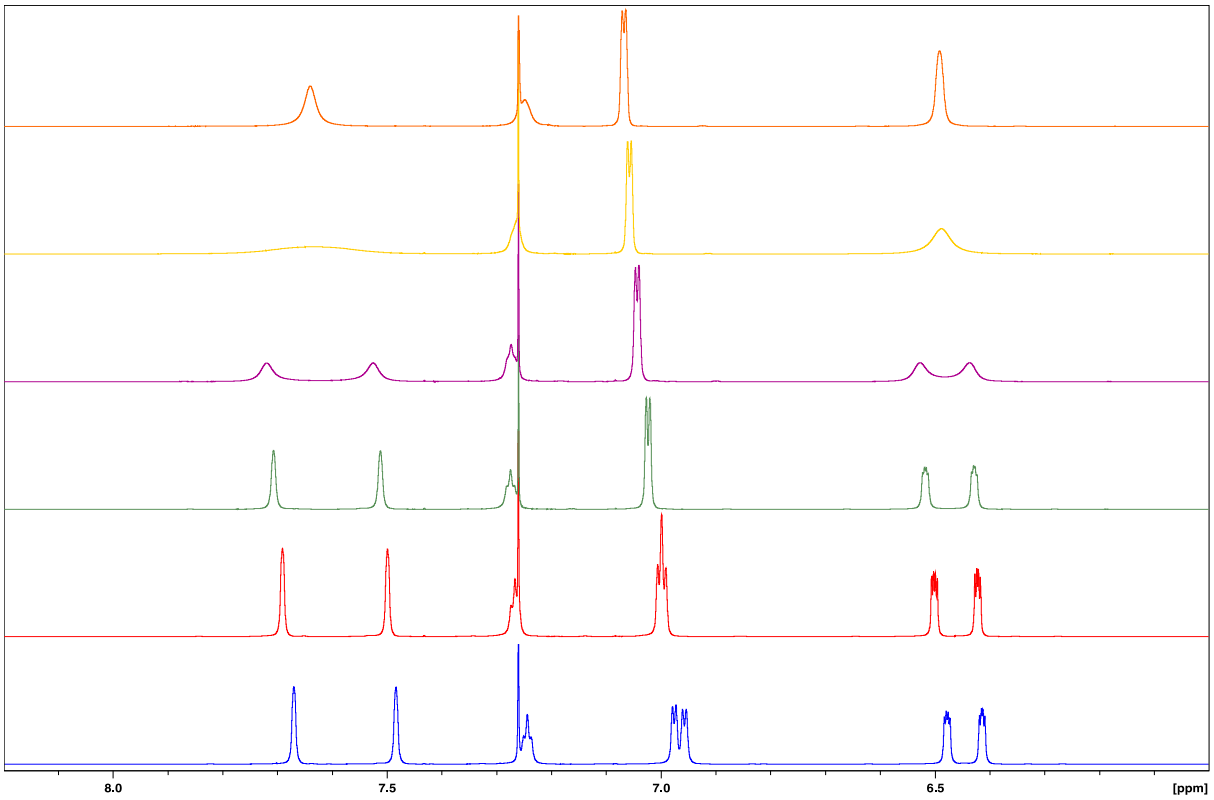

Figure S3. ^{1}H NMR spectrum (zoom, aromatic region) of **6a** ($CDCl_3$, Blue: 220K, Red: 240K, Green: 260K, Violet: 280K, Yellow: 300K, Orange: 320K, 600 MHz).

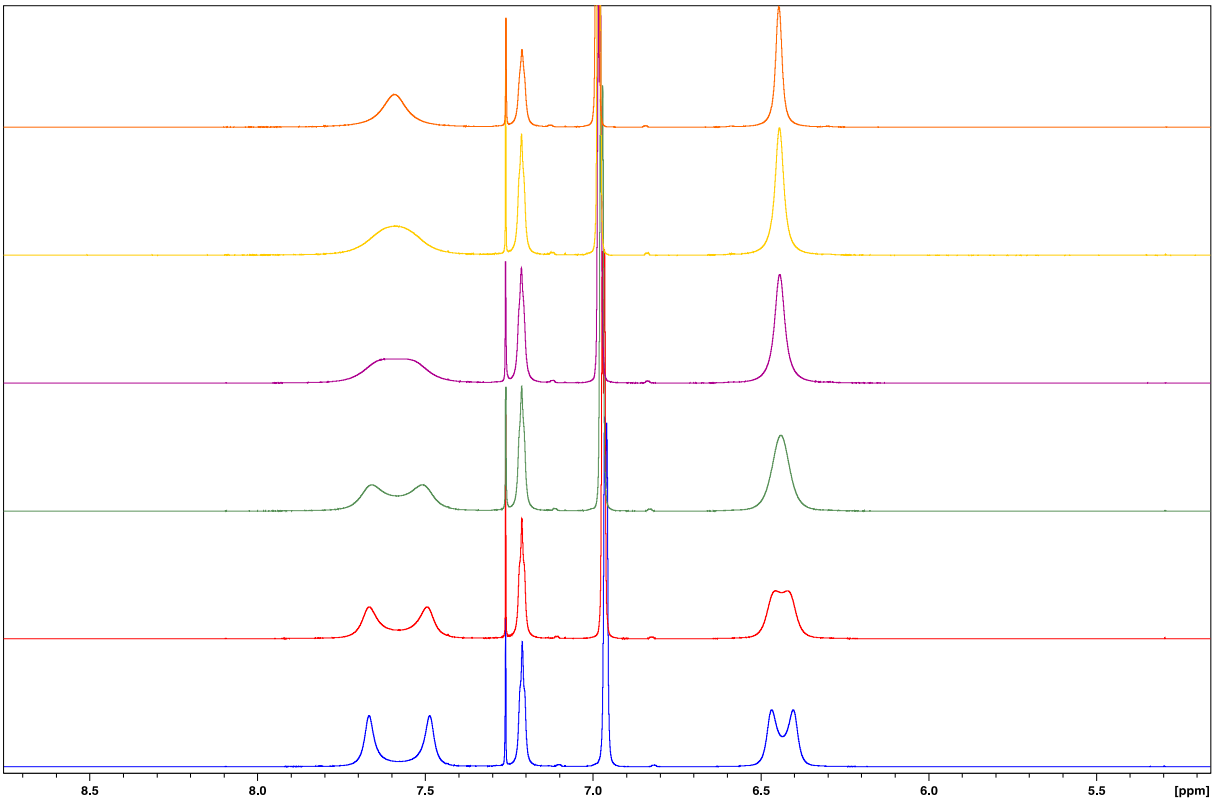

Figure S4. ^{1}H NMR spectrum (coalescence temperature determination, H(1) position) of **6a** ($CDCl_3$, Blue: 285K, Red: 290K, Green: 295K, Violet: 300K, Yellow: 305K, Orange: 310K, 600 MHz).

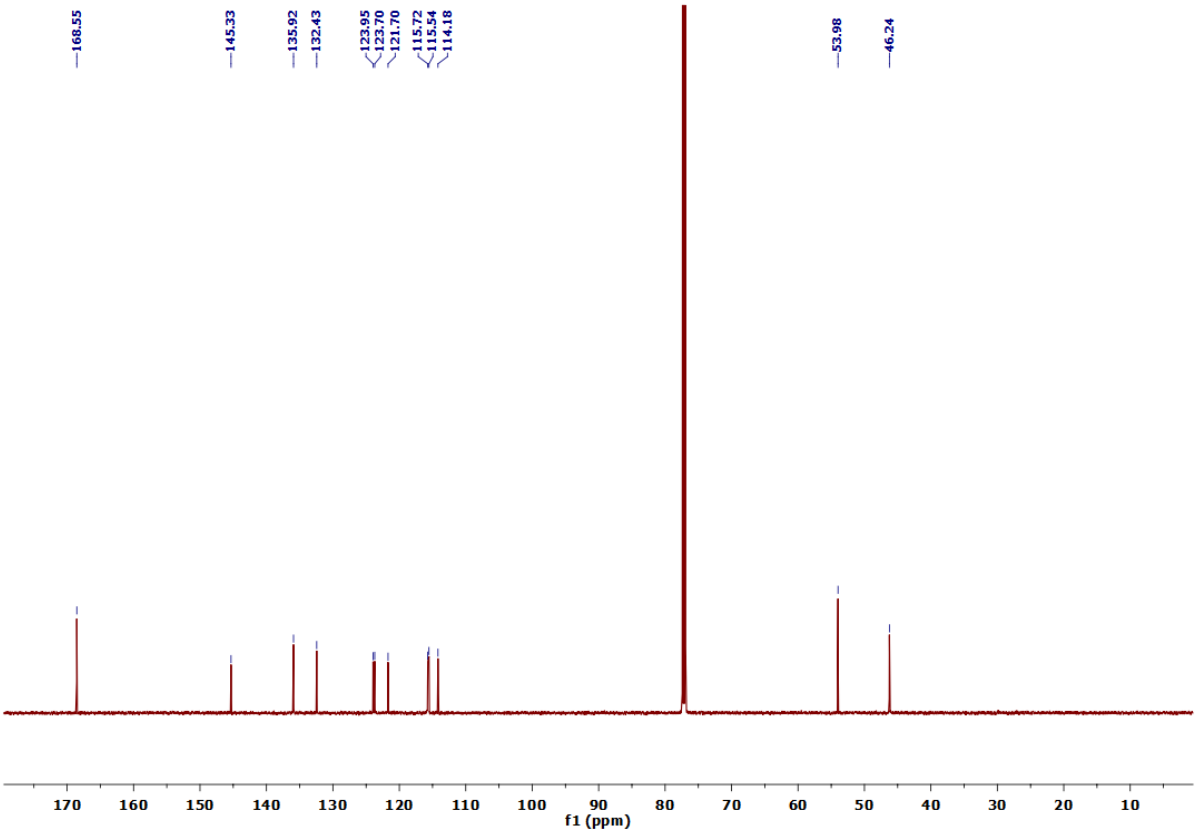

Figure S5. ^{13}C NMR spectrum of **6a** ($CDCl_3$, 220K, 151 MHz).

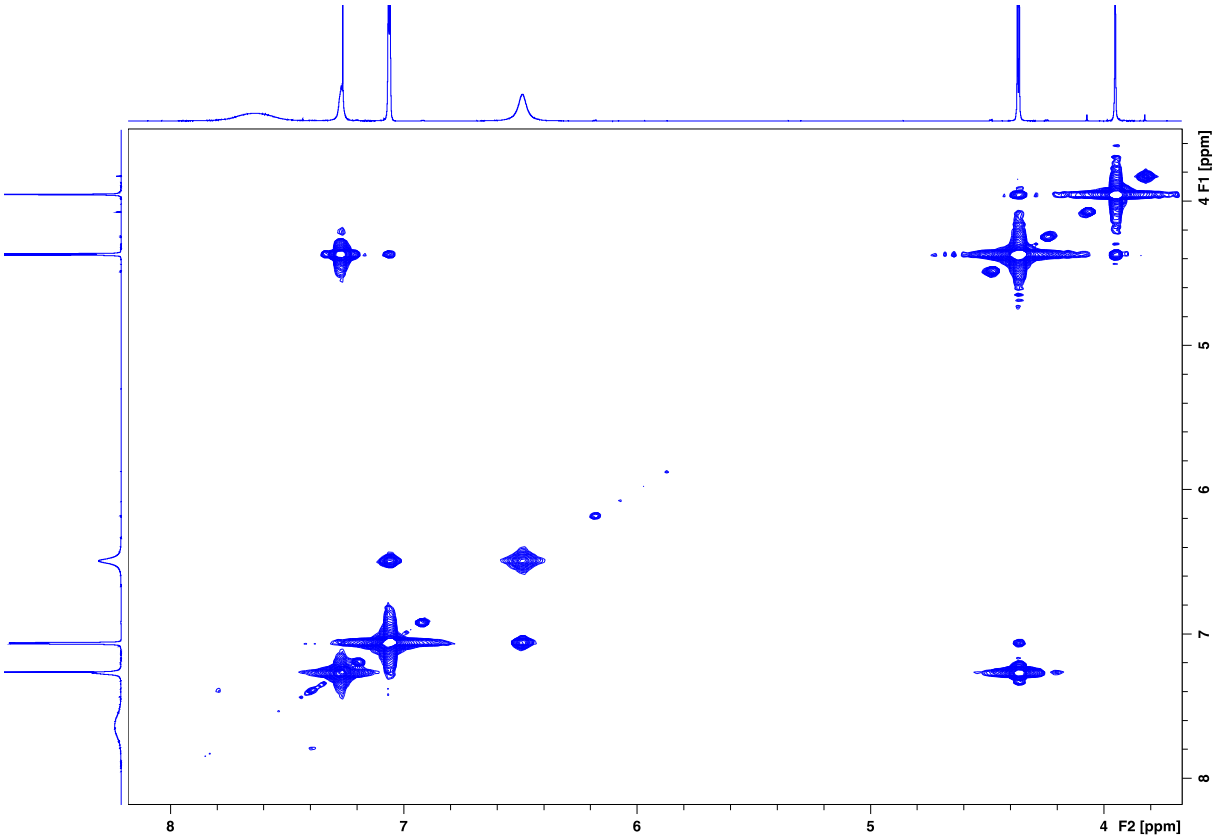

Figure S6. COSY NMR spectrum of **6a** ($CDCl_3$, 300K, 600 MHz).

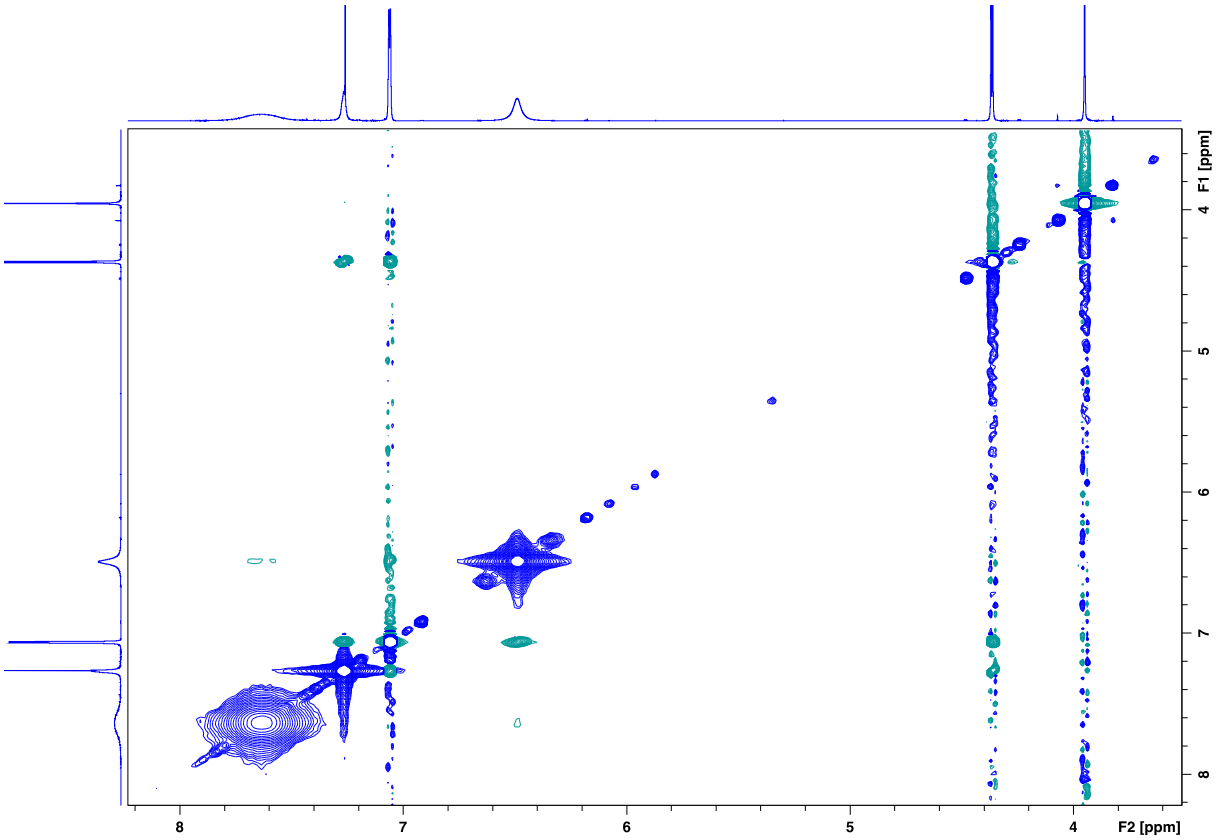

Figure S7. NOESY NMR spectrum of **6a** ($CDCl_3$, 300K, 600 MHz).

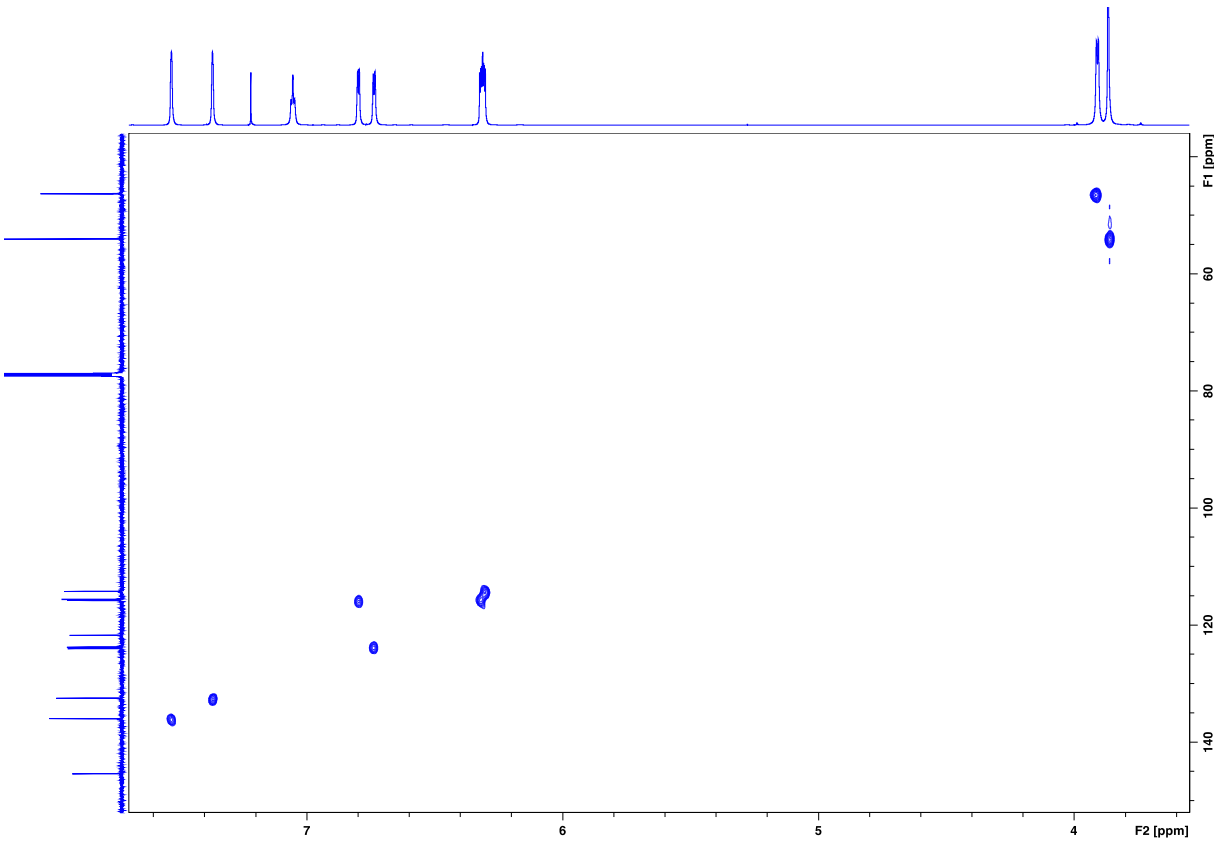

Figure S8. HSQC NMR spectrum of **6a** ($CDCl_3$, 220K, 600, 150 MHz).

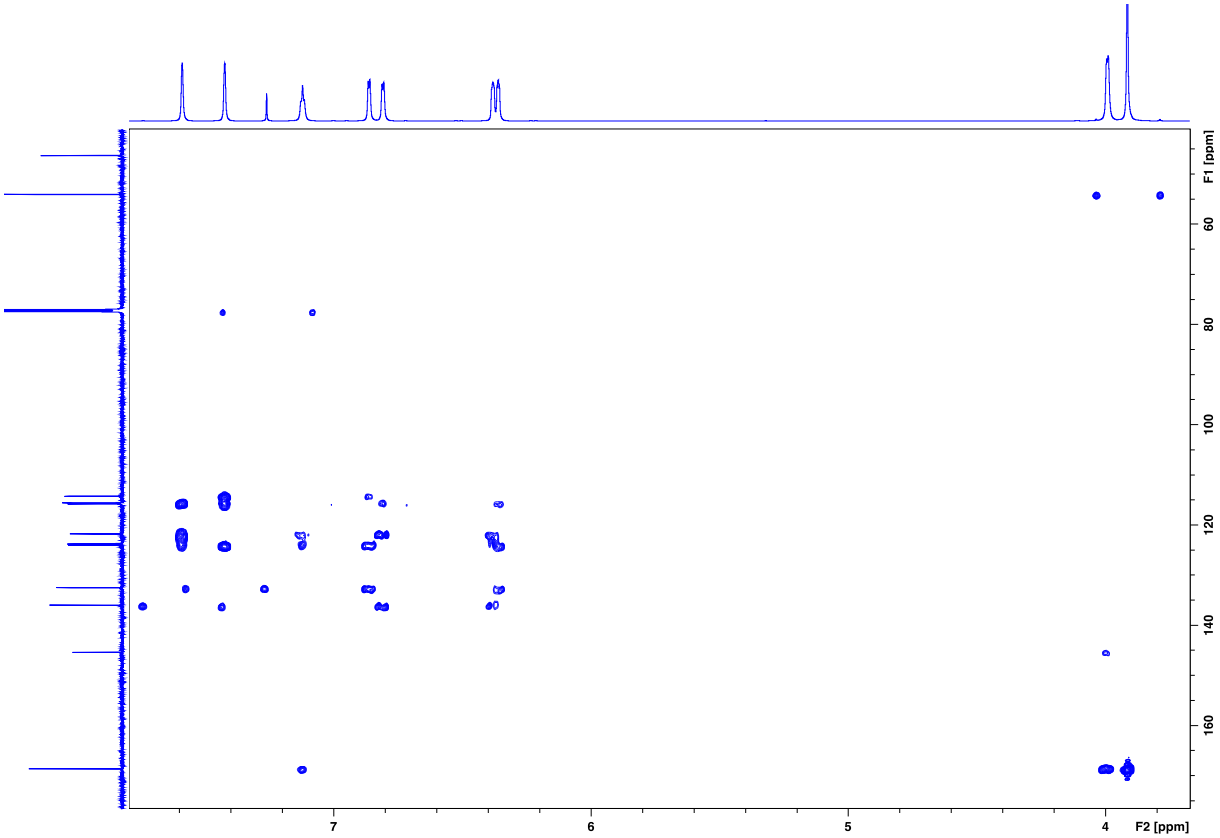

Figure S9. HMBC NMR spectrum of **6a** ($CDCl_3$, 220K, 600, 150 MHz).

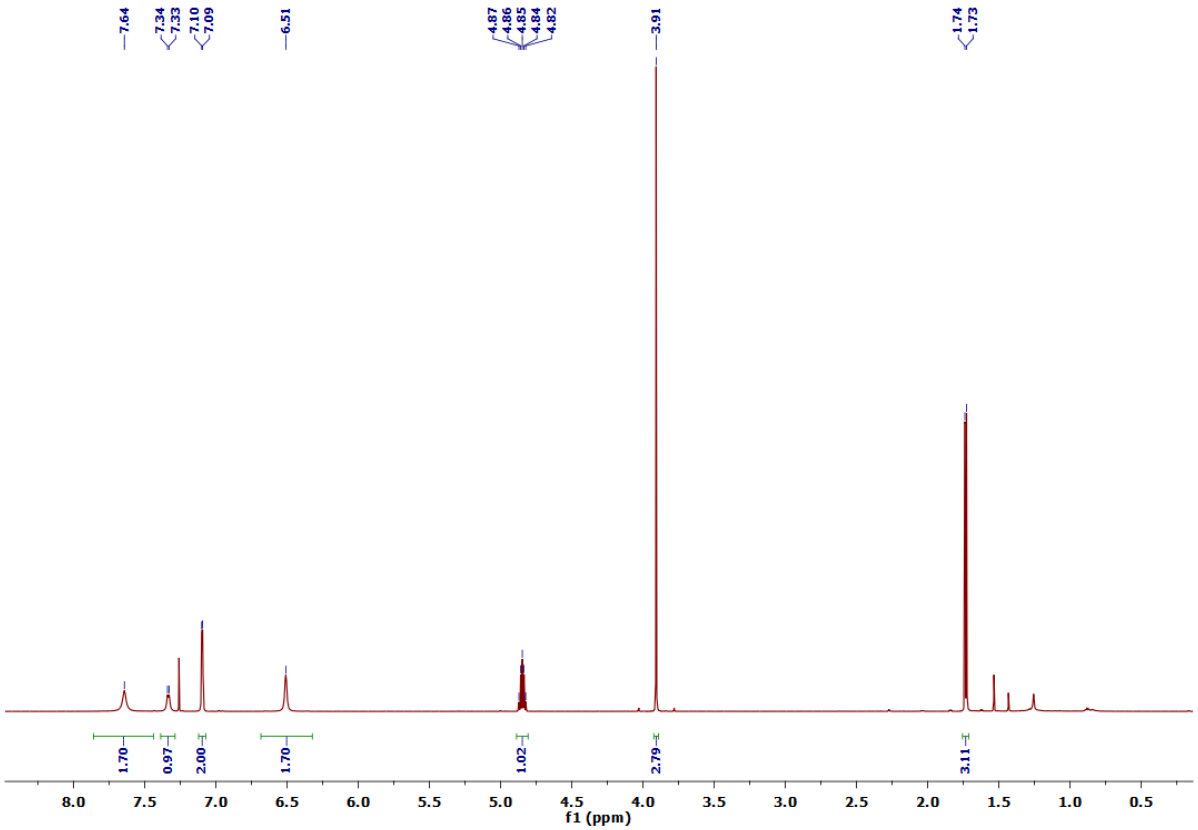

Figure S10. ^1H NMR spectrum of **6b** ($CDCl_3$, 300K, 600 MHz).

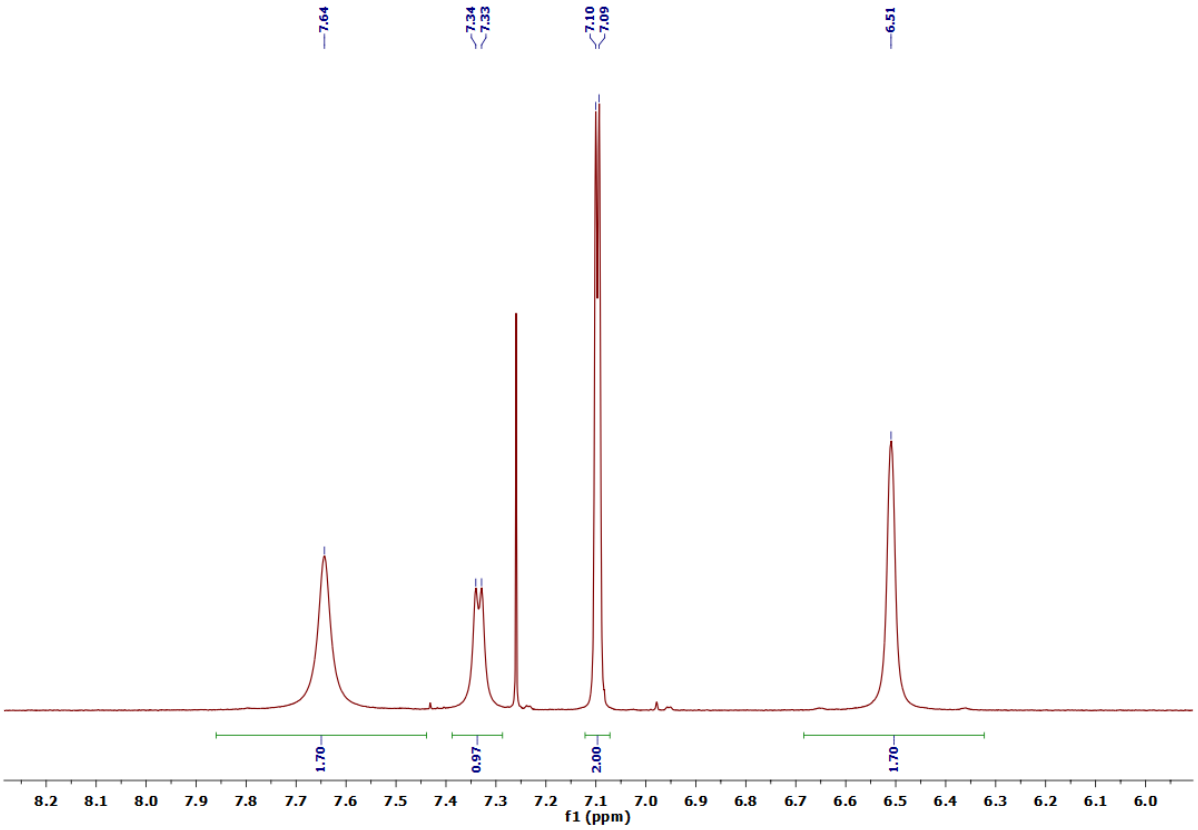

Figure S11. ^{1}H NMR spectrum (zoom, aromatic region) of **6b** ($CDCl_3$, 300K, 600 MHz).

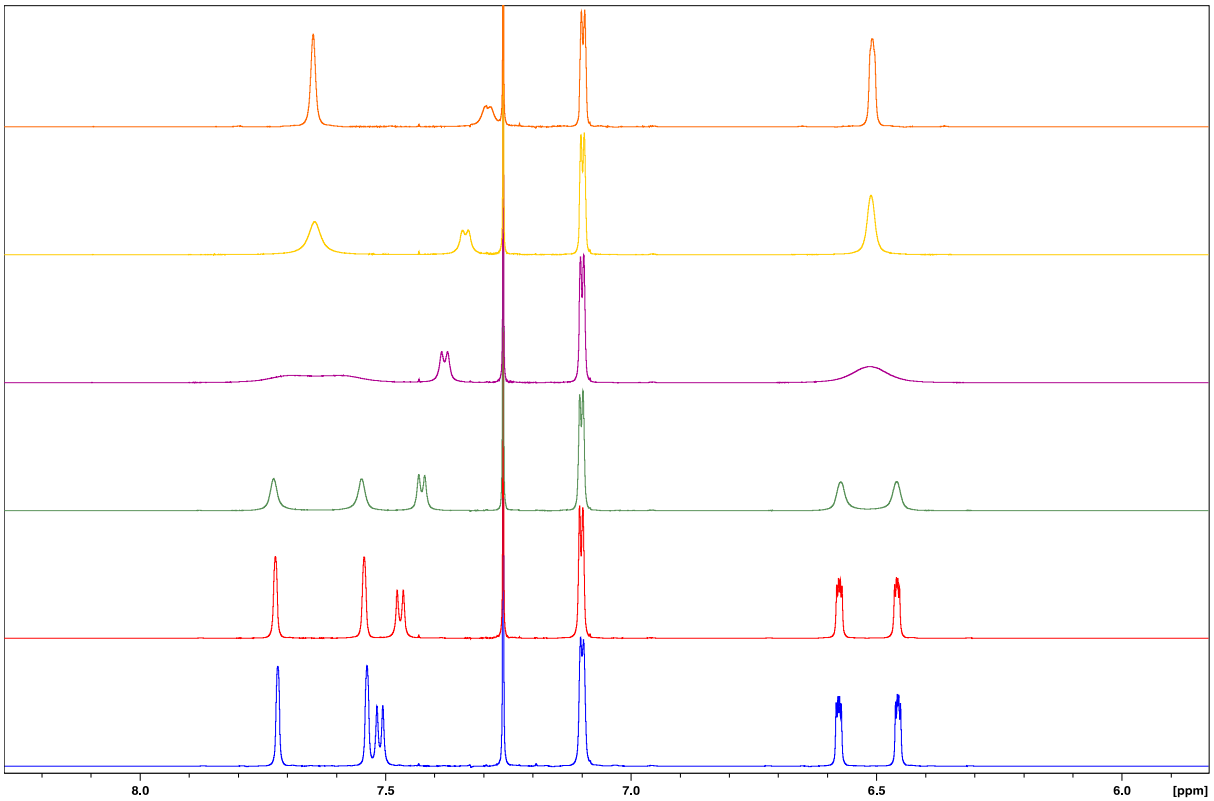

Figure S12. ^{1}H NMR spectrum (zoom, aromatic region) of **6b** ($CDCl_3$, Blue: 220K, Red: 240K, Green: 260K, Violet: 280K, Yellow: 300K, Orange: 320K, 600 MHz).

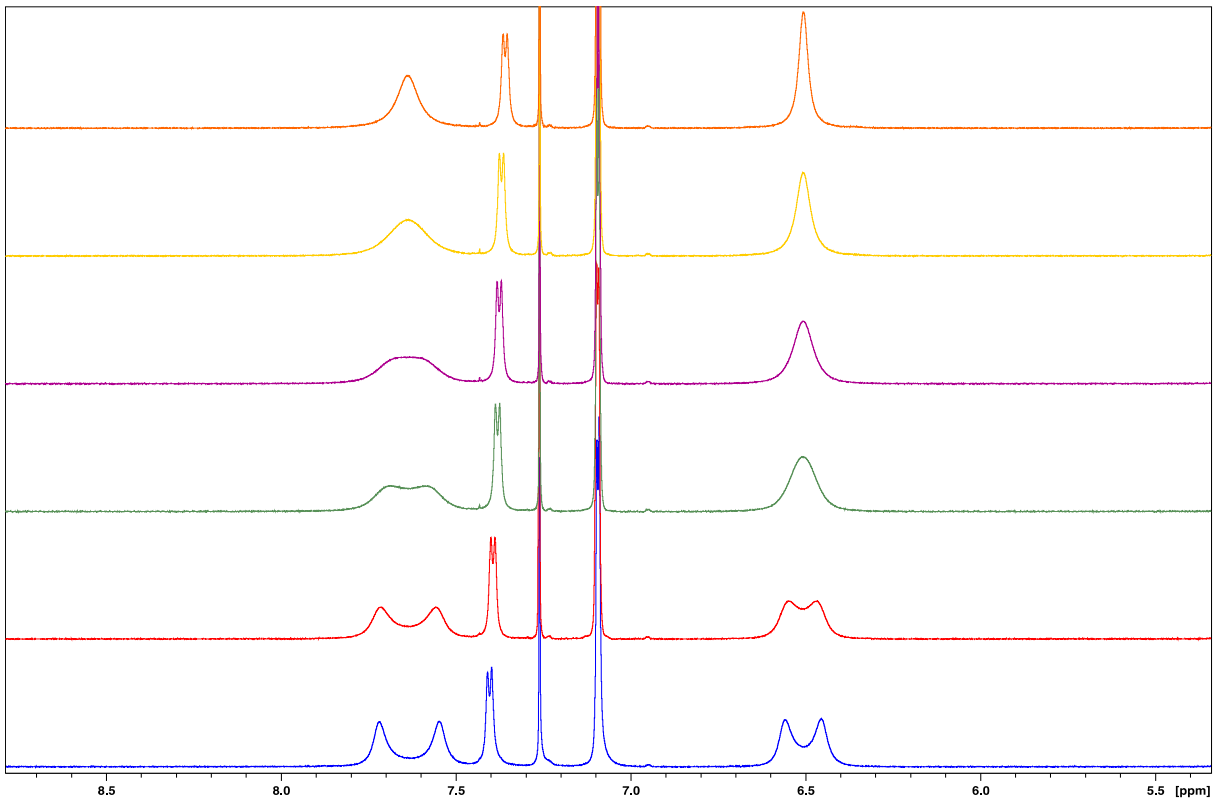

Figure S13. ^{1}H NMR spectrum (coalescence temperature determination, H(1) position) of **6b** ($CDCl_3$, Blue: 270K, Red: 275K, Green: 280K, Violet: 282K, Yellow: 258K, Orange: 290K, 600 MHz).

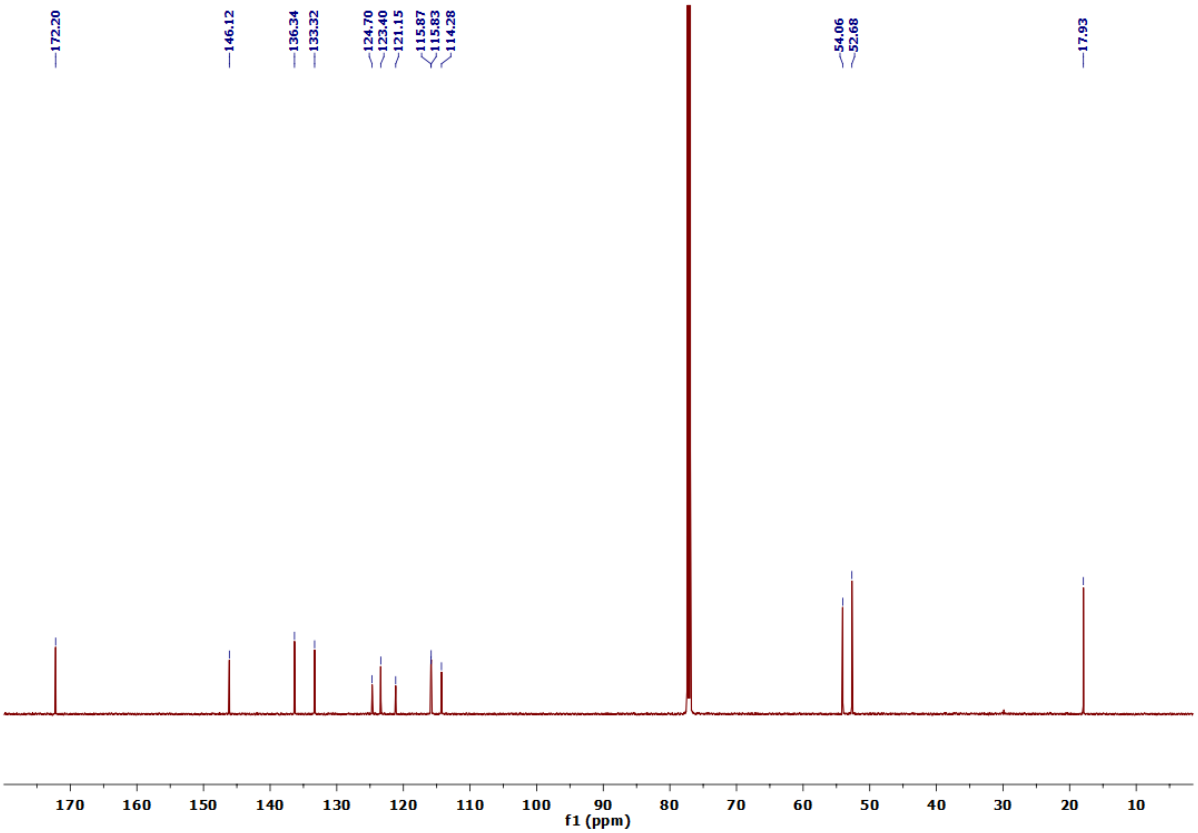

Figure S14. ^{13}C NMR spectrum of **6b** ($CDCl_3$, 240K, 150 MHz).

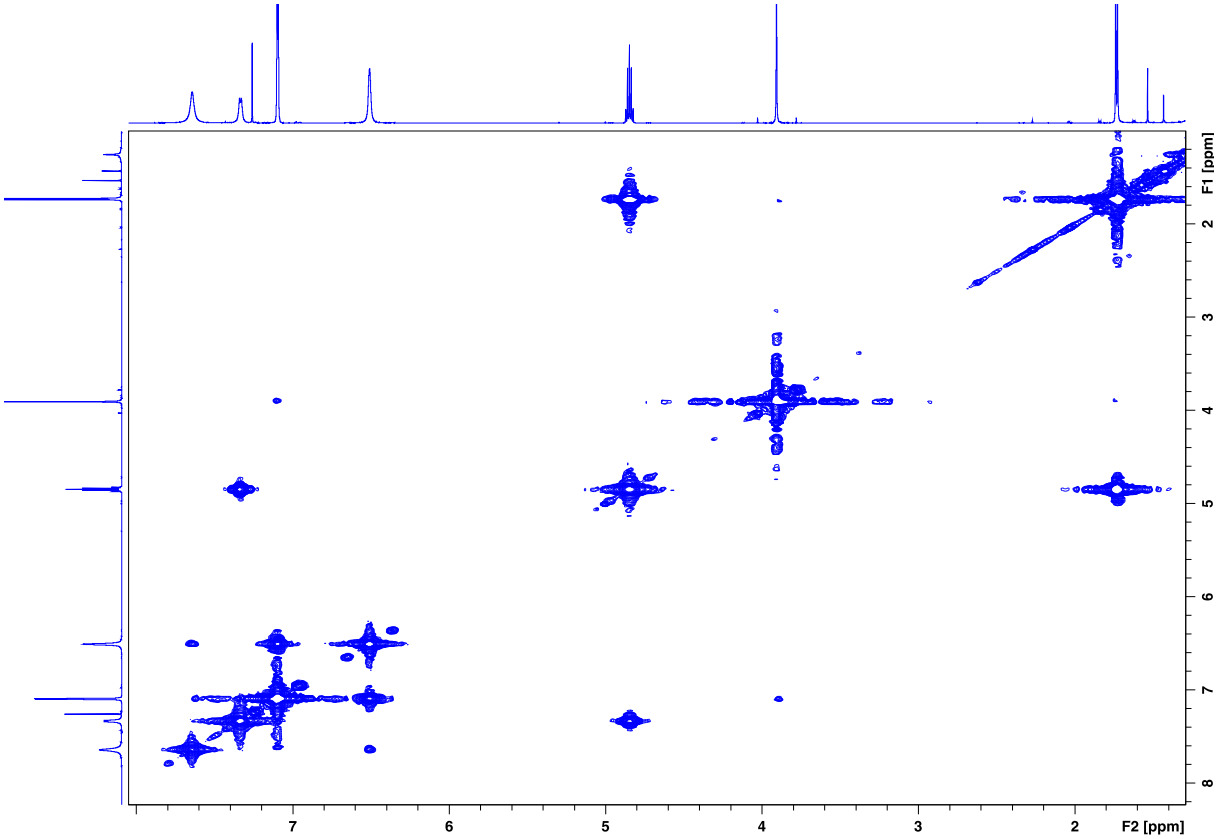

Figure S15. COSY NMR spectrum of **6b** ($CDCl_3$, 300K, 600 MHz).

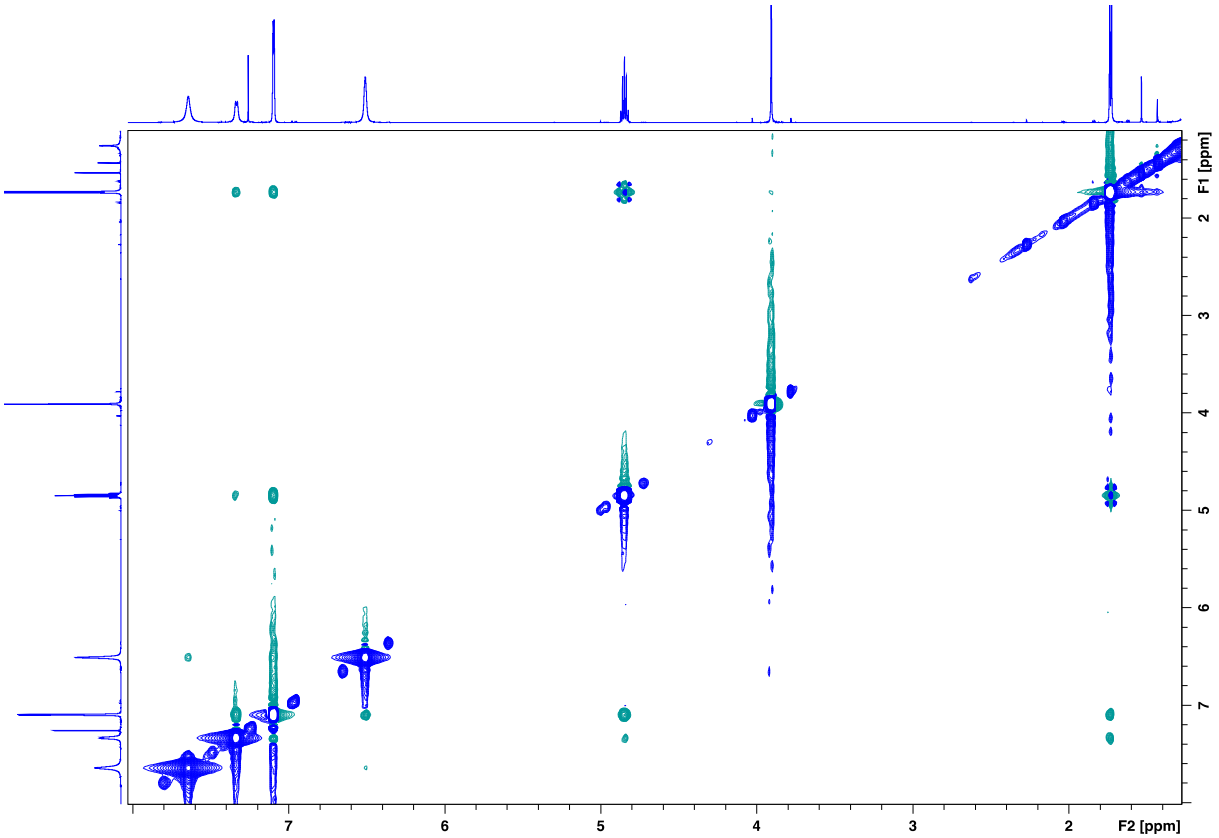

Figure S16. NOESY NMR spectrum of **6b** ($CDCl_3$, 300K, 600 MHz).

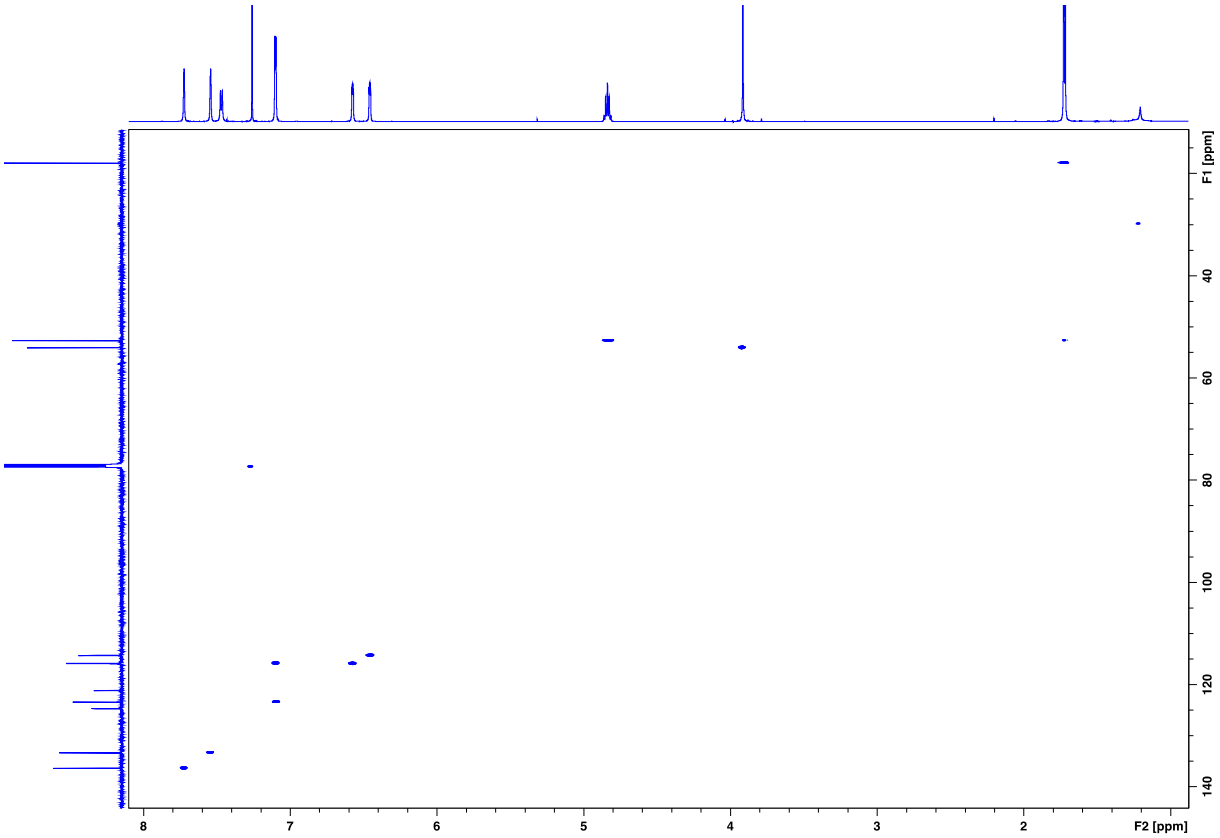

Figure S17. HSQC NMR spectrum of **6b** ($CDCl_3$, 240K, 600, 150 MHz).

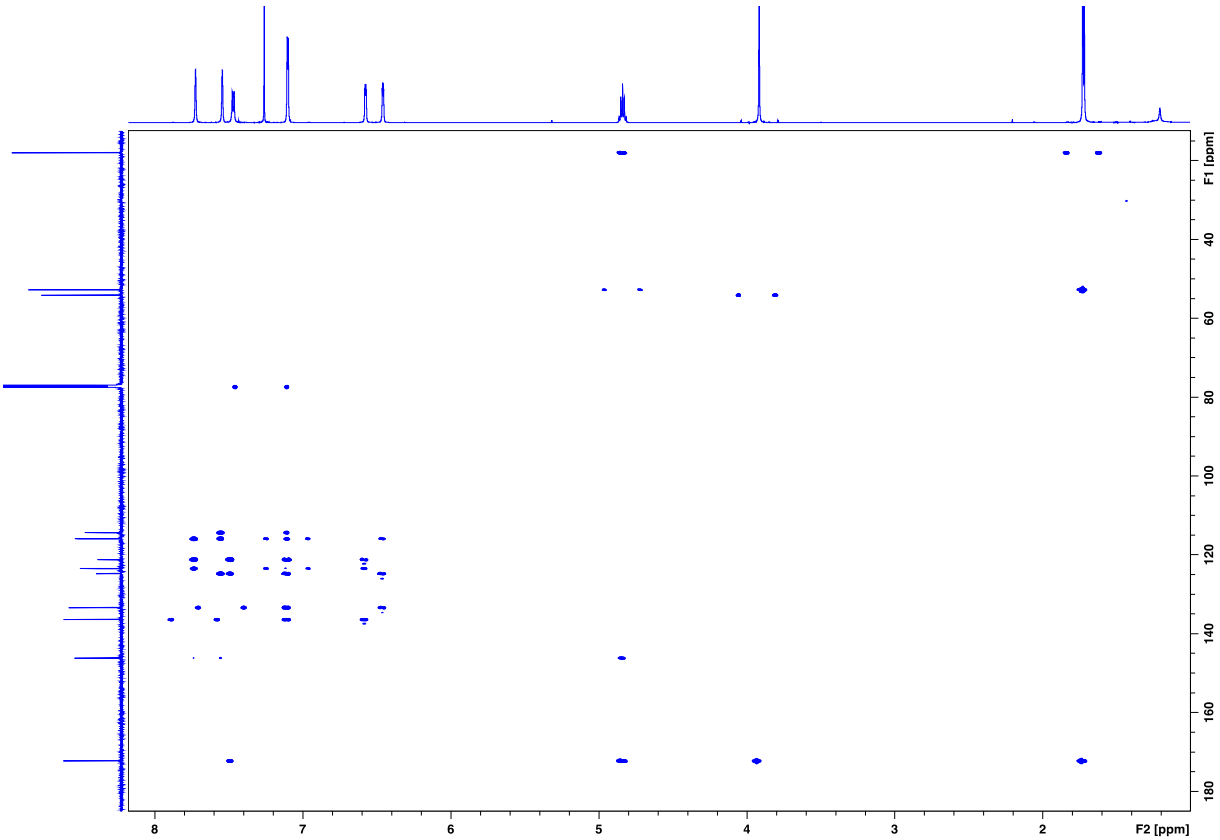

Figure S18. HMBC NMR spectrum of **6b** ($CDCl_3$, 240K, 600, 150 MHz).

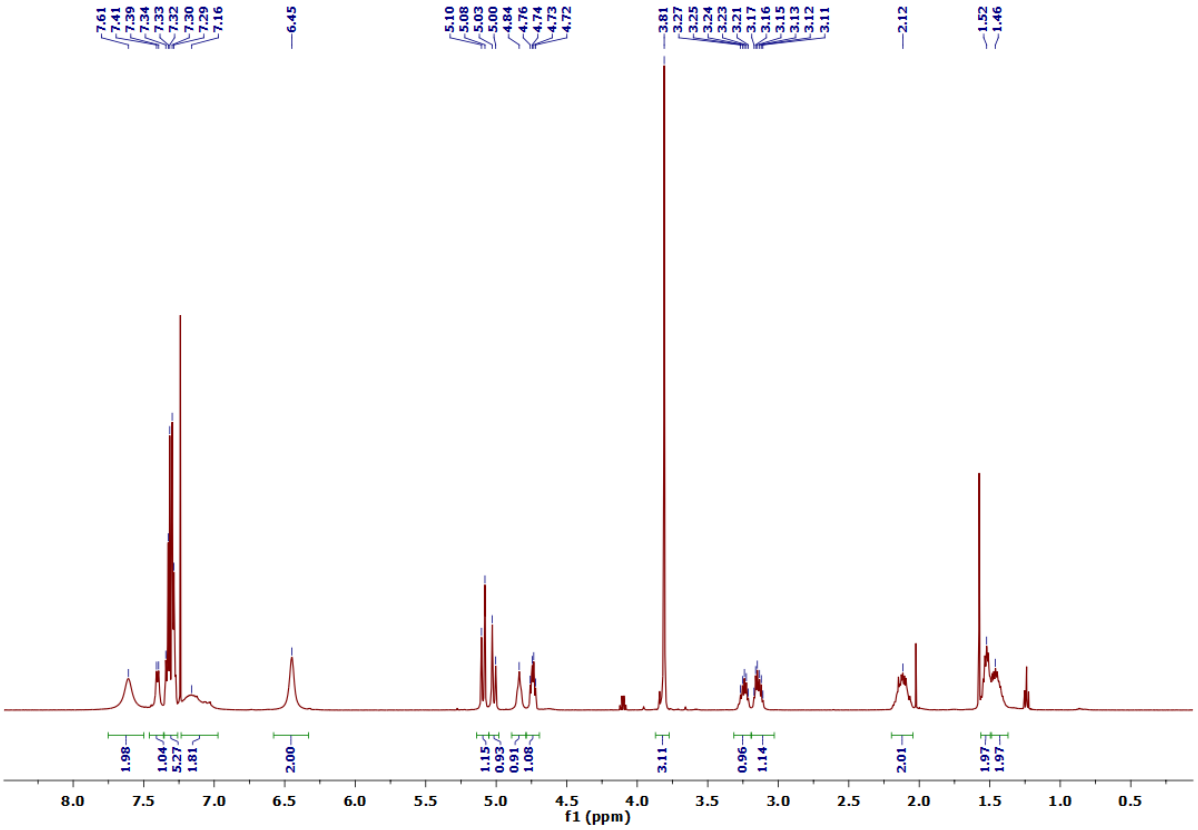

Figure S19. ^{1}H NMR spectrum of **6c** ($CDCl_3$, 300K, 600 MHz).

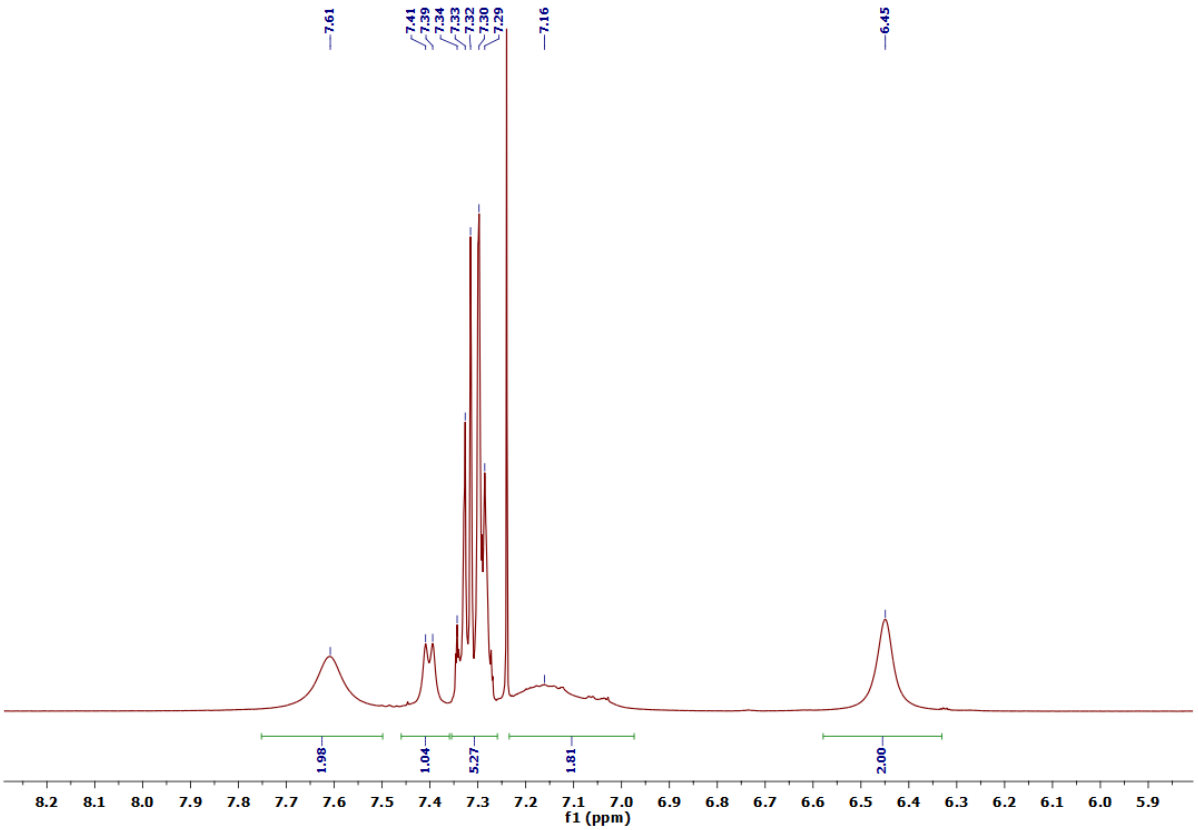

Figure S20. ^{1}H NMR spectrum (zoom, aromatic region) of **6c** ($CDCl_3$, 300K, 600 MHz).

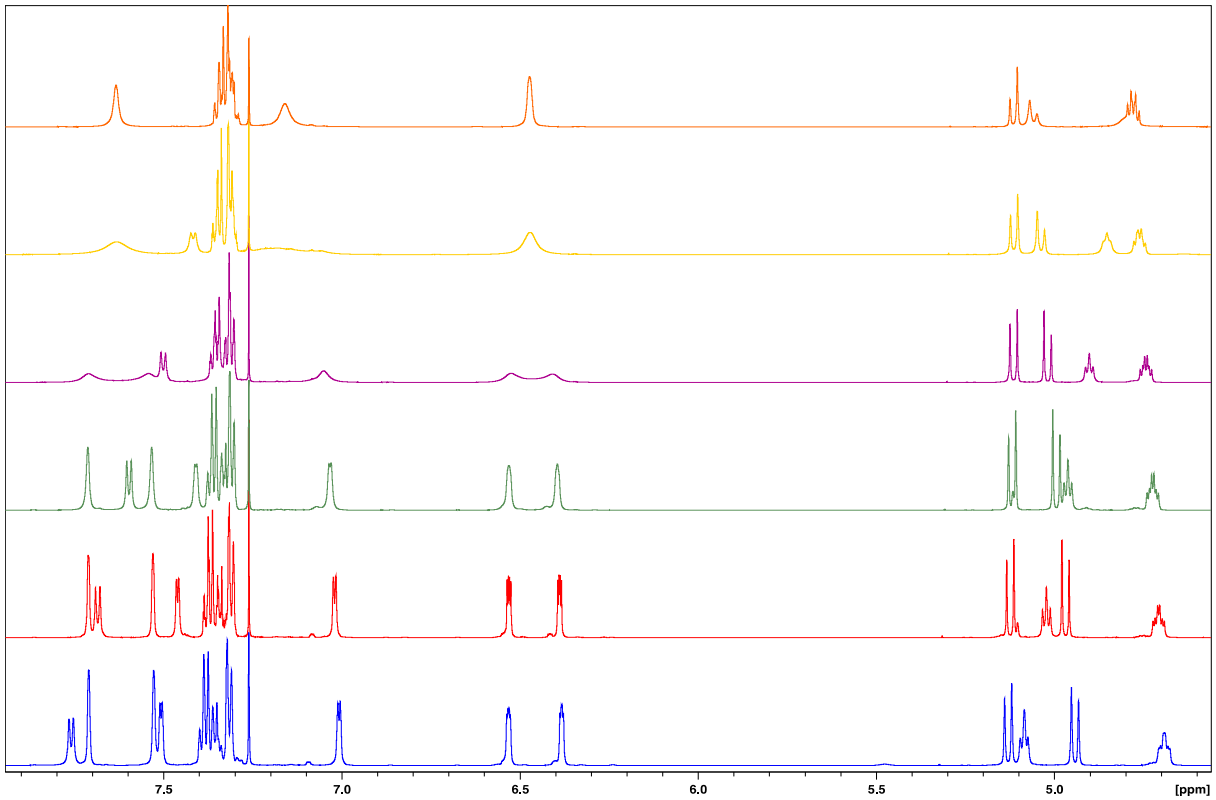

Figure S21. ^{1}H NMR spectrum (zoom, aromatic region) of **6c** (CDCl3, Blue: 220K, Red: 240K, Green: 260K, Violet: 280K, Yellow: 300K, Orange: 320K, 600 MHz).

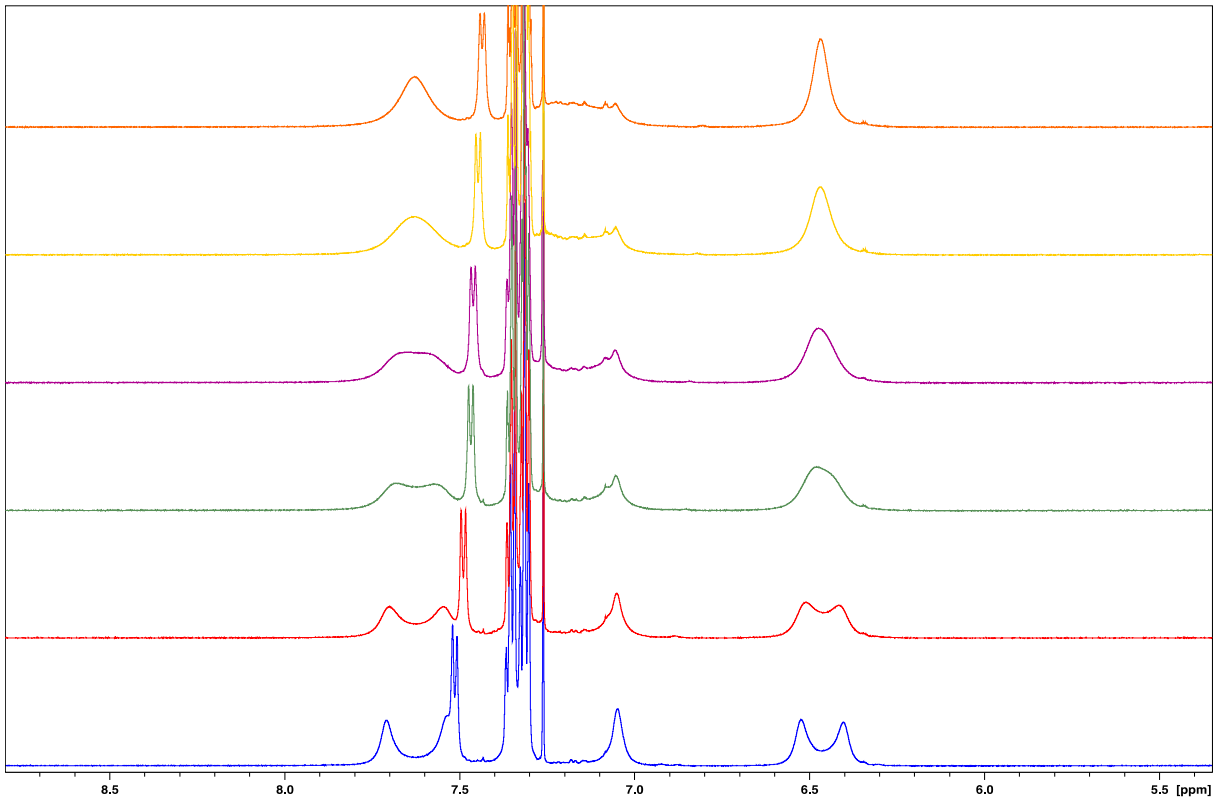

Figure S22. ^{1}H NMR spectrum (coalescence temperature determination, H(1) position) of **6c** ($CDCl_3$, Blue: 280K, Red: 285K, Green: 290K, Violet: 292K, Yellow: 295K, Orange: 300K, 600 MHz).

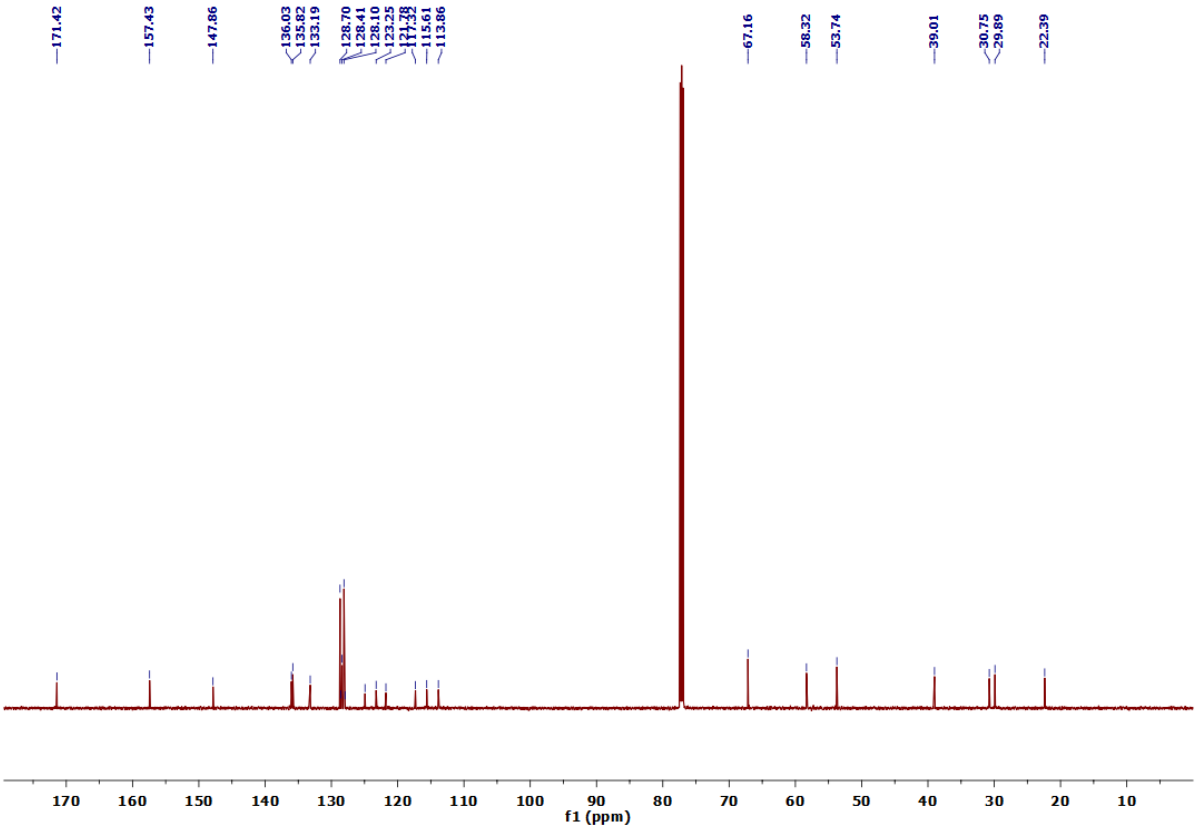

Figure S23. ^{13}C NMR spectrum of **6c** ($CDCl_3$, 240K, 150 MHz).

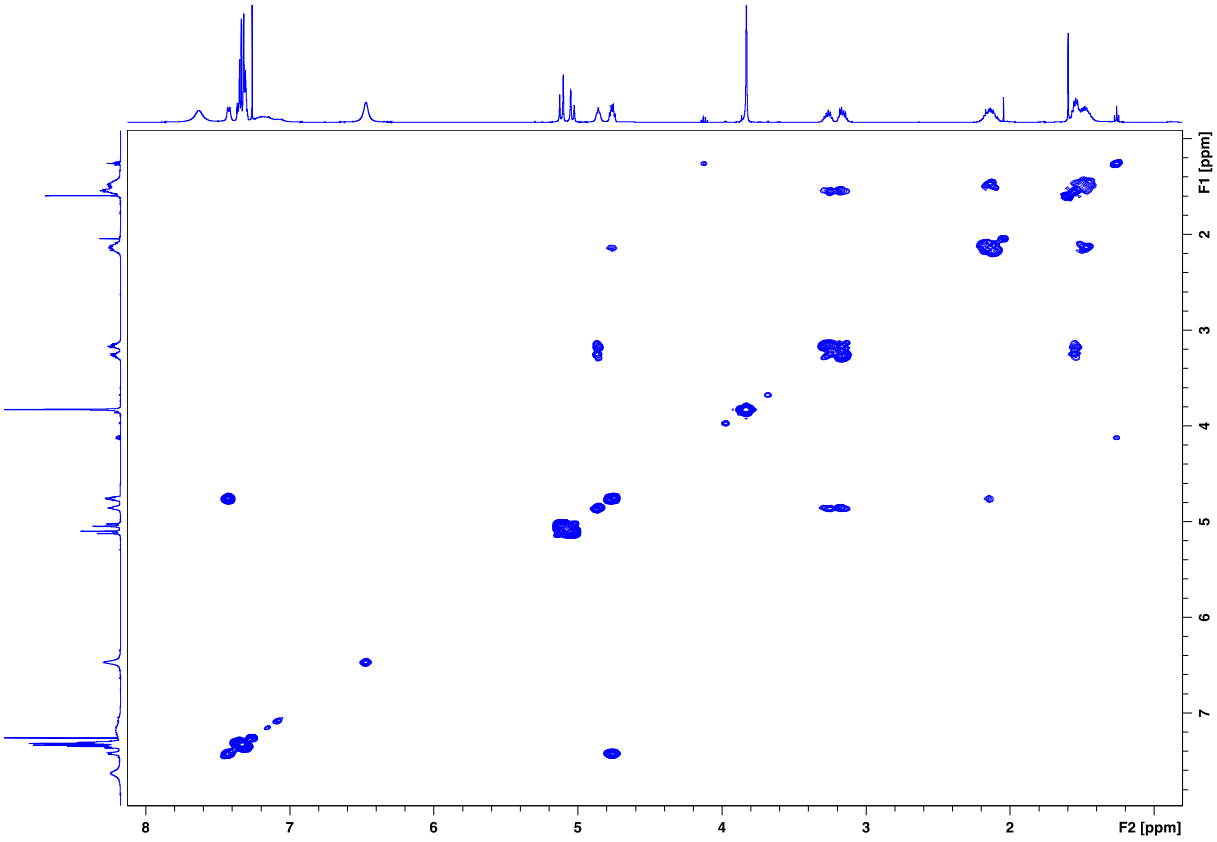

Figure S24. COSY NMR spectrum of **6c** ($CDCl_3$, 300K, 600 MHz).

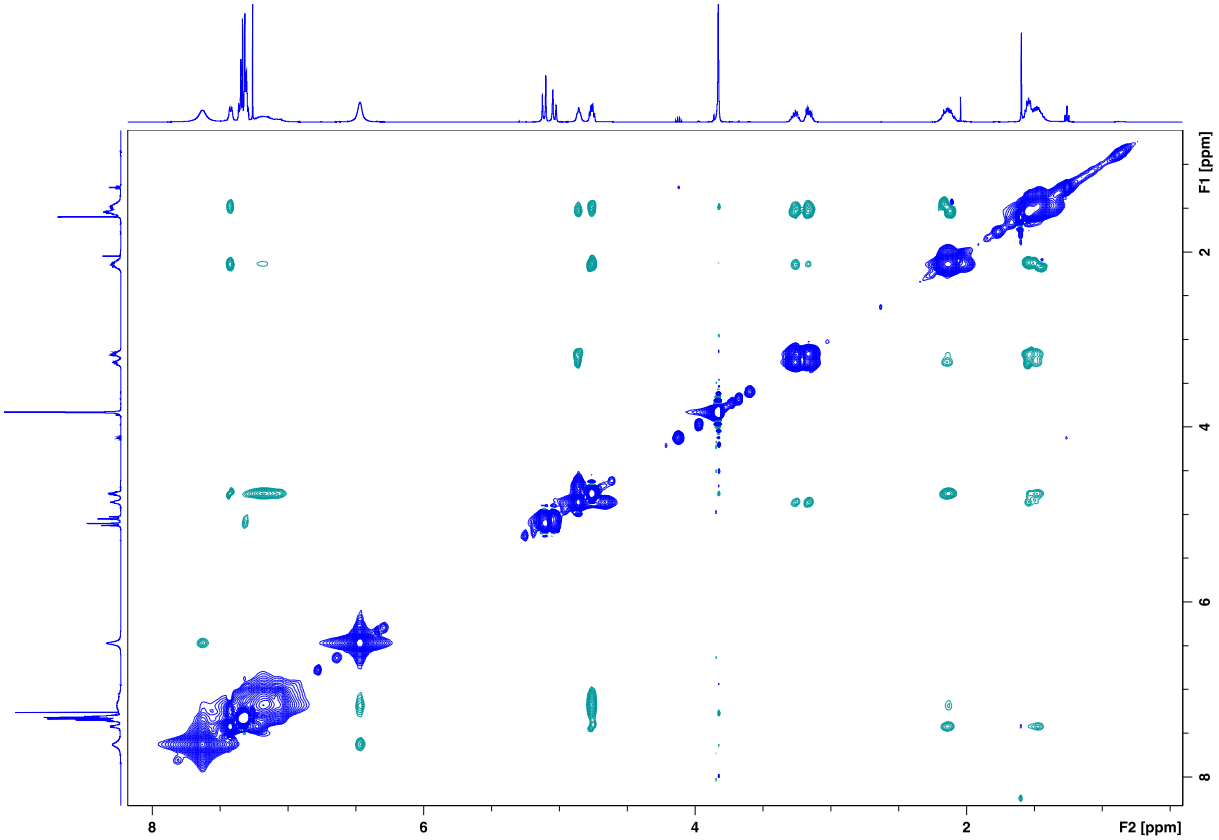

Figure S25. NOESY NMR spectrum of **6c** ($CDCl_3$, 300K, 600 MHz).

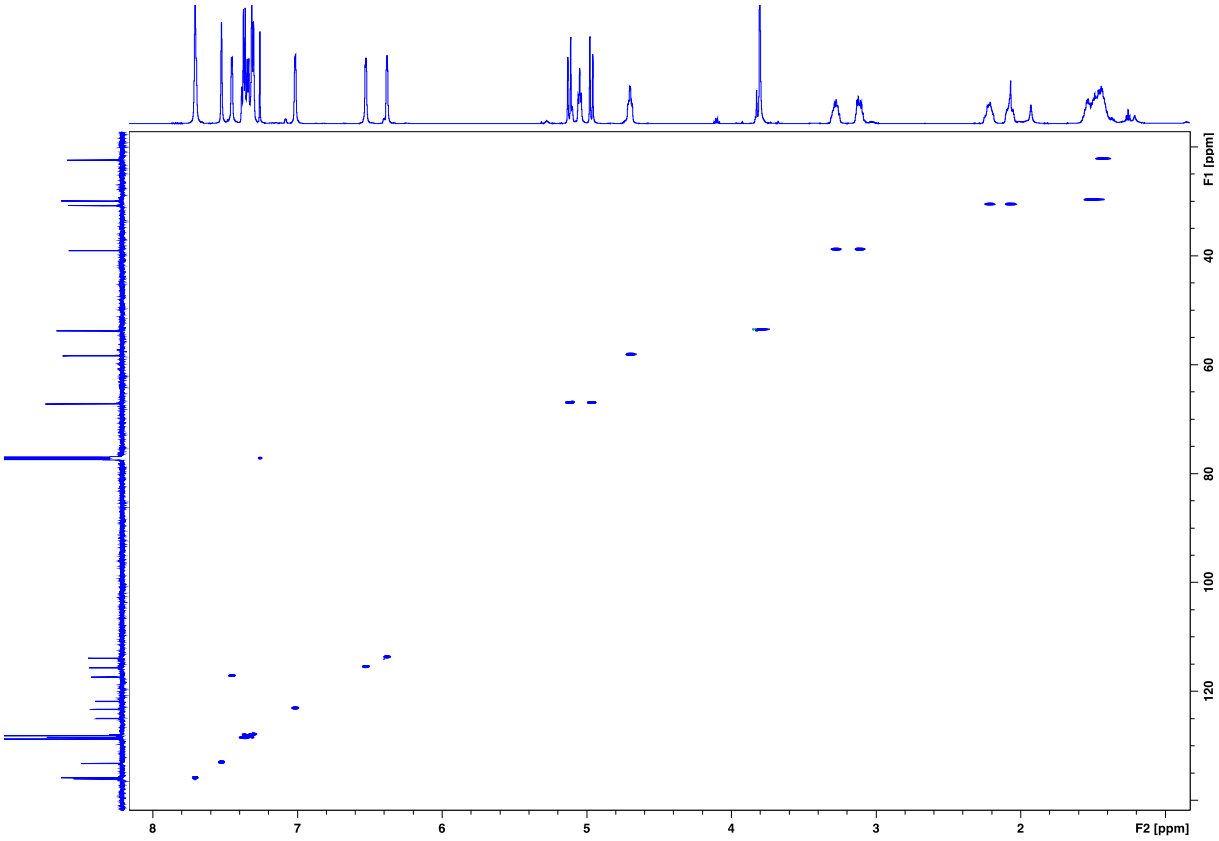

Figure S26. HSCQ NMR spectrum of **6c** ($CDCl_3$, 240K, 600, 150 MHz).

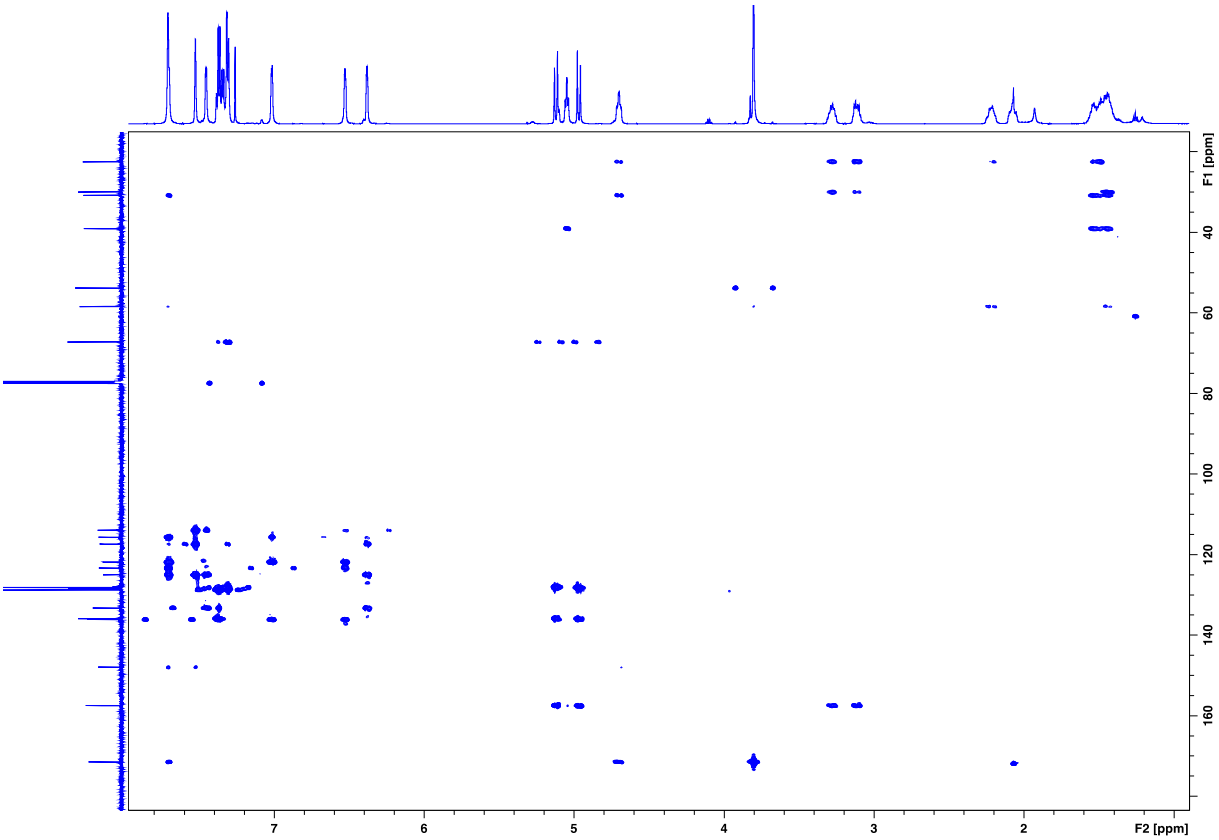

Figure S27. HMBC NMR spectrum of **6c** ($CDCl_3$, 240K, 600, 150 MHz).

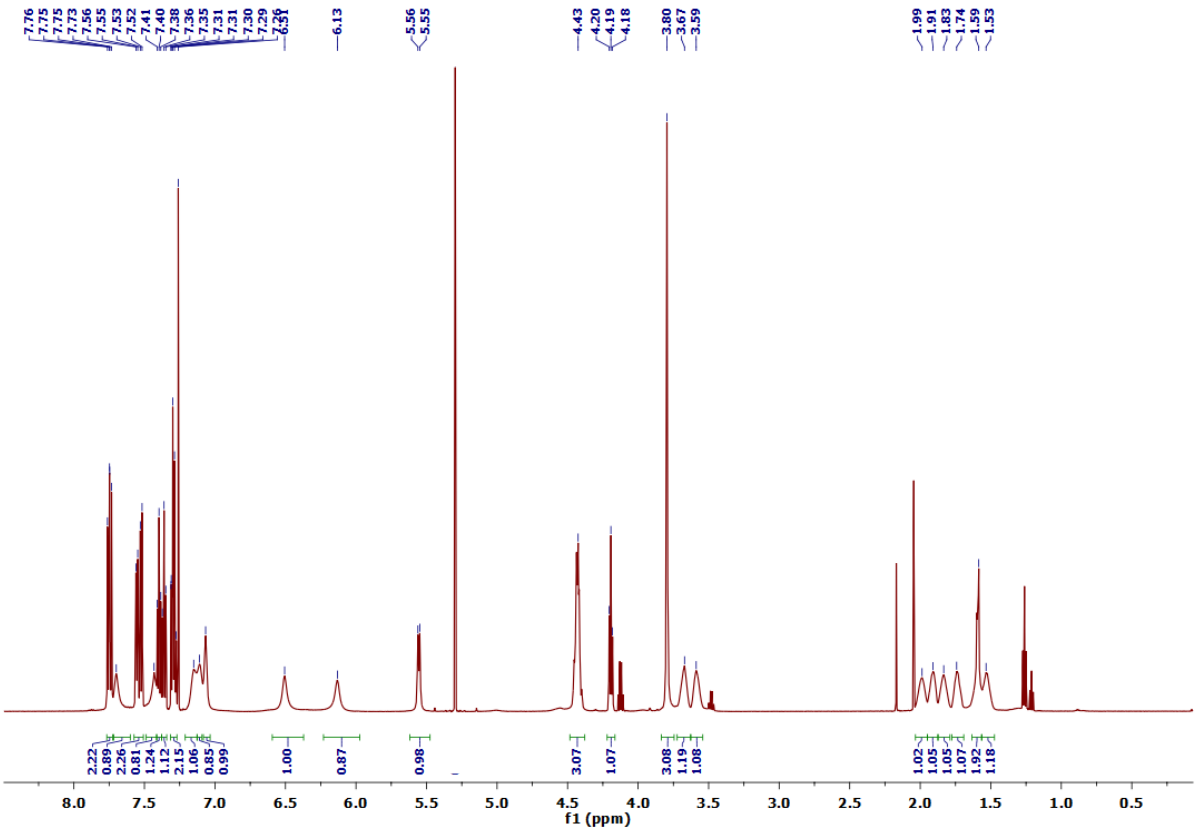

Figure S28. ^1H NMR spectrum of **7a** ($CDCl_3$, 300K, 600 MHz).

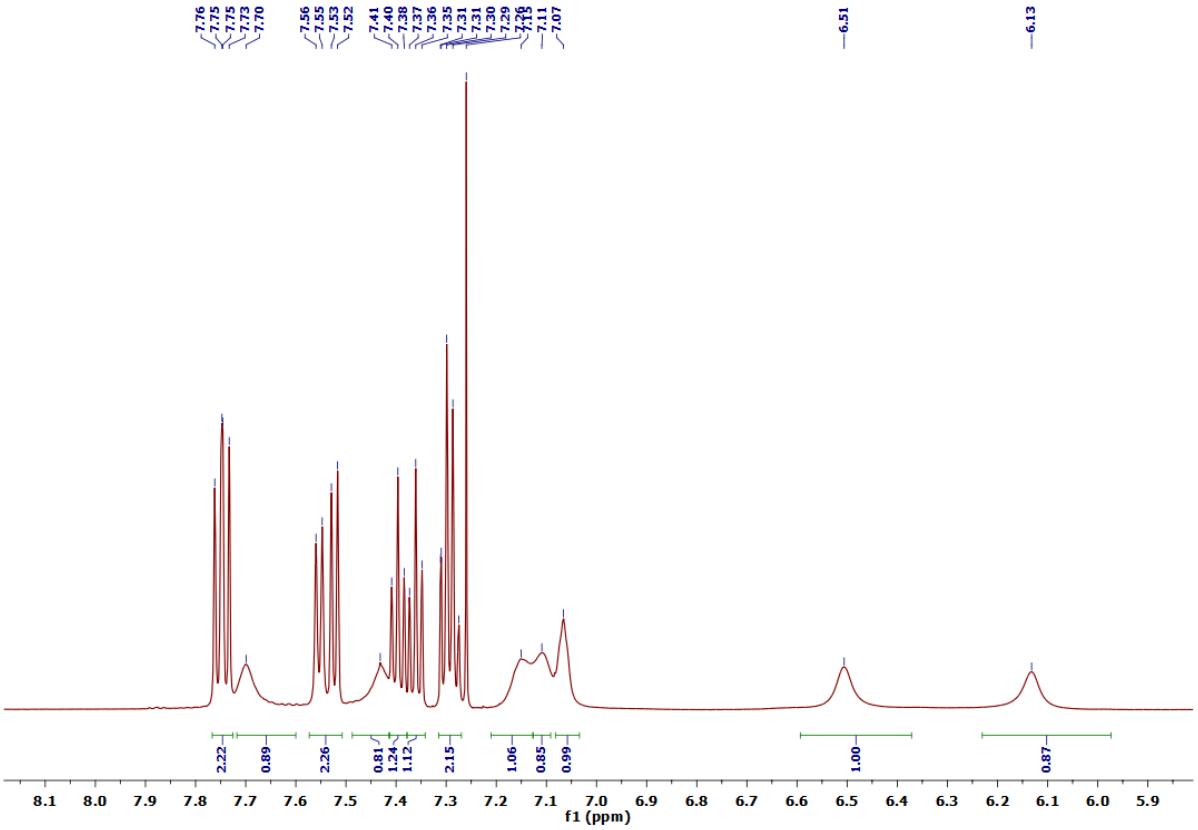

Figure S29. ^{1}H NMR spectrum (zoom, aromatic region) of **7a** ($CDCl_3$, 300K, 600 MHz).

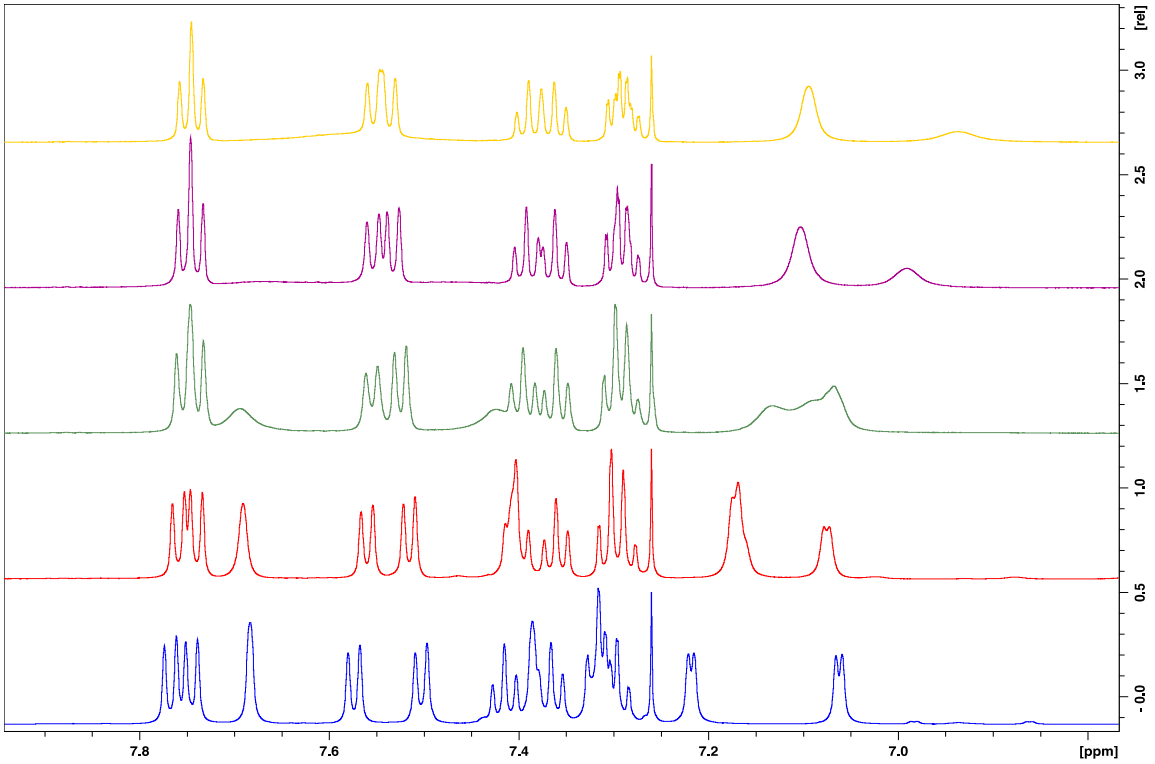

Figure S30. ^{1}H NMR spectrum (zoom, aromatic region) of **7a** (CDCl3, Blue: 250K, Red: 280K, Green: 300K, Violet: 315K, Yellow: 325K, 600 MHz).

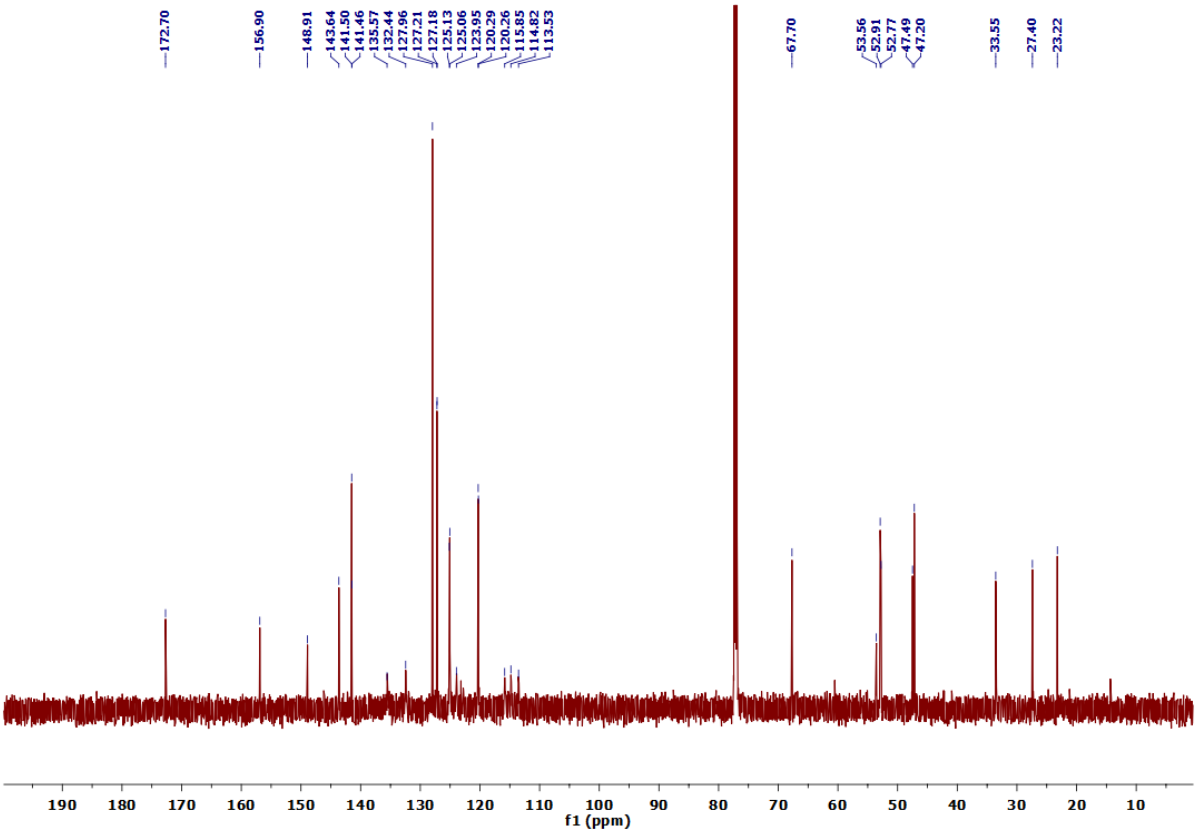

Figure S31. ^{13}C NMR spectrum of **7a** ($CDCl_3$, 300K, 150 MHz).

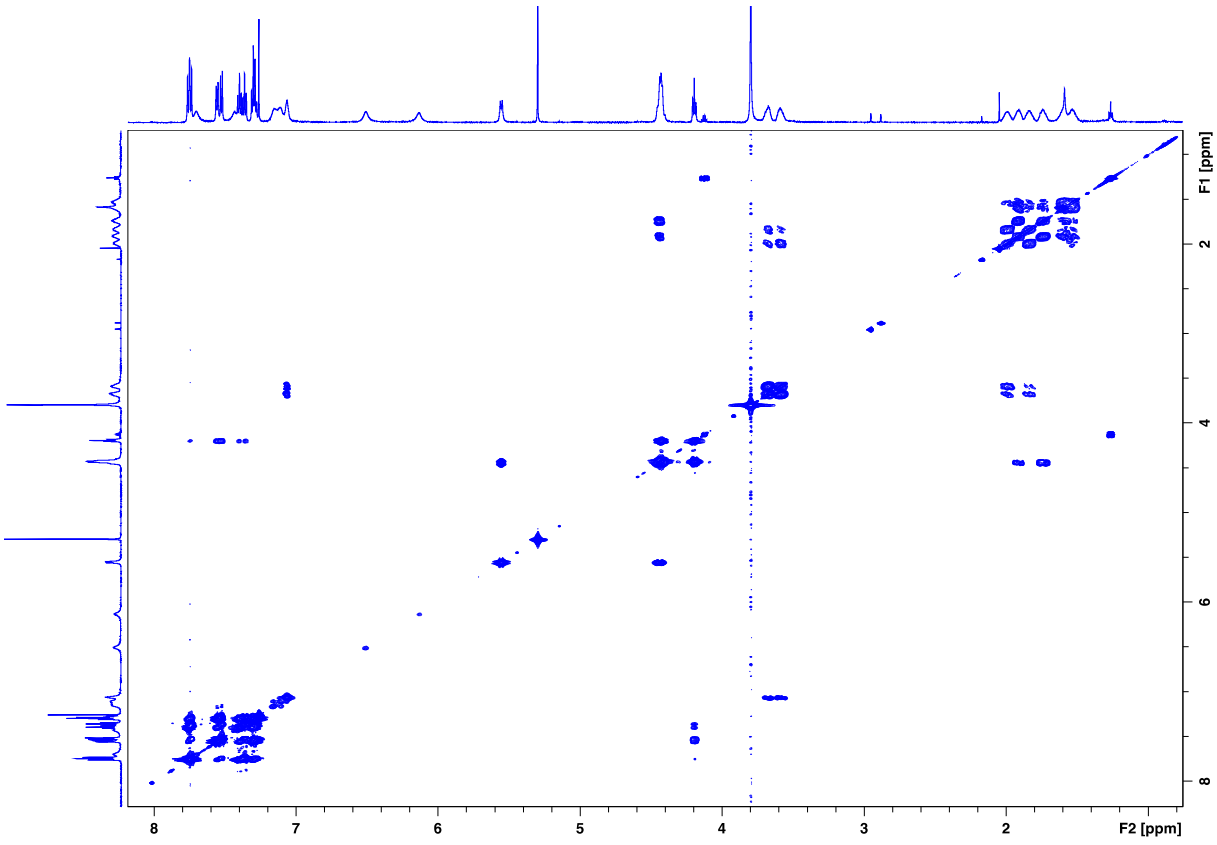

Figure S32. COSY NMR spectrum of **7a** ($CDCl_3$, 300K, 600 MHz).

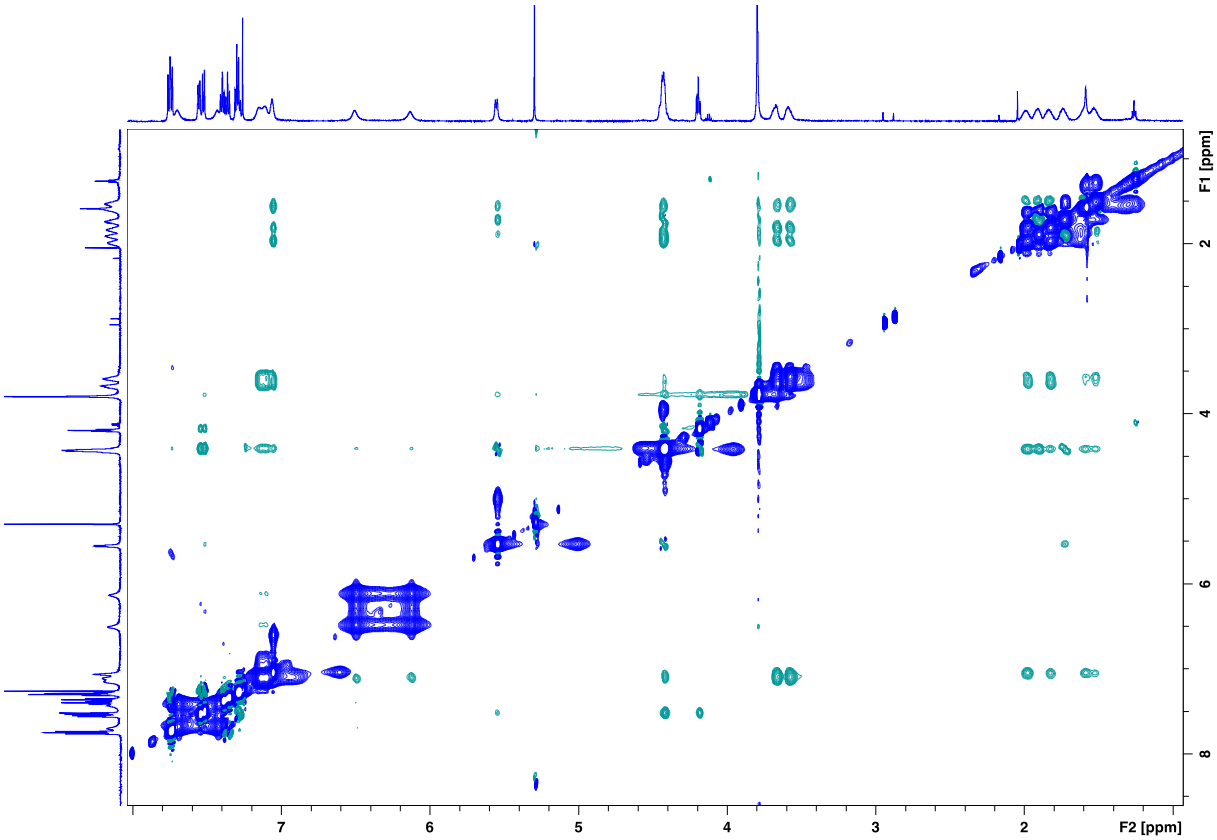

Figure S33. NOESY NMR spectrum of **7a** ($CDCl_3$, 300K, 600 MHz).

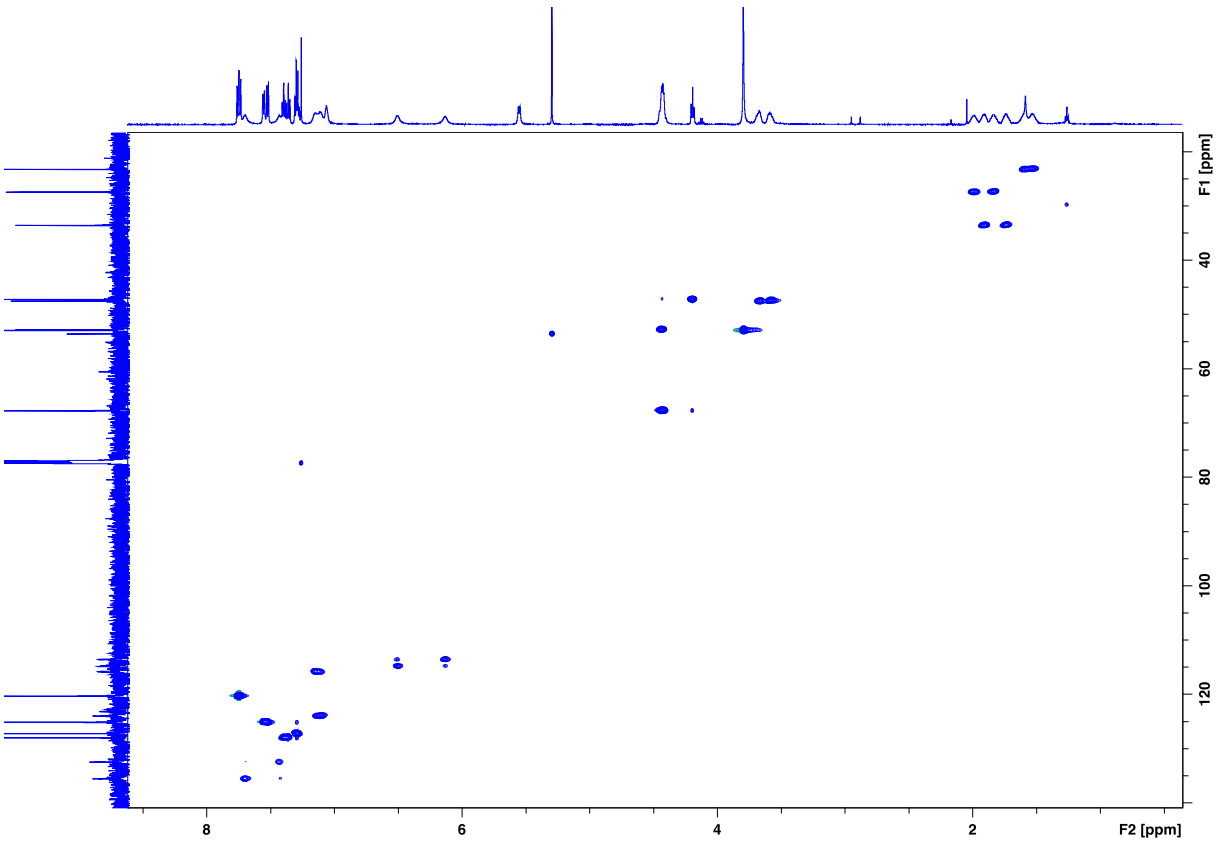

Figure S34. HSQC NMR spectrum of **7a** ($CDCl_3$, 300K, 600, 150 MHz).

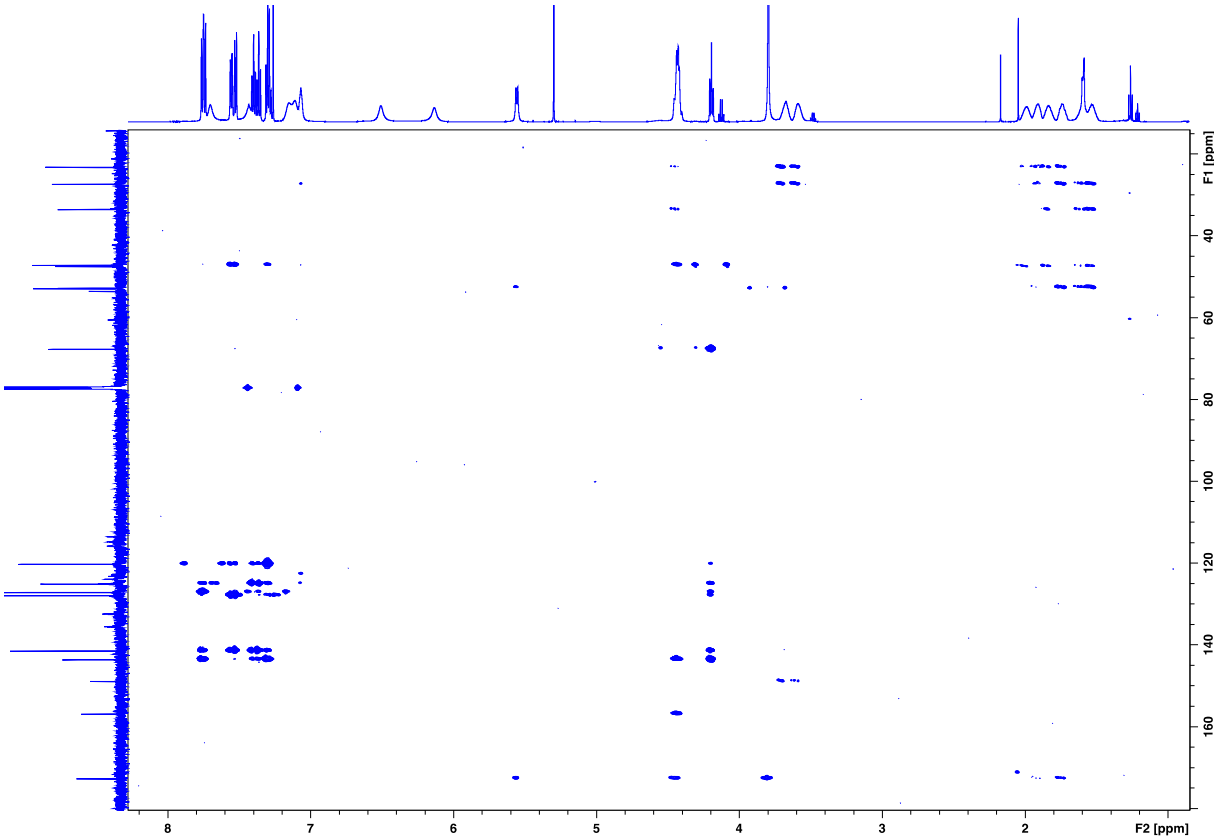

Figure S35. HMBC NMR spectrum of **7a** ($CDCl_3$, 300K, 600, 150 MHz).

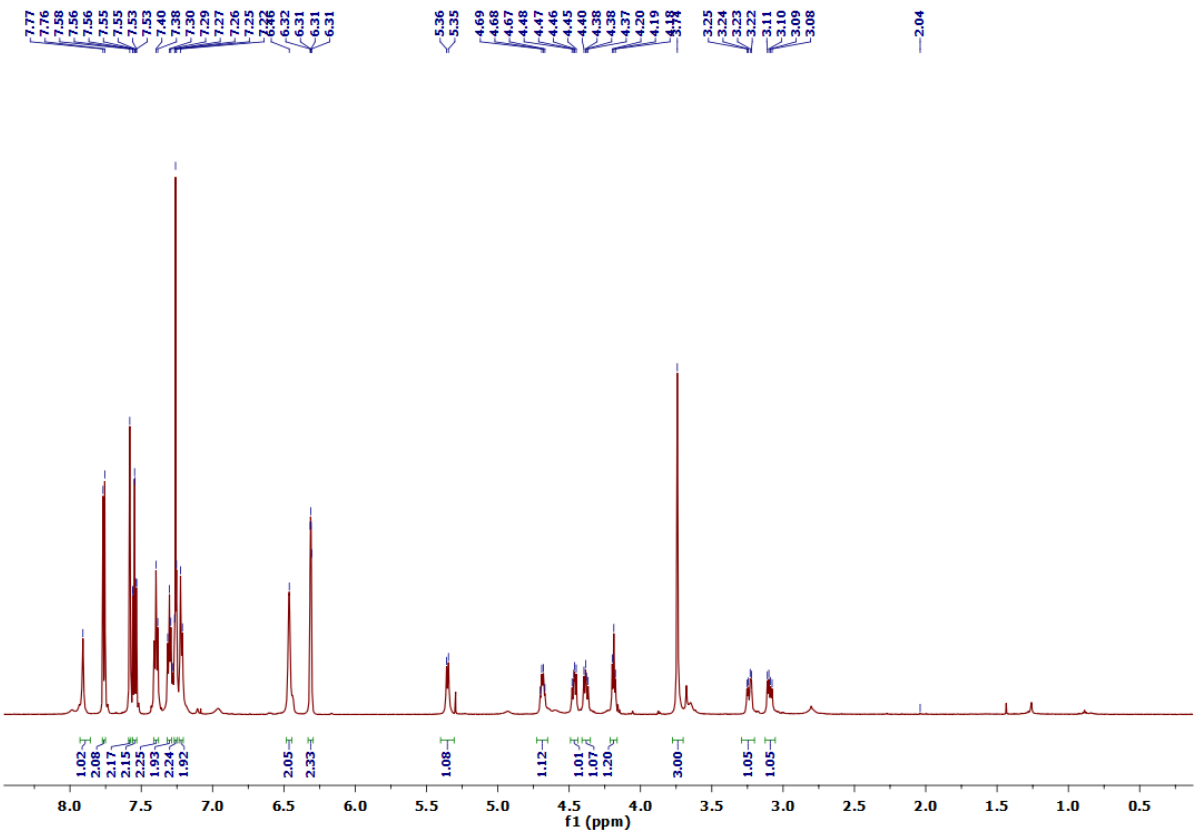

Figure S36. ^1H NMR spectrum of **7b** ($CDCl_3$, 300K, 600 MHz).

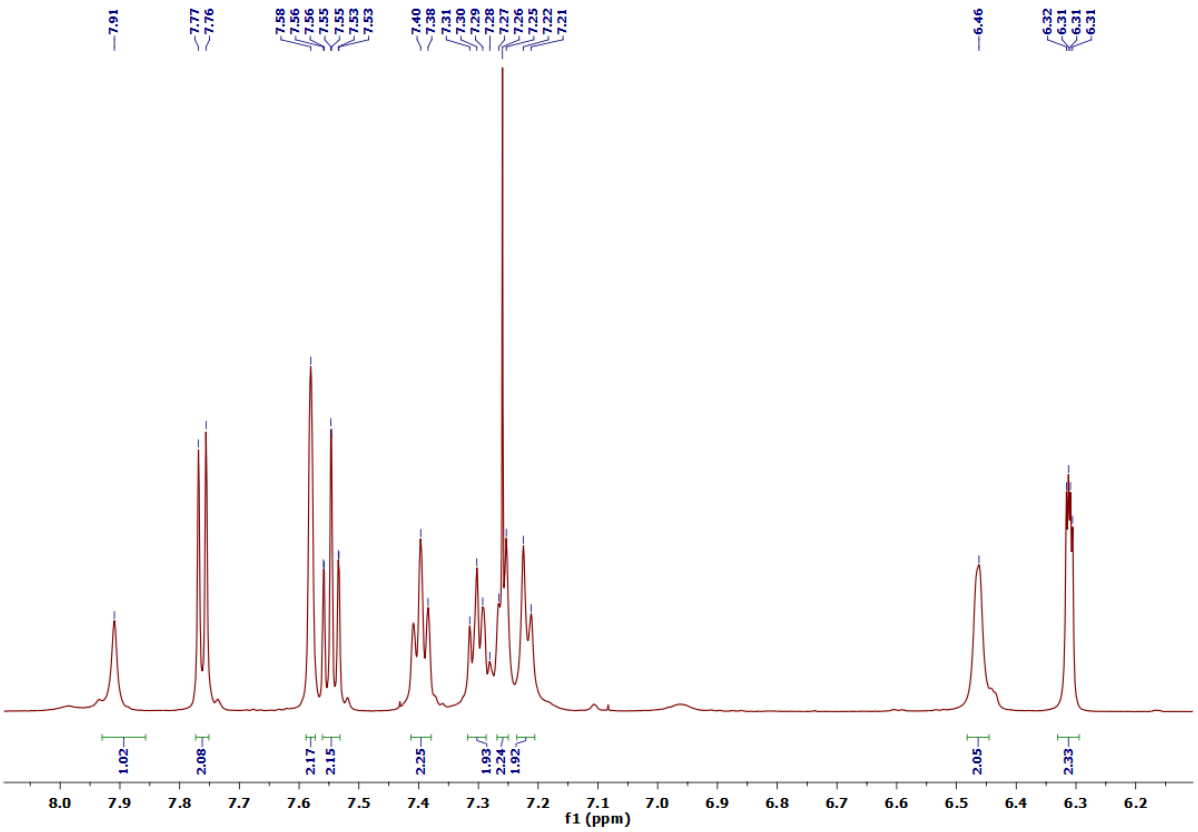

Figure S37. ^{1}H NMR spectrum (zoom, aromatic region) of **7b** ($CDCl_3$, 300K, 600 MHz).

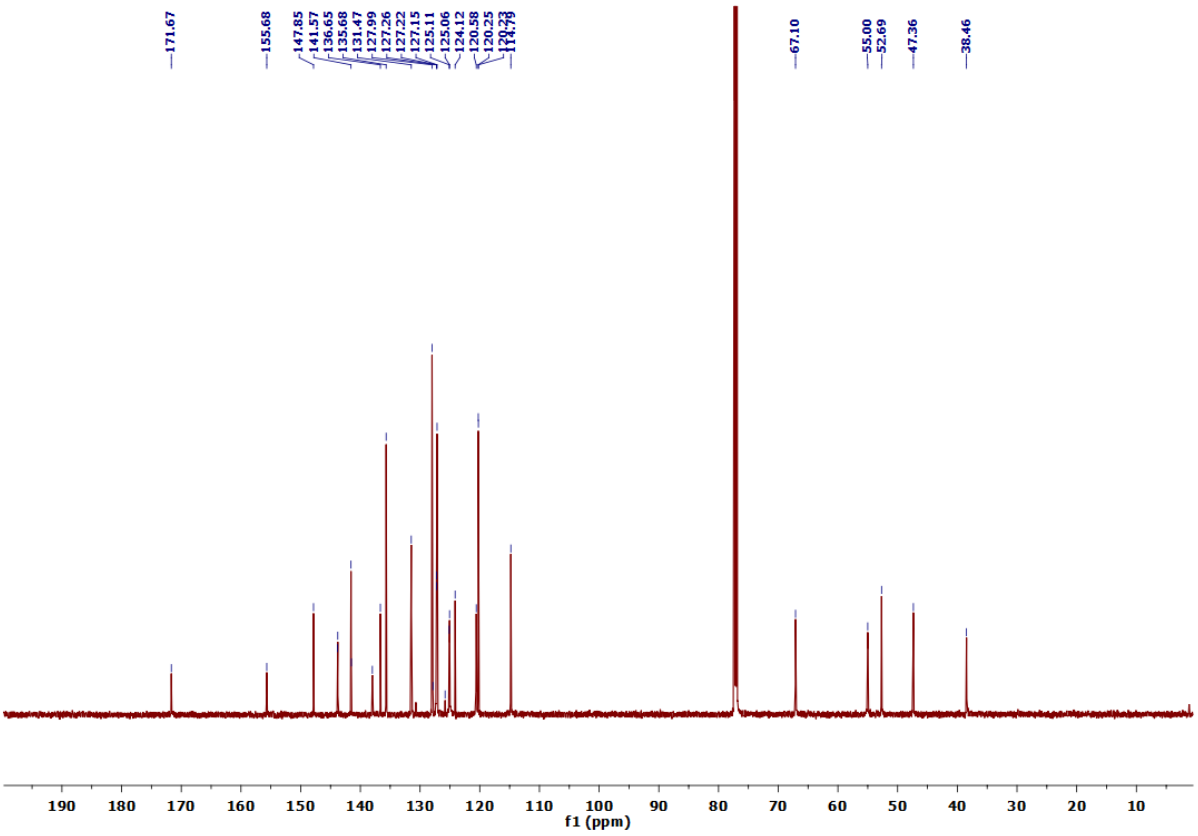

Figure S38. ^{13}C NMR spectrum of **7b** ($CDCl_3$, 300K, 150 MHz).

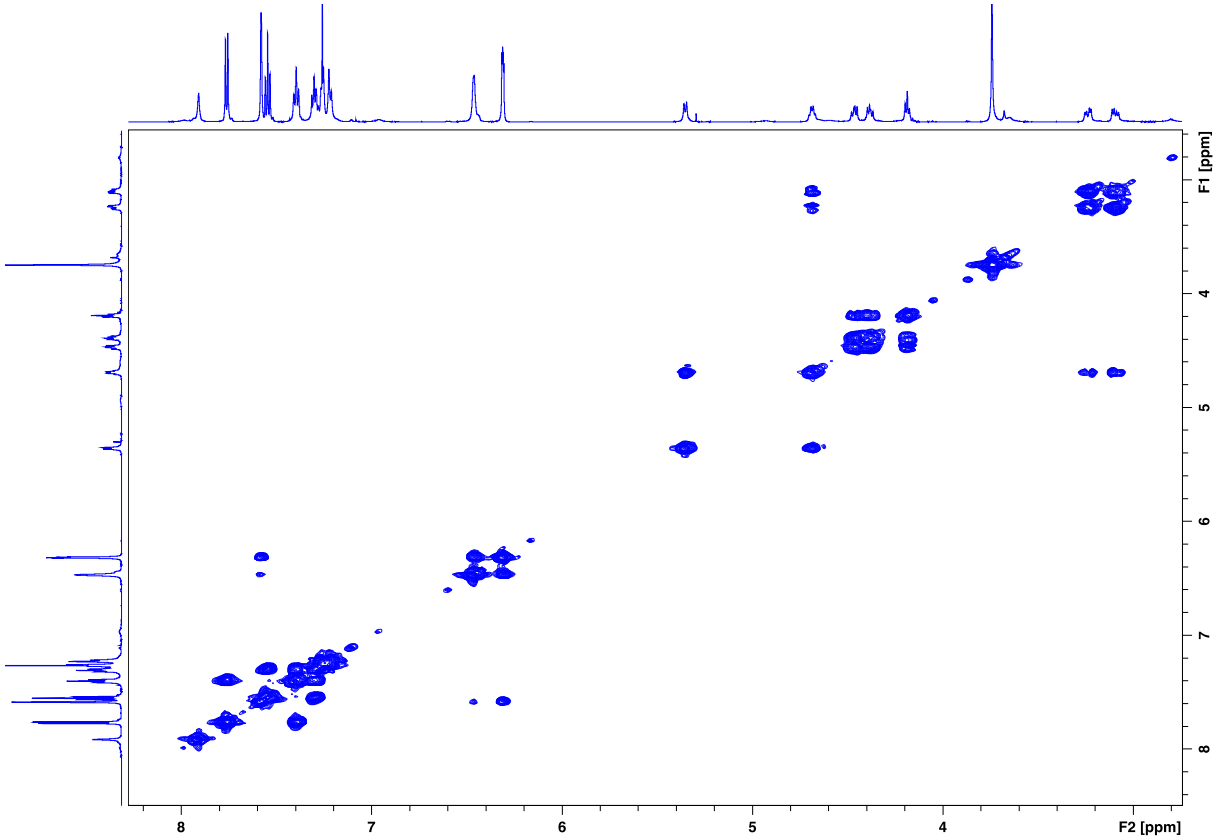

Figure S39. COSY NMR spectrum of **7b** ($CDCl_3$, 300K, 600 MHz).

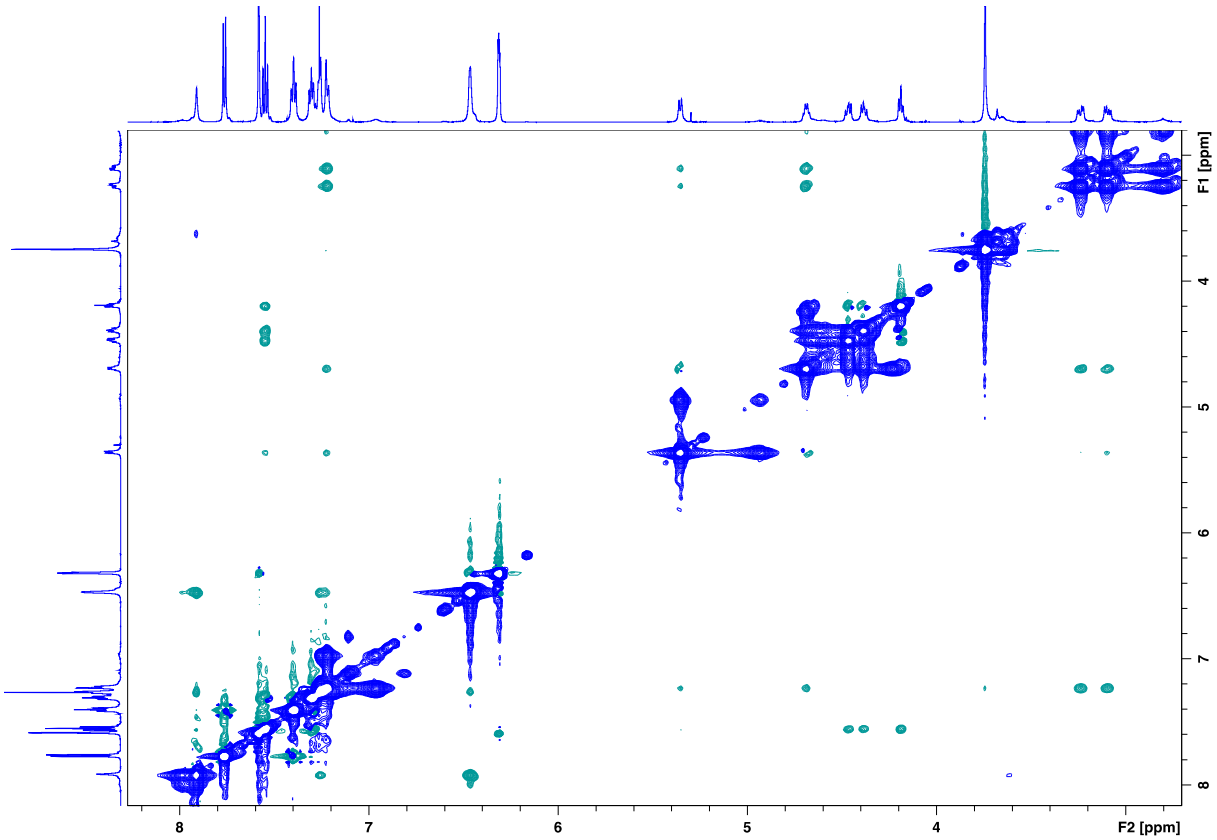

Figure S40. NOESY NMR spectrum of **7b** ($CDCl_3$, 300K, 600 MHz).

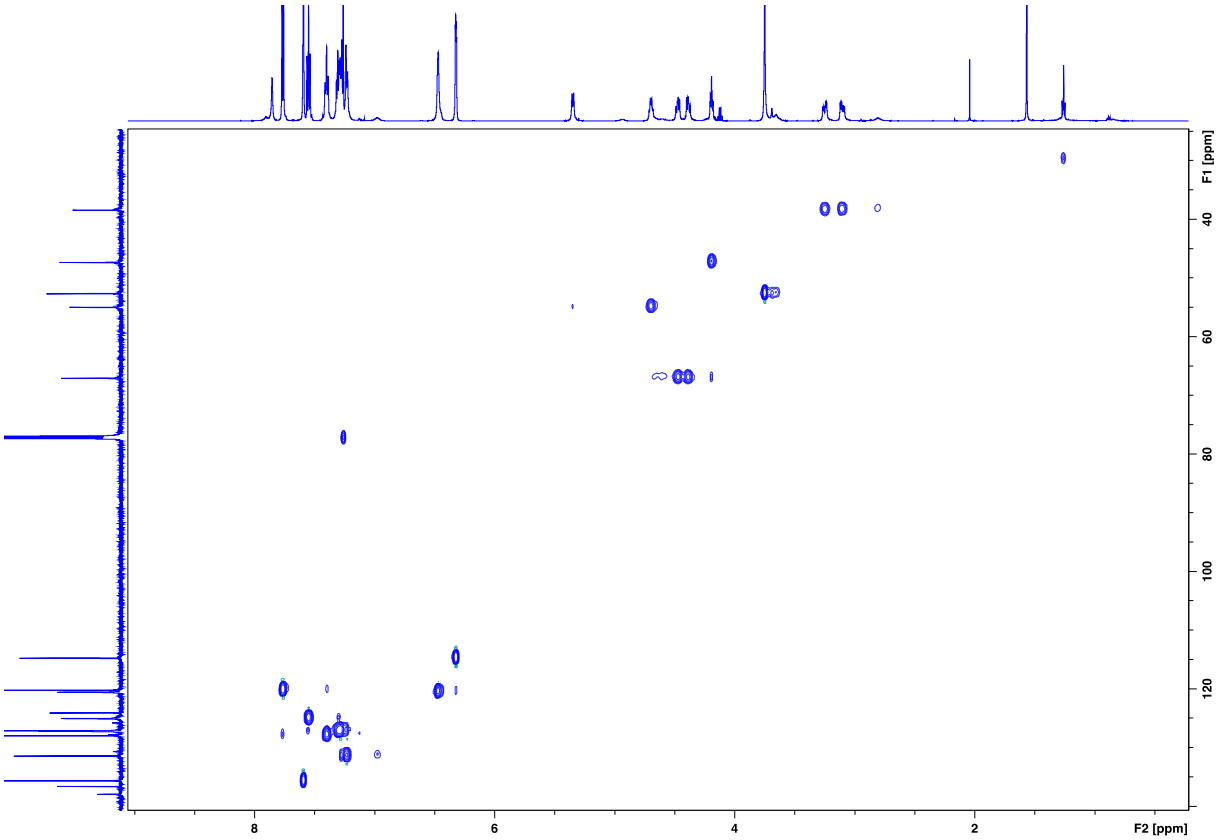

Figure S41. HSQC NMR spectrum of **7b** ($CDCl_3$, 300K, 600, 150 MHz).

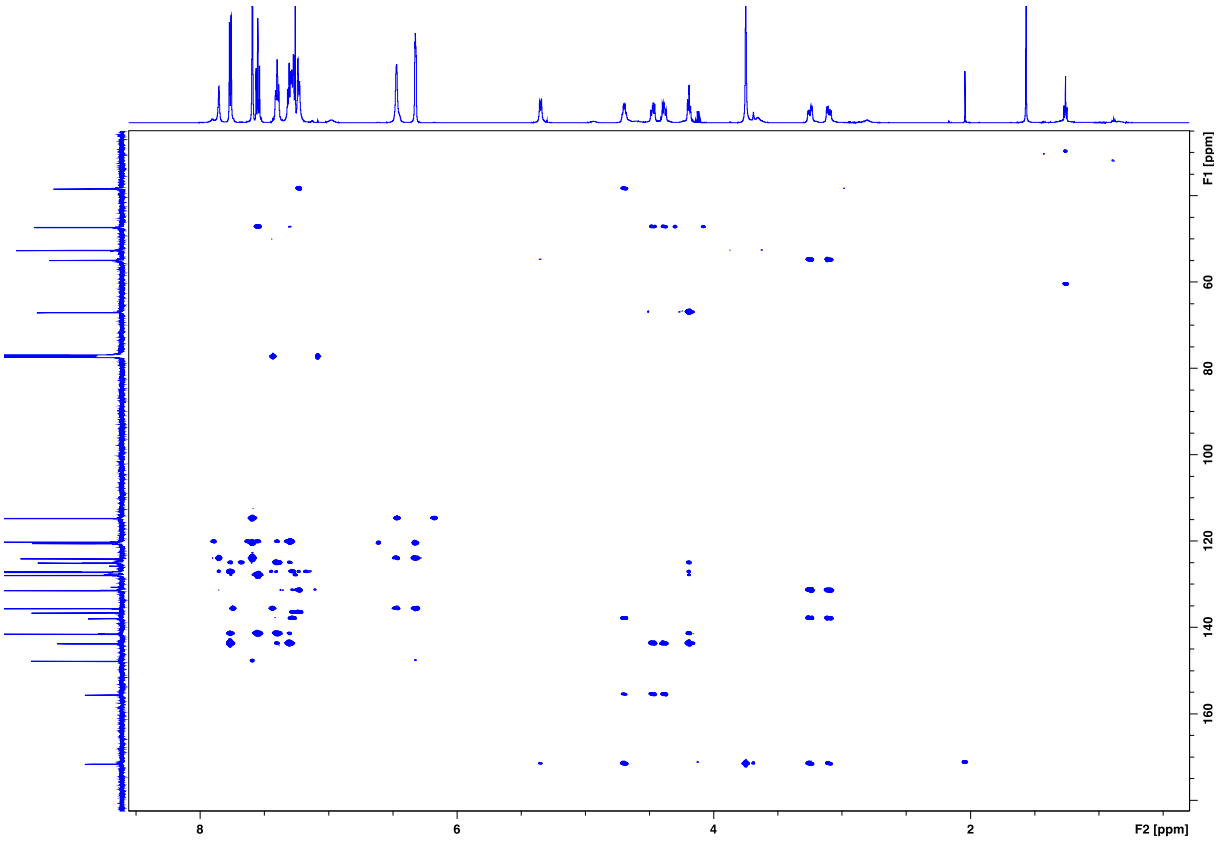

Figure S42. HMBC NMR spectrum of **7b** ($CDCl_3$, 300K, 600, 150 MHz).

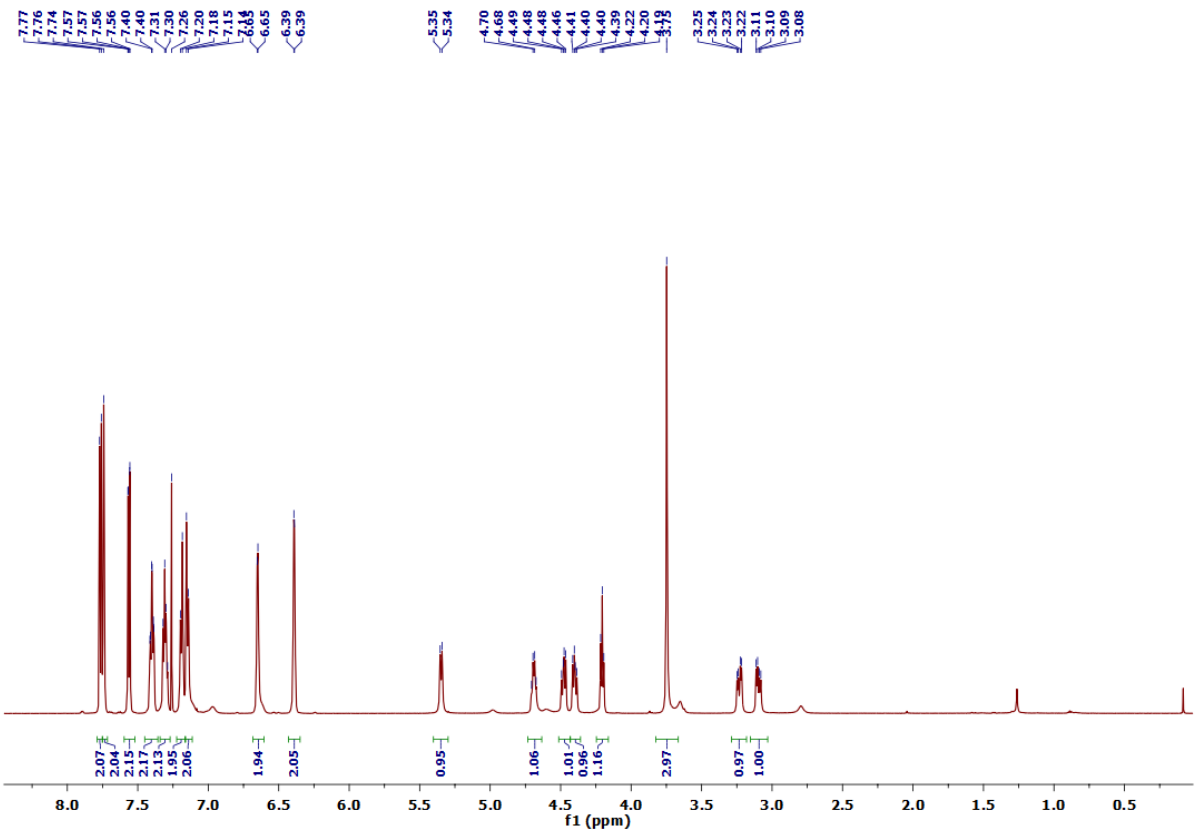

Figure S43. ^{1}H NMR spectrum of **7c** ($CDCl_3$, 300K, 600 MHz).

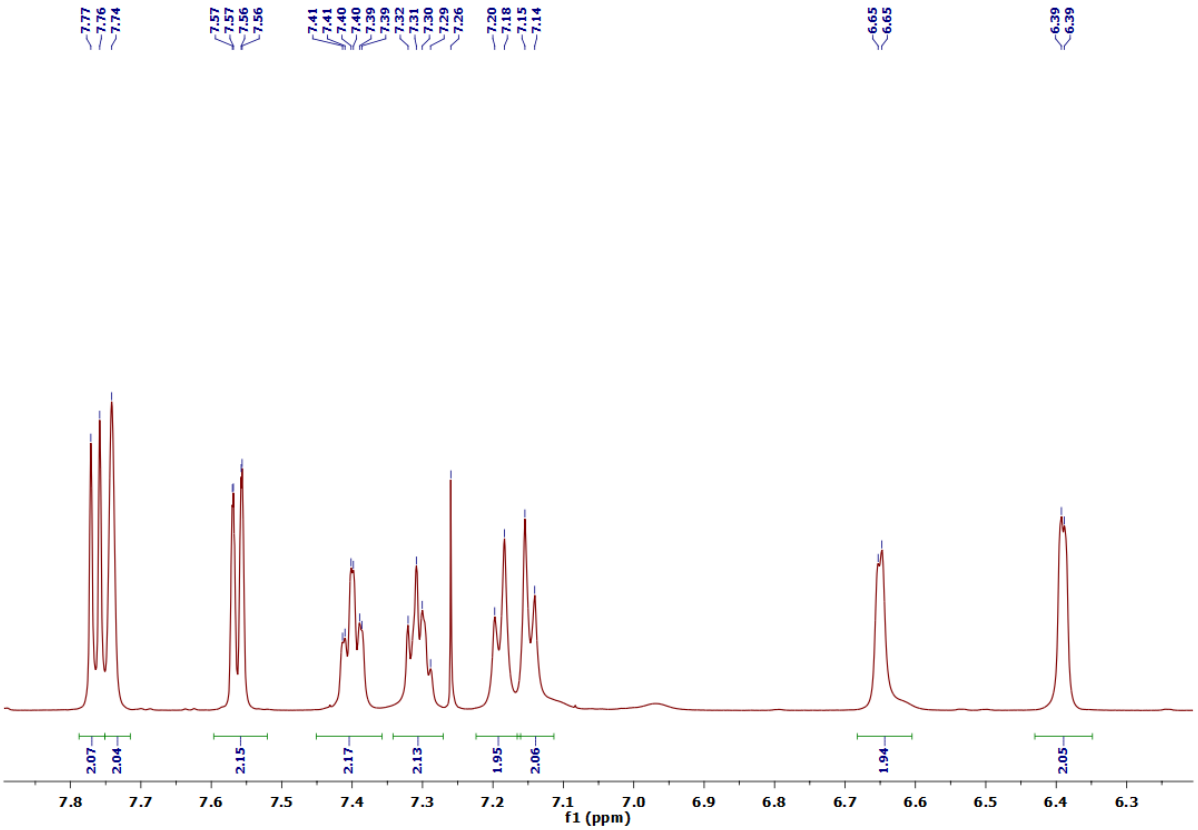

Figure S44. ^{1}H NMR spectrum (zoom, aromatic region) of **7c** ($CDCl_3$, 300K, 600 MHz).

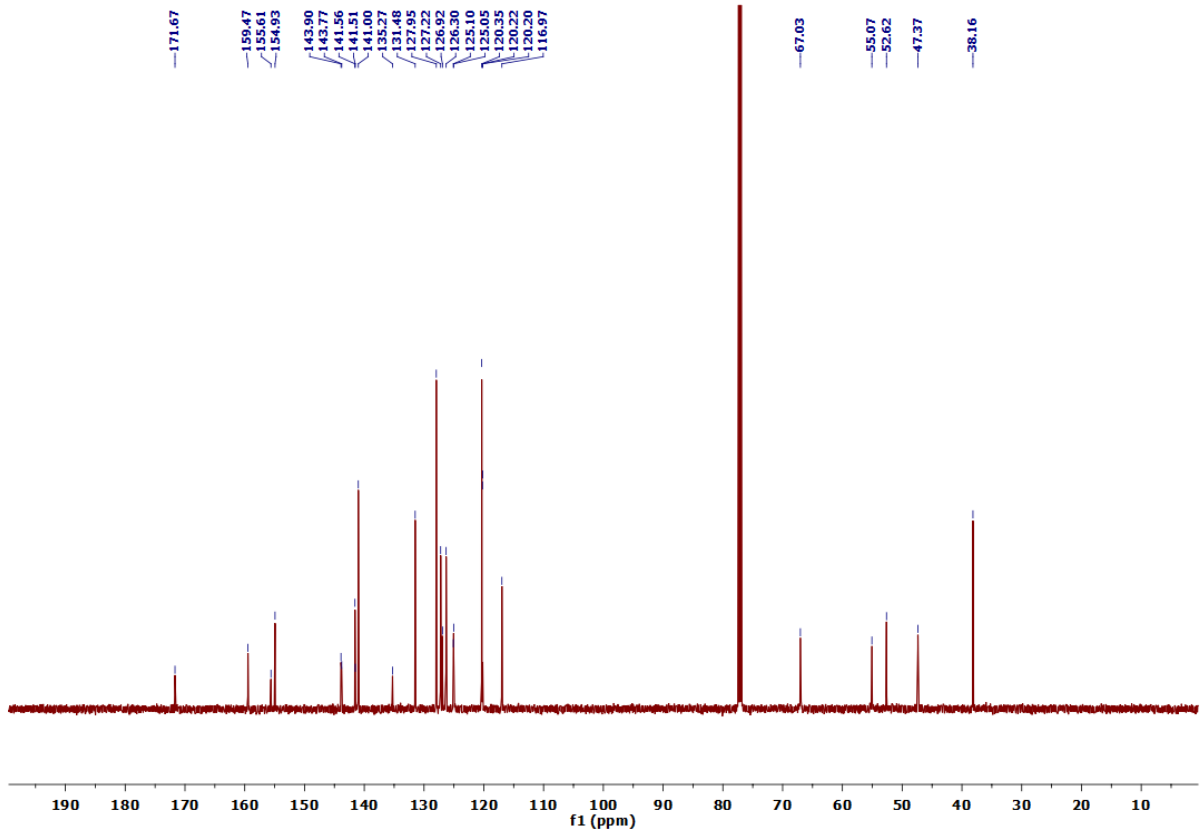

Figure S45. ^{13}C NMR spectrum of **7c** ($CDCl_3$, 300K, 150 MHz).

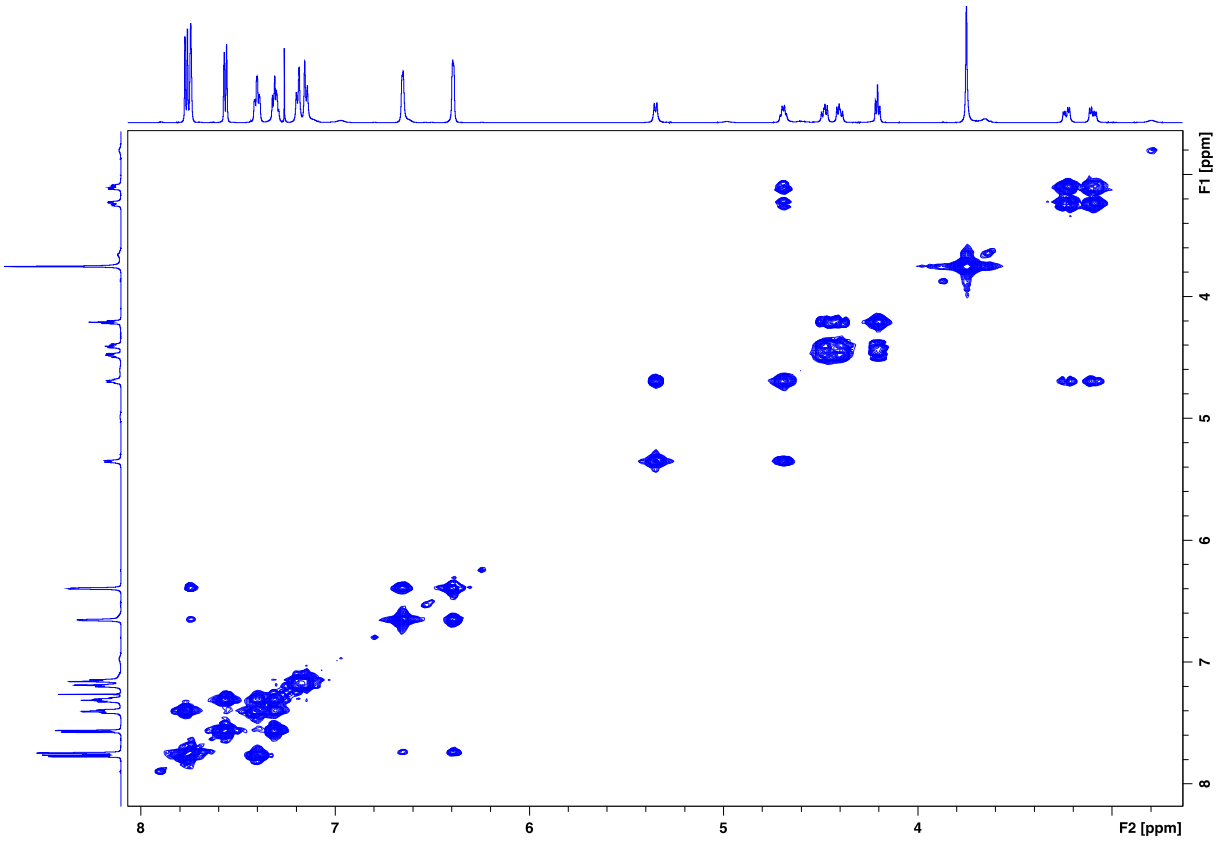

Figure S46. COSY NMR spectrum of **7c** ($CDCl_3$, 300K, 600 MHz).

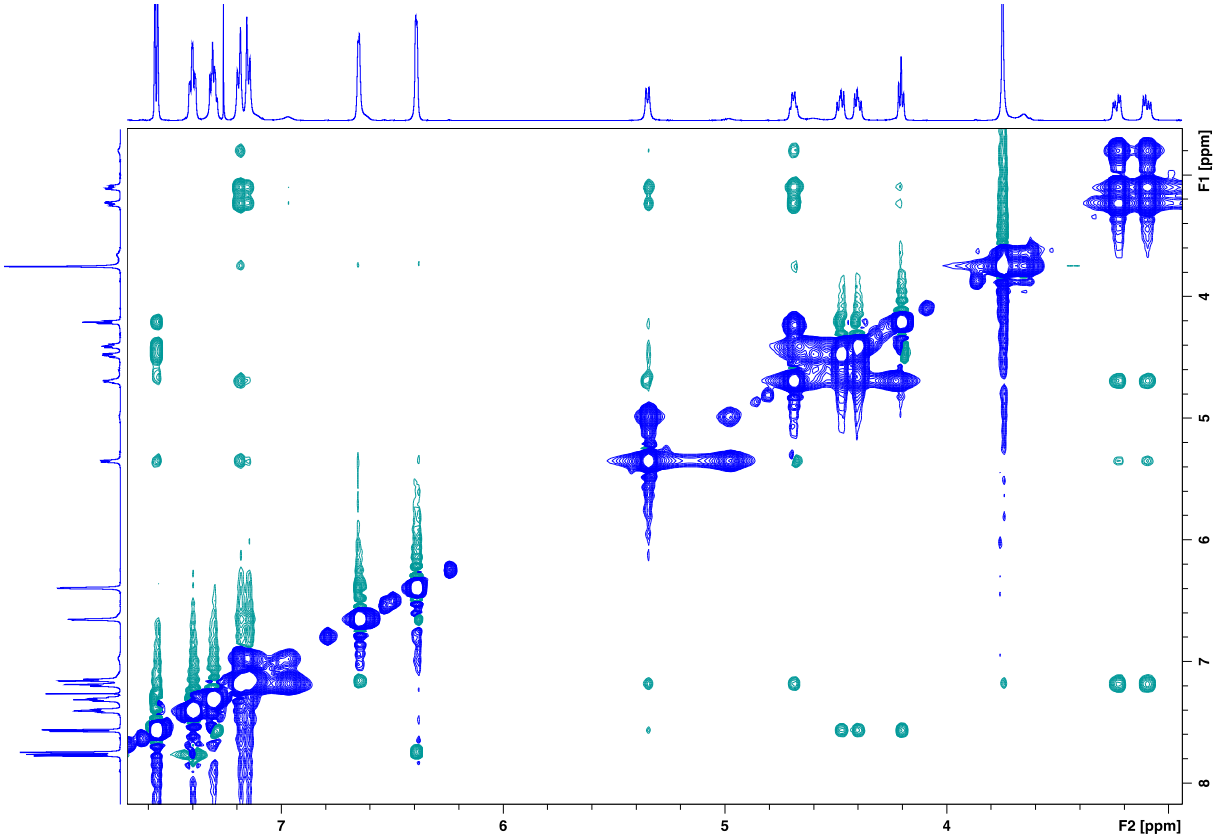

Figure S47. NOESY NMR spectrum of **7c** ($CDCl_3$, 300K, 600 MHz).

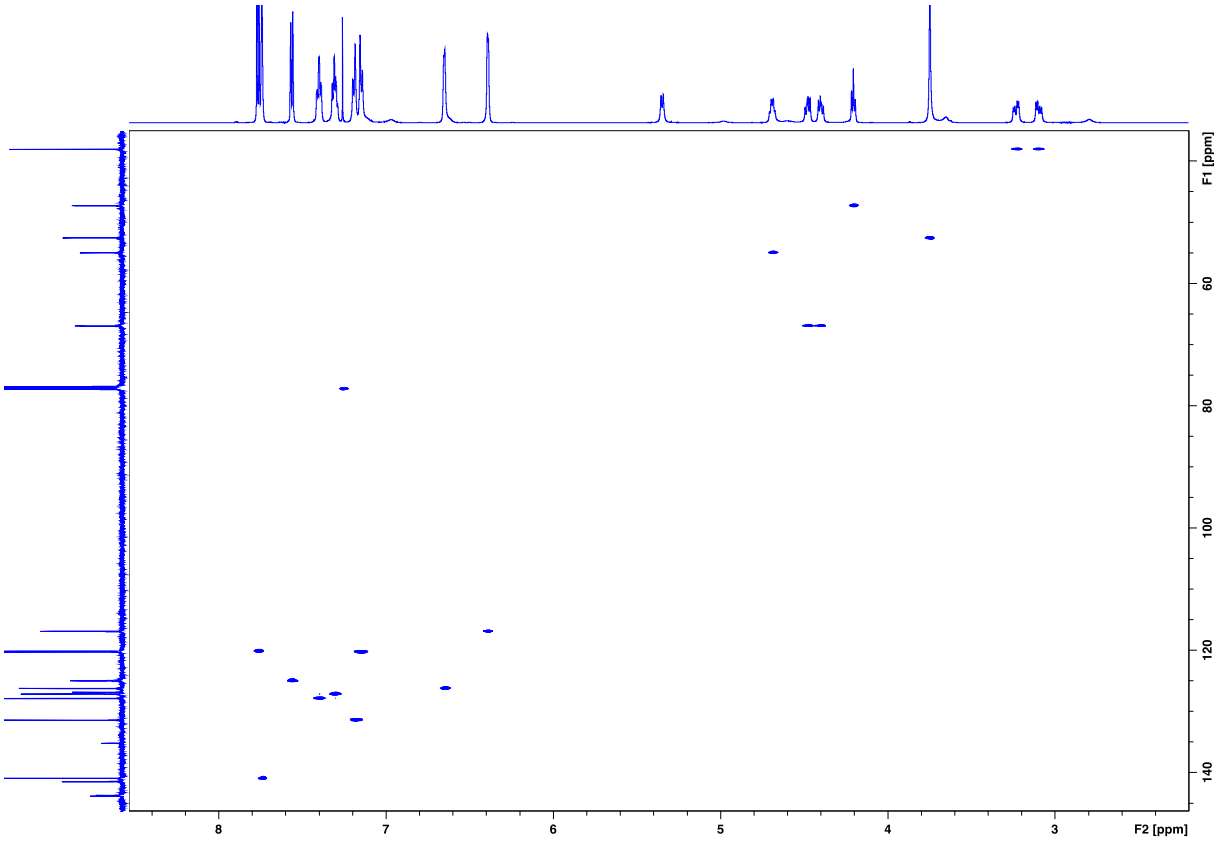

Figure S48. HSQC NMR spectrum of **7c** ($CDCl_3$, 300K, 600, 150 MHz).

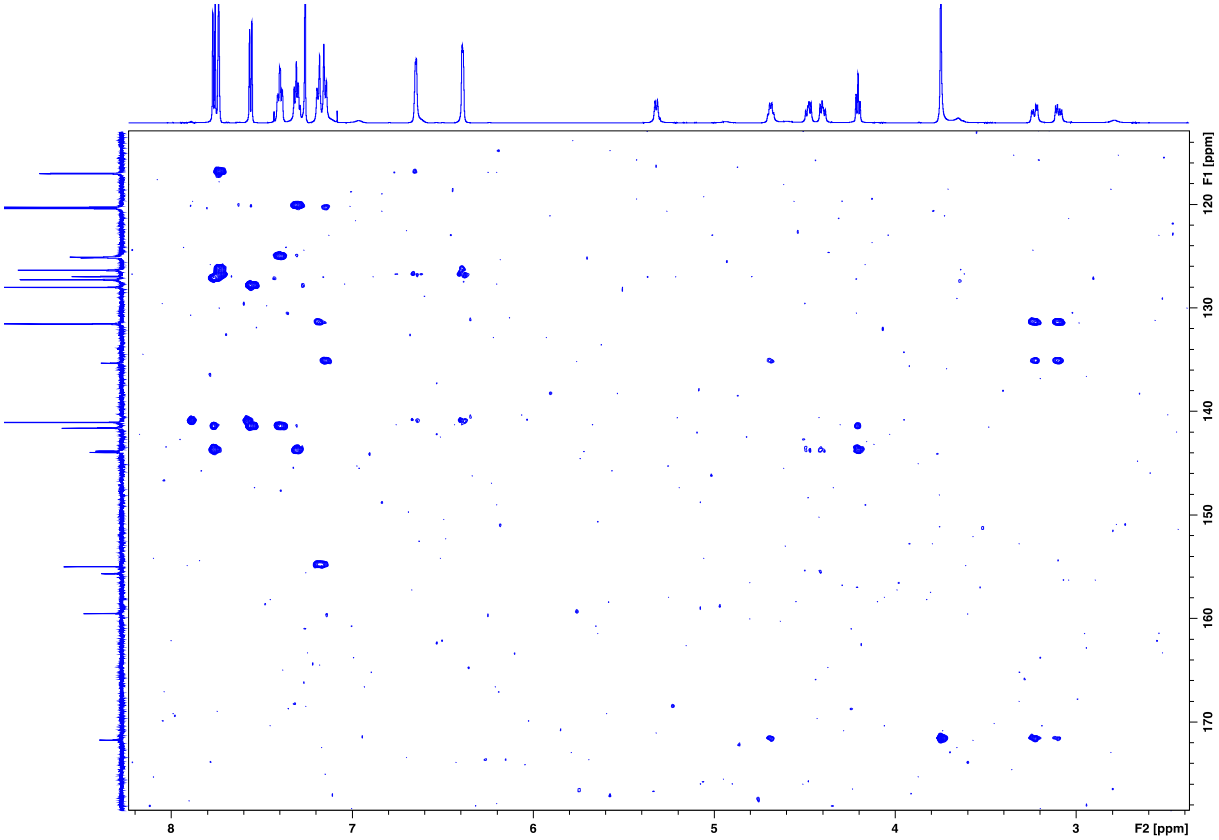

Figure S49. HMBC NMR spectrum of **7c** ($CDCl_3$, 300K, 600, 150 MHz).

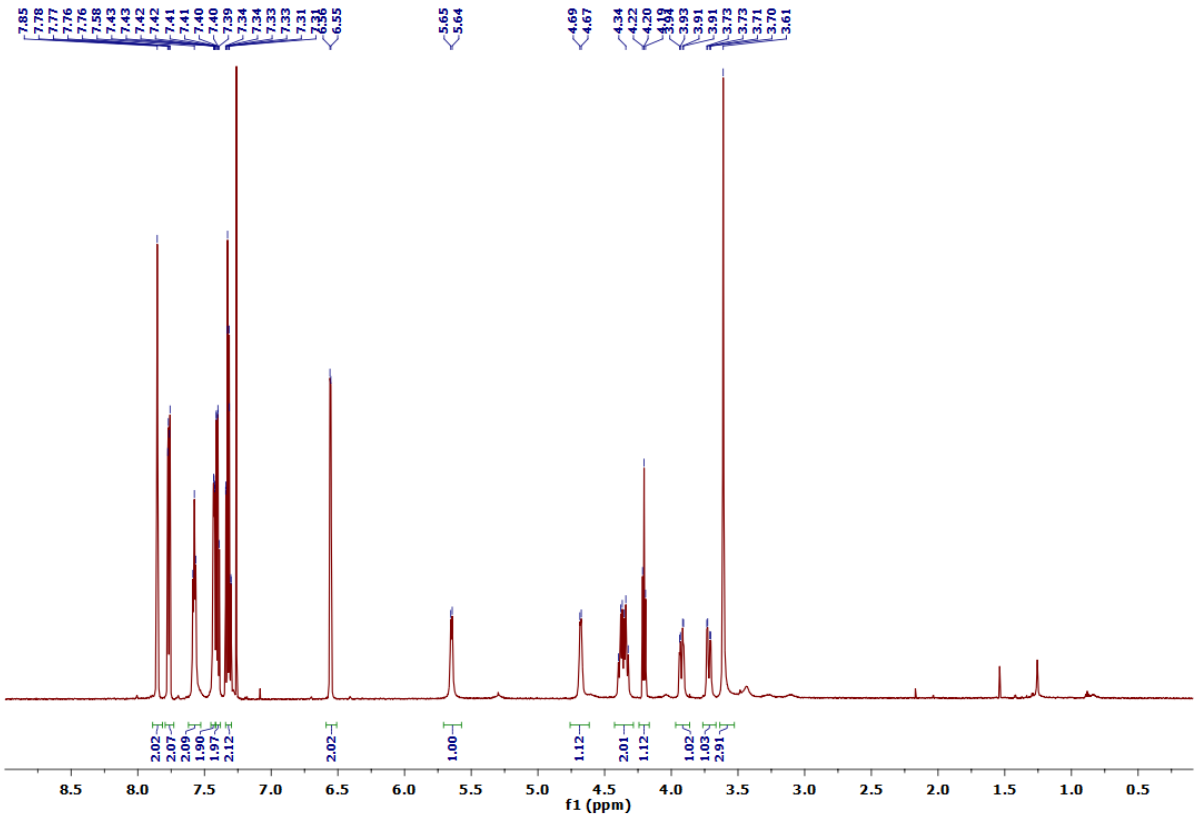

Figure S50. ^1H NMR spectrum of **7d** ($CDCl_3$, 300K, 600 MHz).

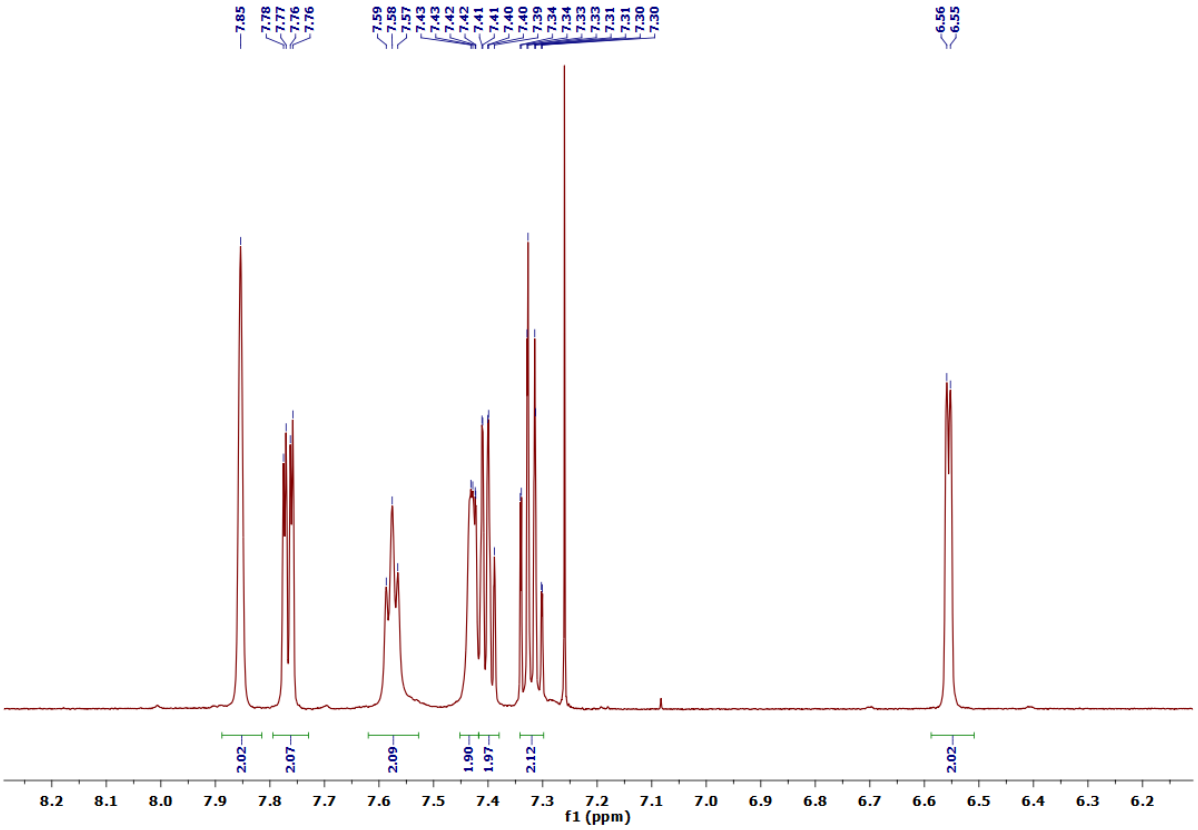

Figure S51. ^{1}H NMR spectrum (zoom, aromatic region) of **7d** ($CDCl_3$, 300K, 600 MHz).

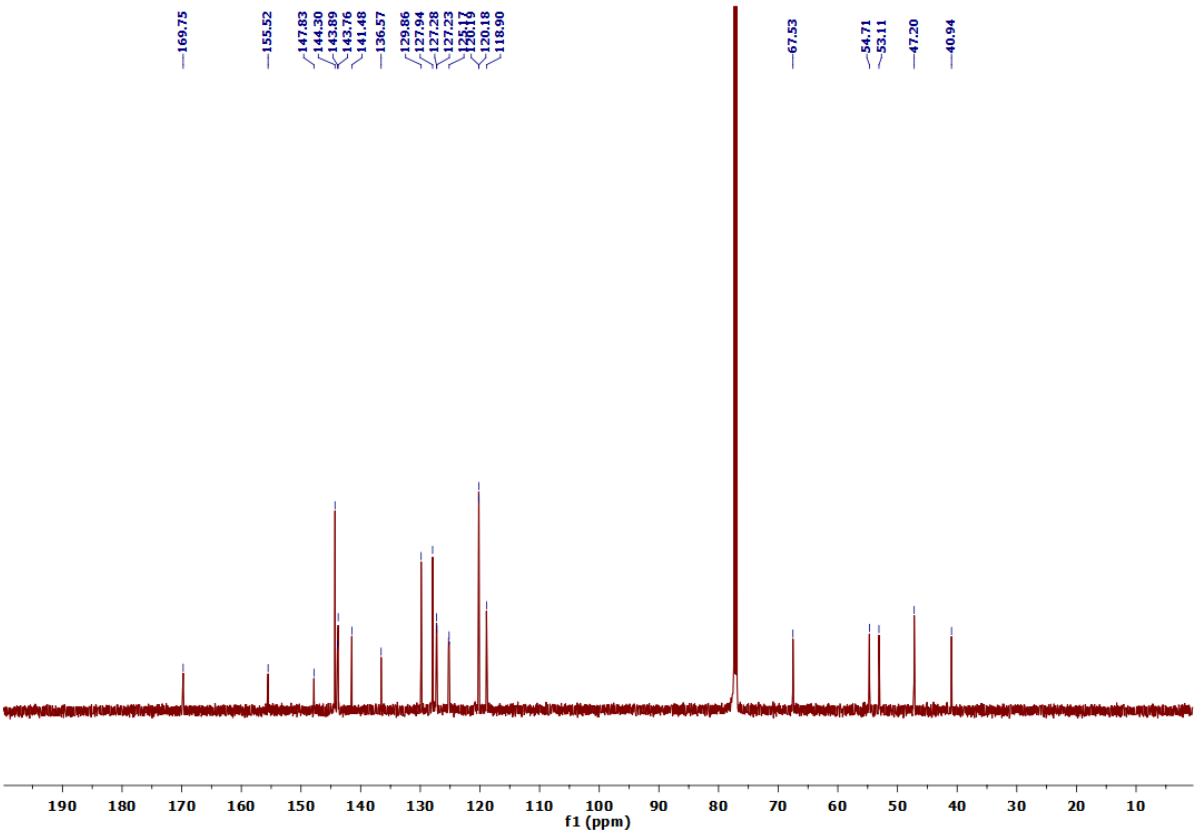

Figure S52. ^{13}C NMR spectrum of **7d** ($CDCl_3$, 300K, 150 MHz).

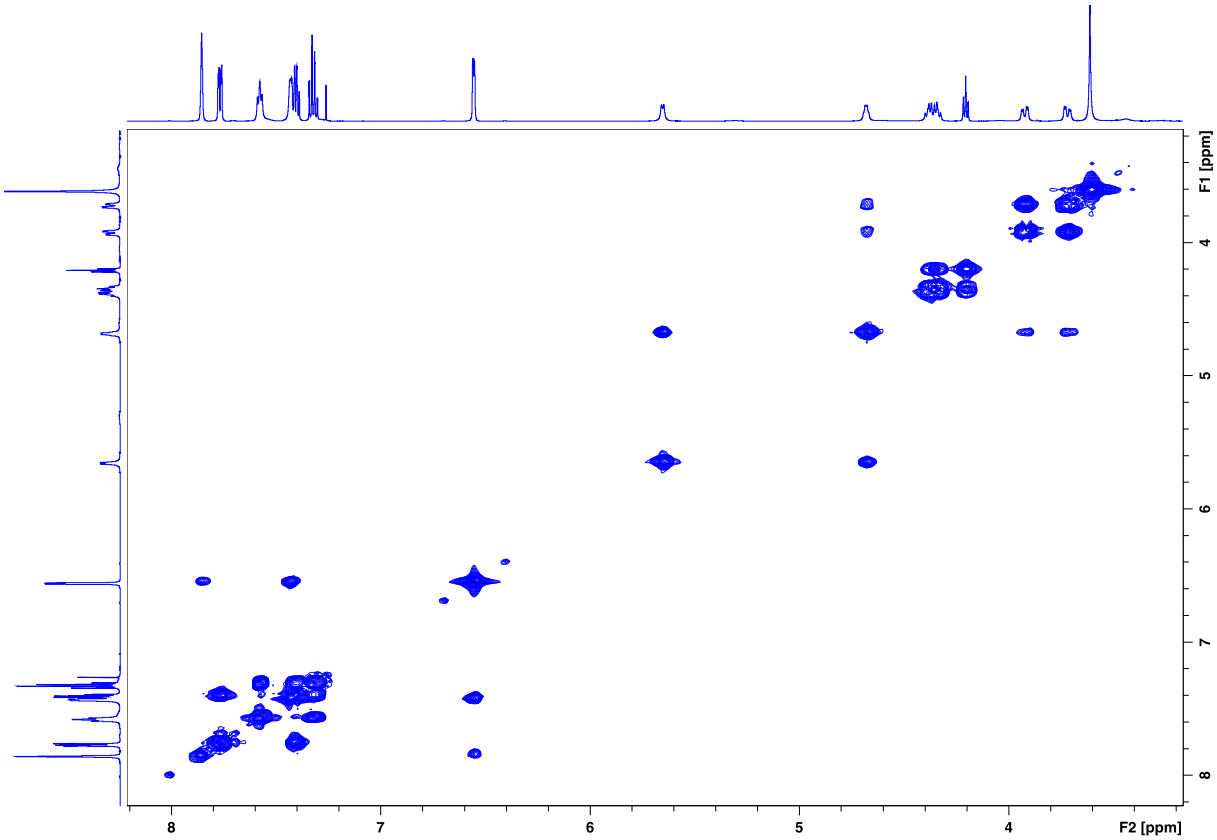

Figure S53. COSY NMR spectrum of **7d** ($CDCl_3$, 300K, 600 MHz).

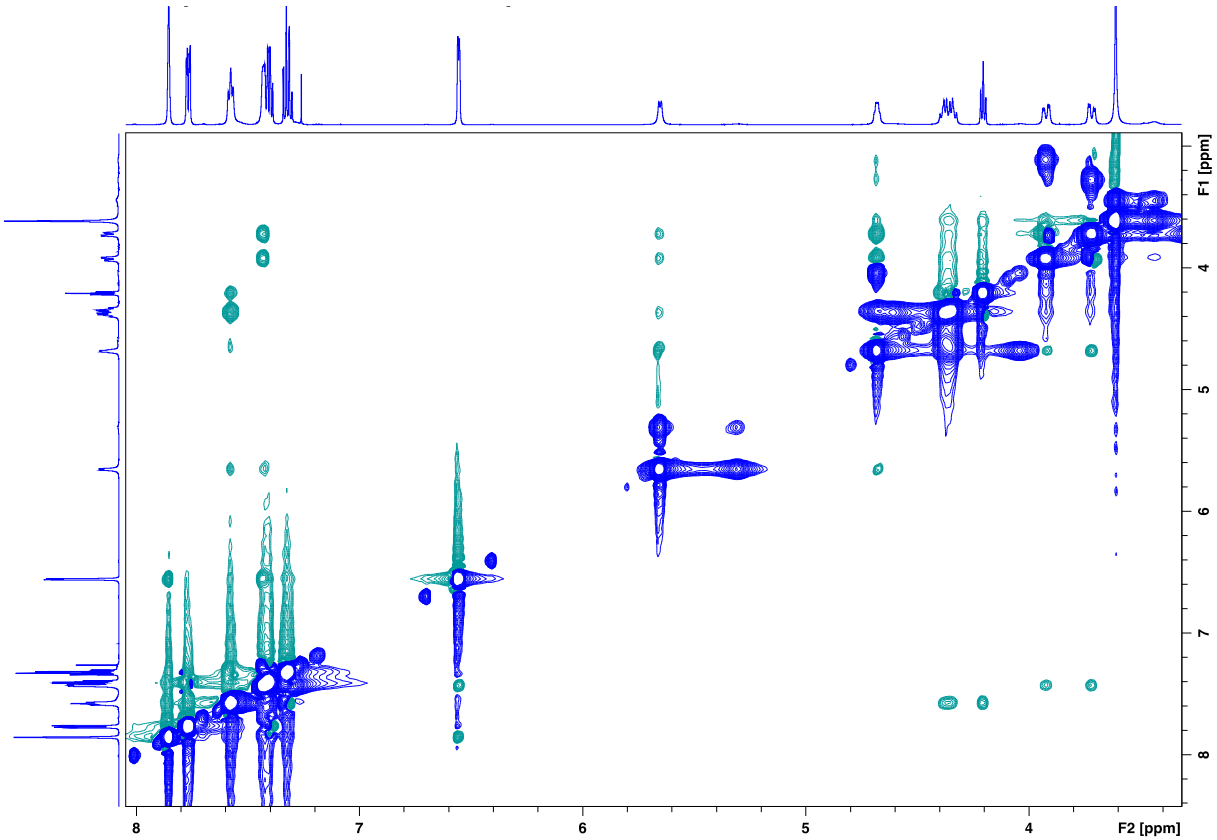

Figure S54. NOESY NMR spectrum of **7d** ($CDCl_3$, 300K, 600 MHz).

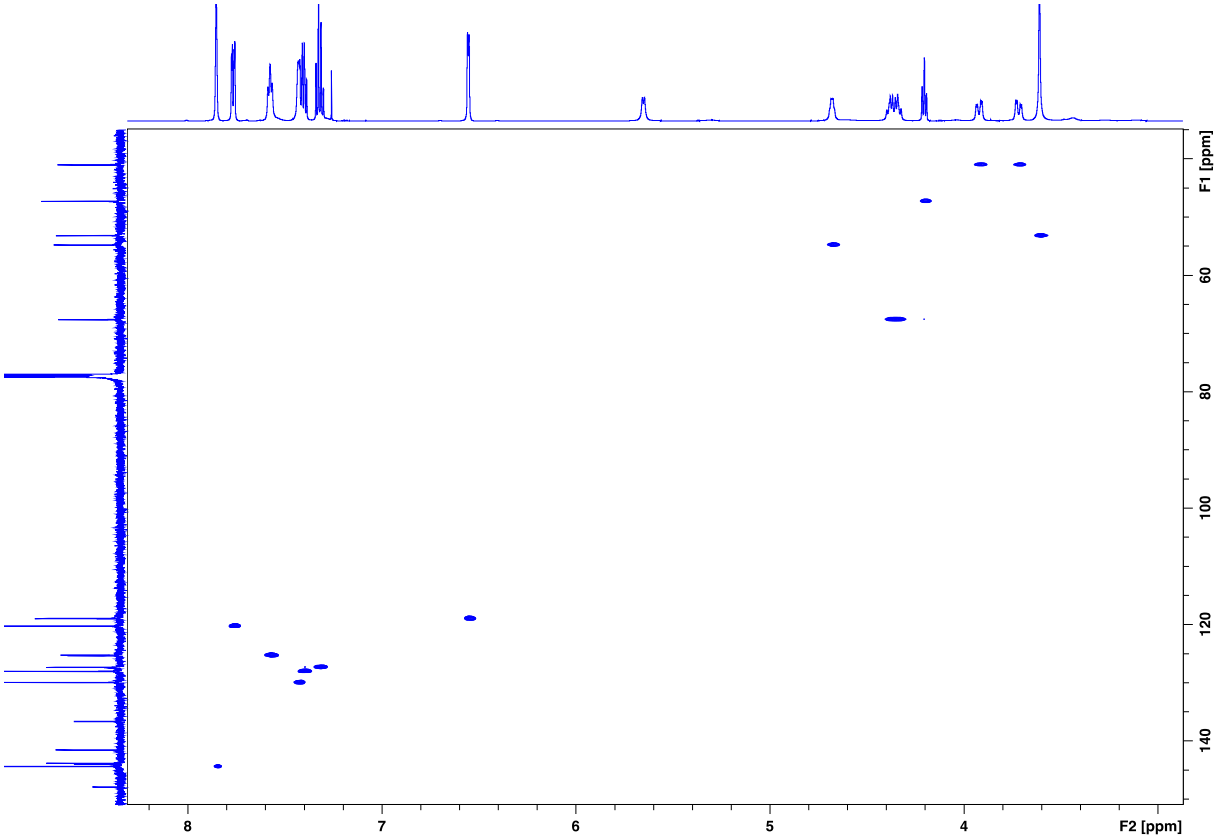

Figure S55. HSQC NMR spectrum of **7d** ($CDCl_3$, 300K, 600, 150 MHz).

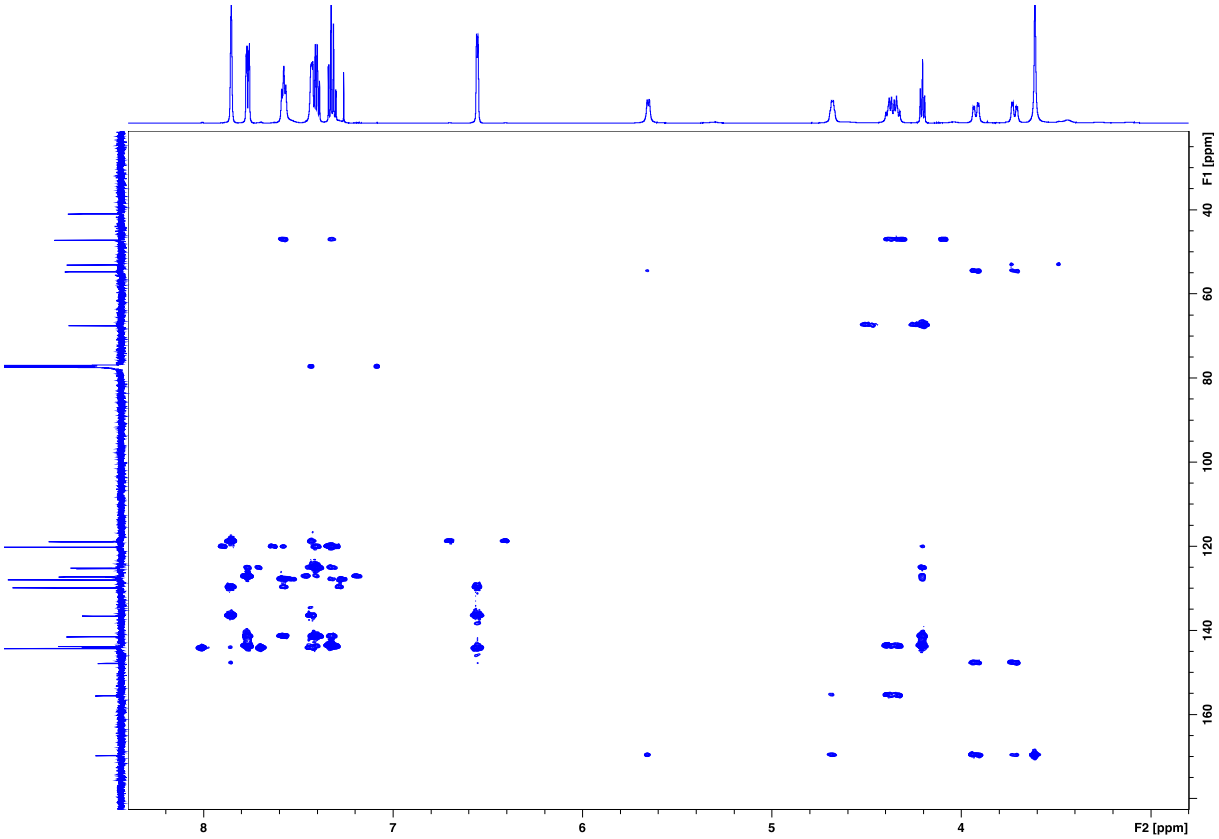

Figure S56. HMBC NMR spectrum of **7d** ($CDCl_3$, 300K, 600, 150 MHz).

4. Mass spectra.

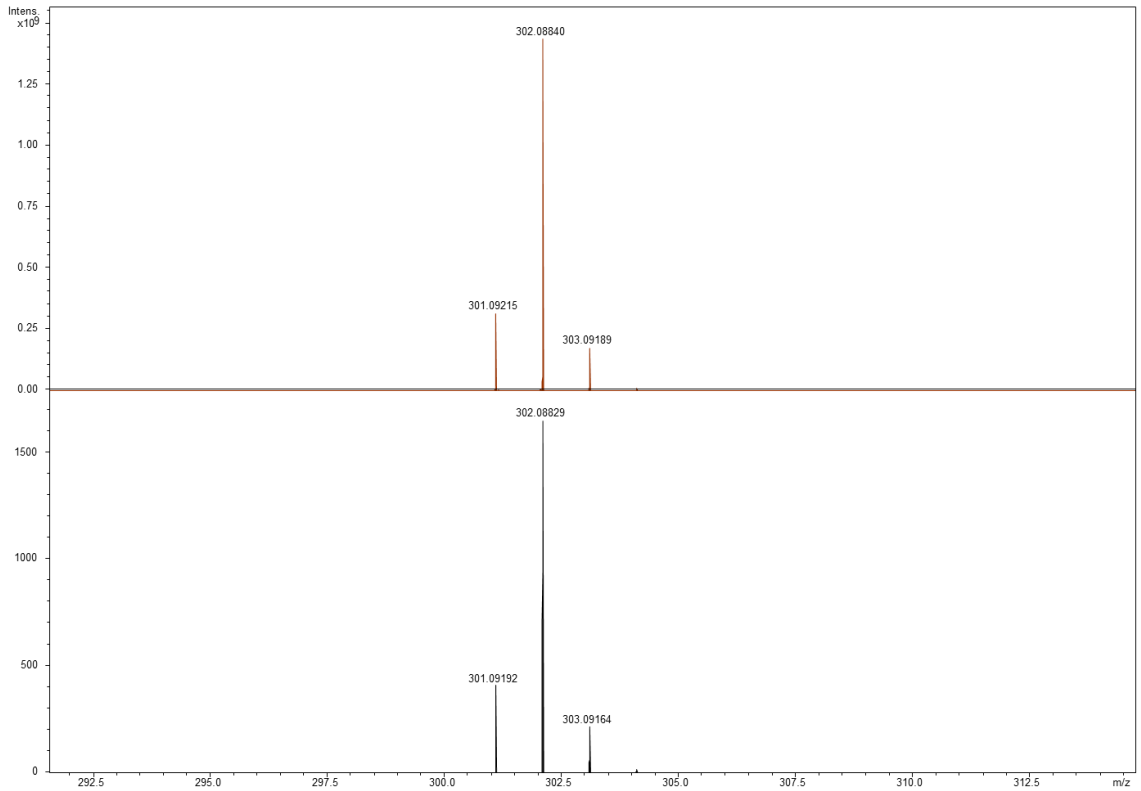

Figure S57. MS spectrum recorded for **6a** (above) compared with simulated pattern (below).

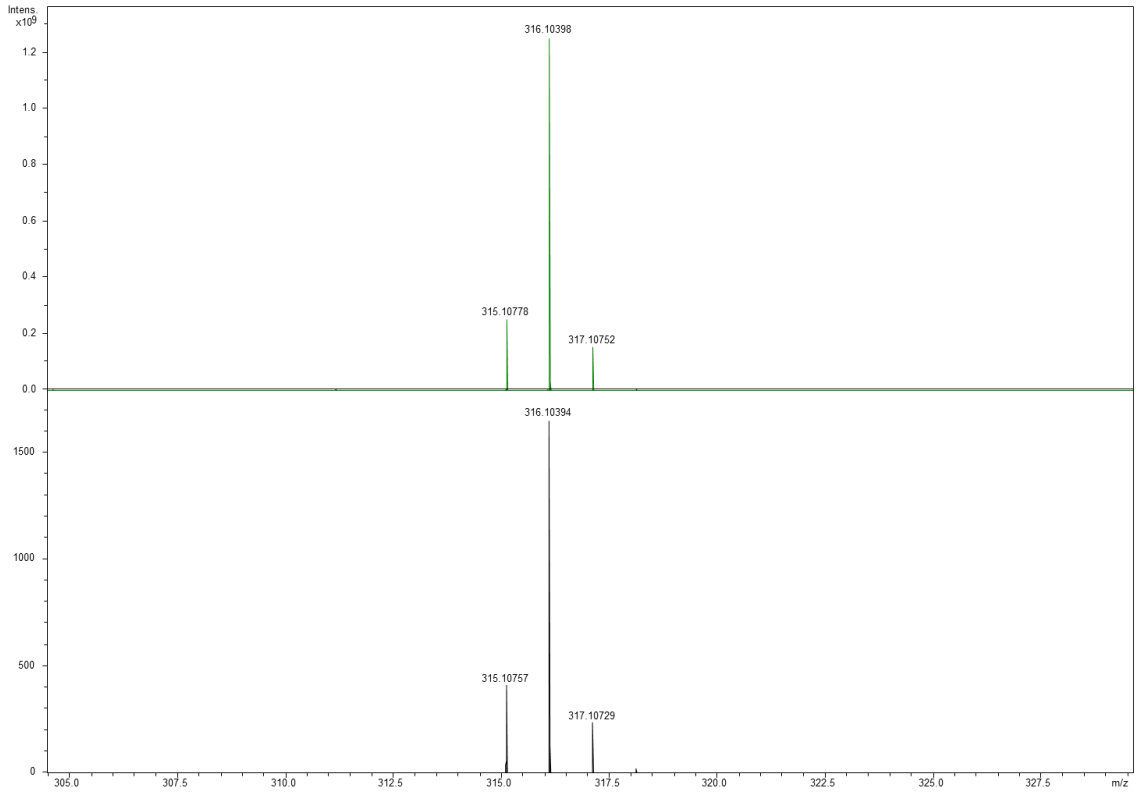

Figure S58. MS spectrum recorded for **6b** (above) compared with simulated pattern (below).

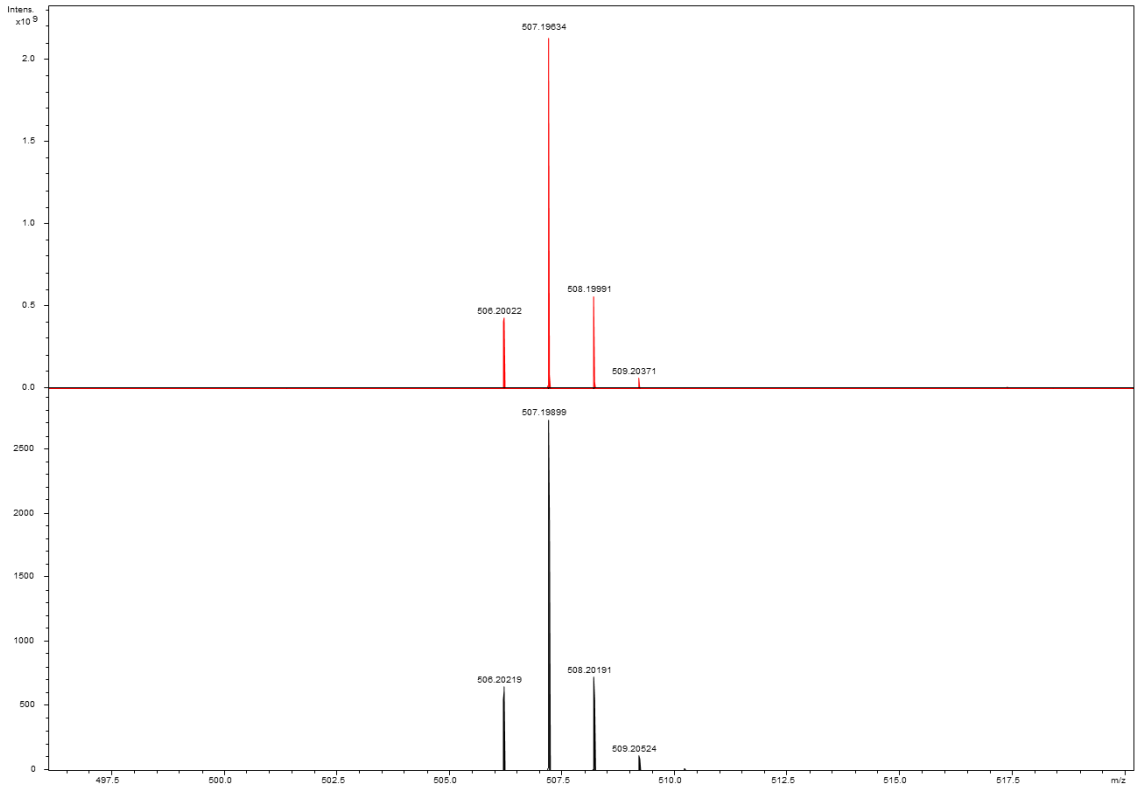

Figure S59. MS spectrum recorded for **6c** (above) compared with simulated pattern (below).

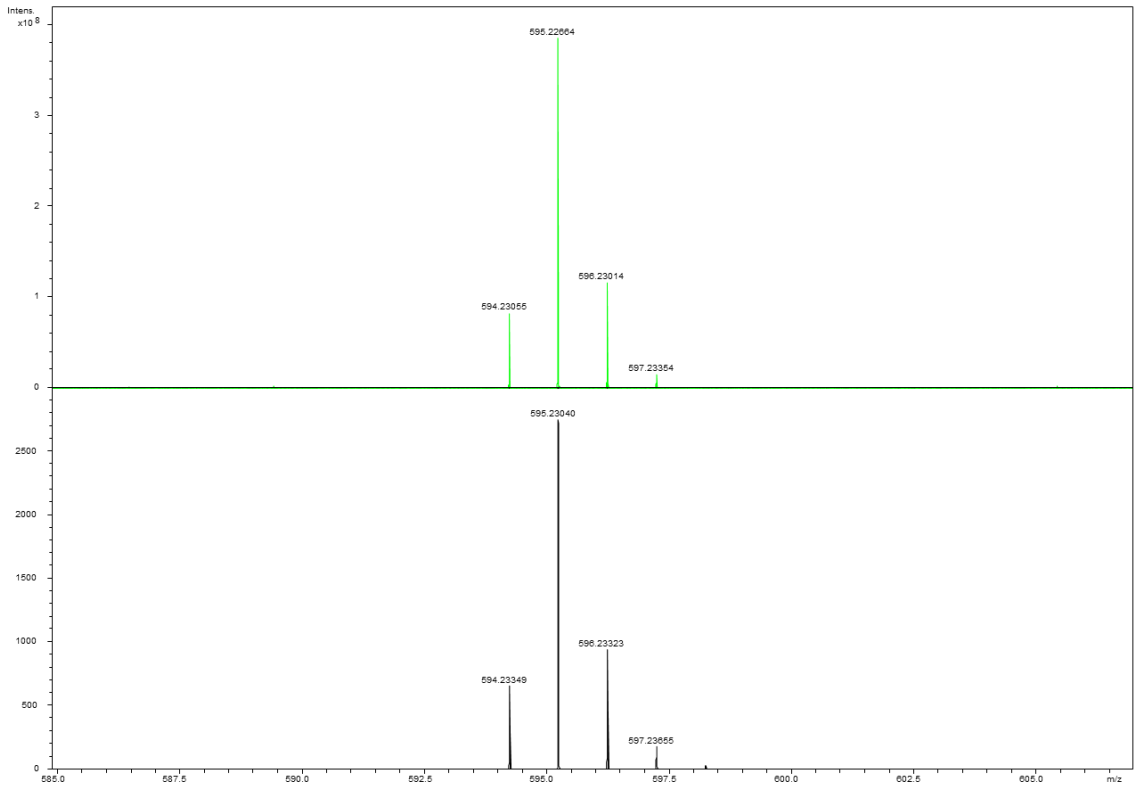

Figure S60. MS spectrum recorded for **7a** (above) compared with simulated pattern (below).

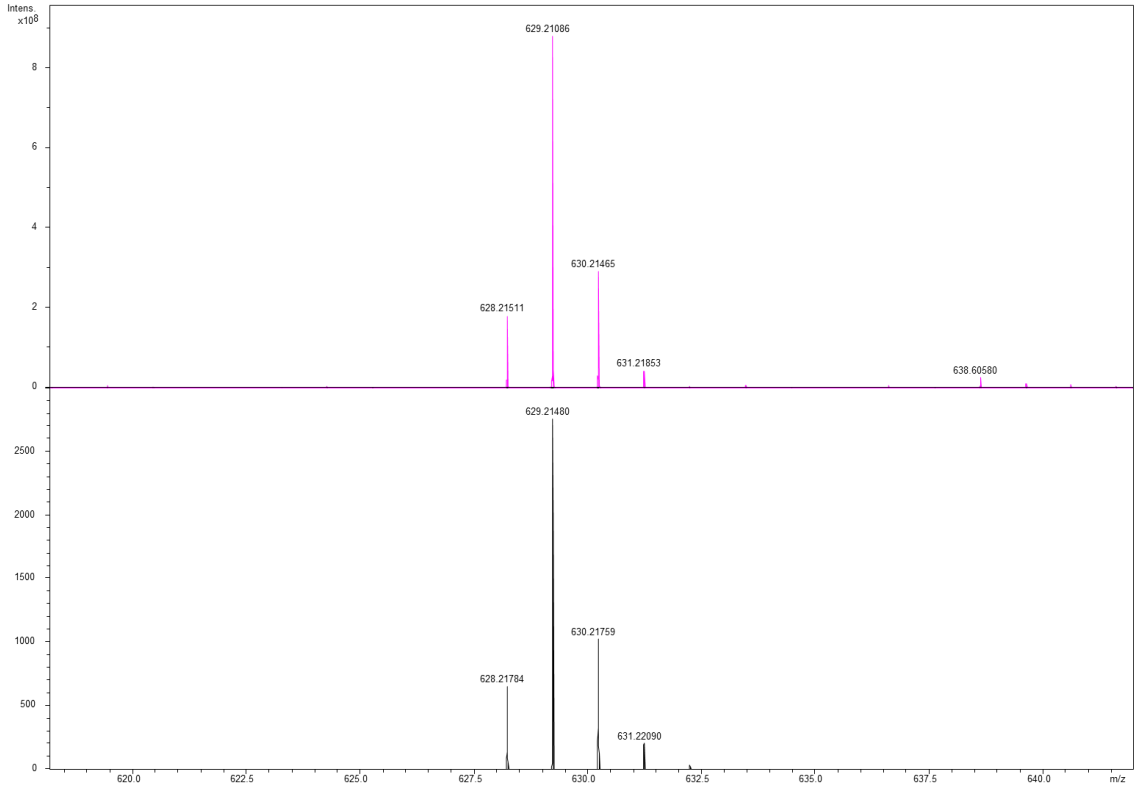

Figure S61. MS spectrum recorded for **7b** (above) compared with simulated pattern (below).

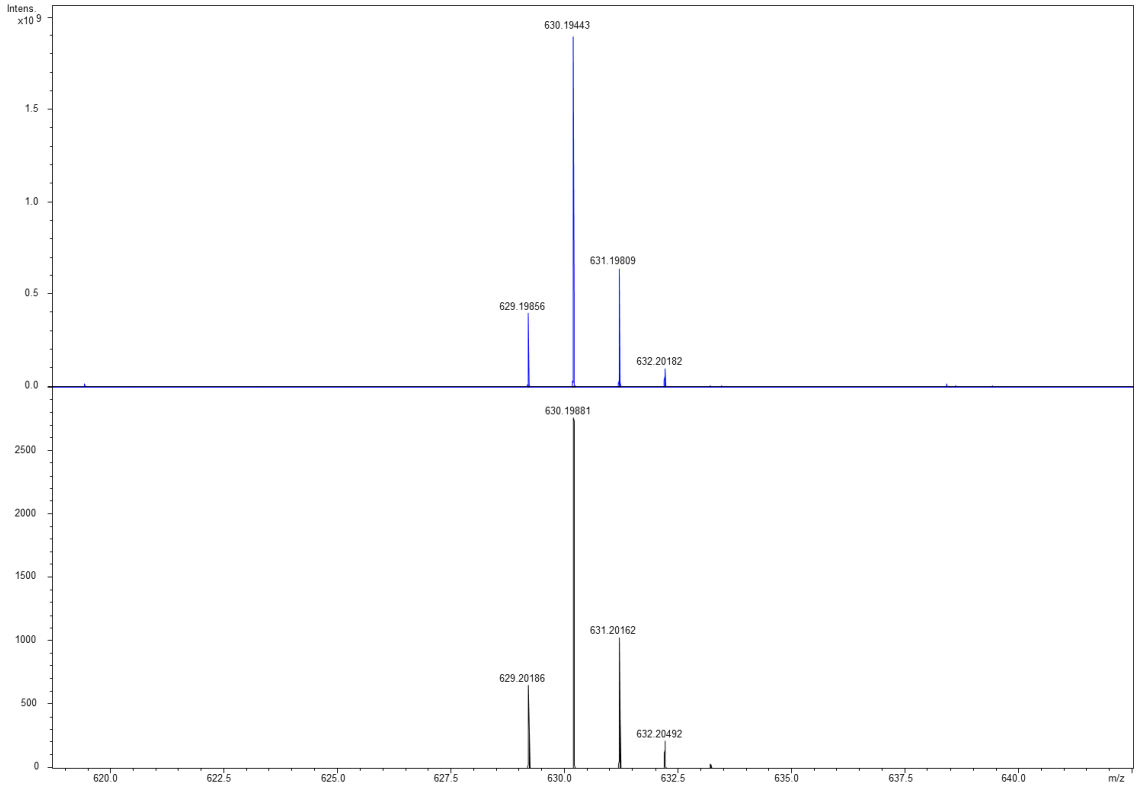

Figure S62. MS spectrum recorded for **7c** (above) compared with simulated pattern (below).

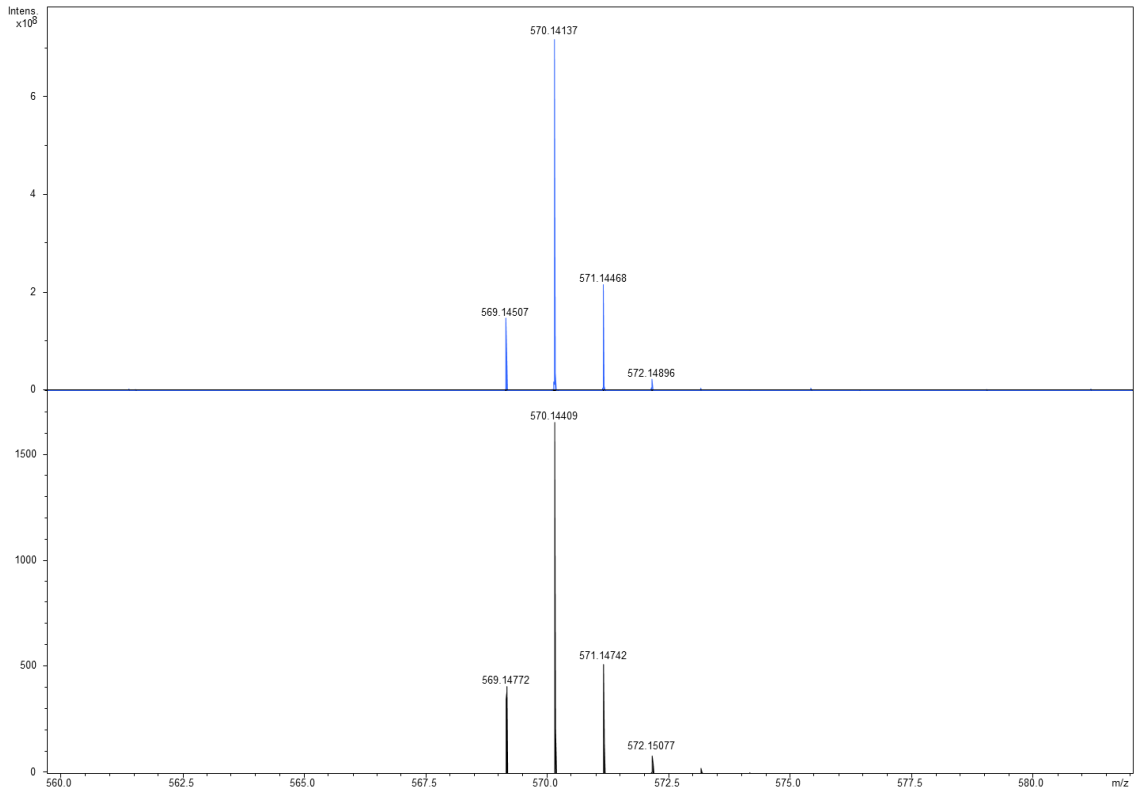

Figure S63. MS spectrum recorded for **7d** (above) compared with simulated pattern (below).

5. UV-VIS spectra.

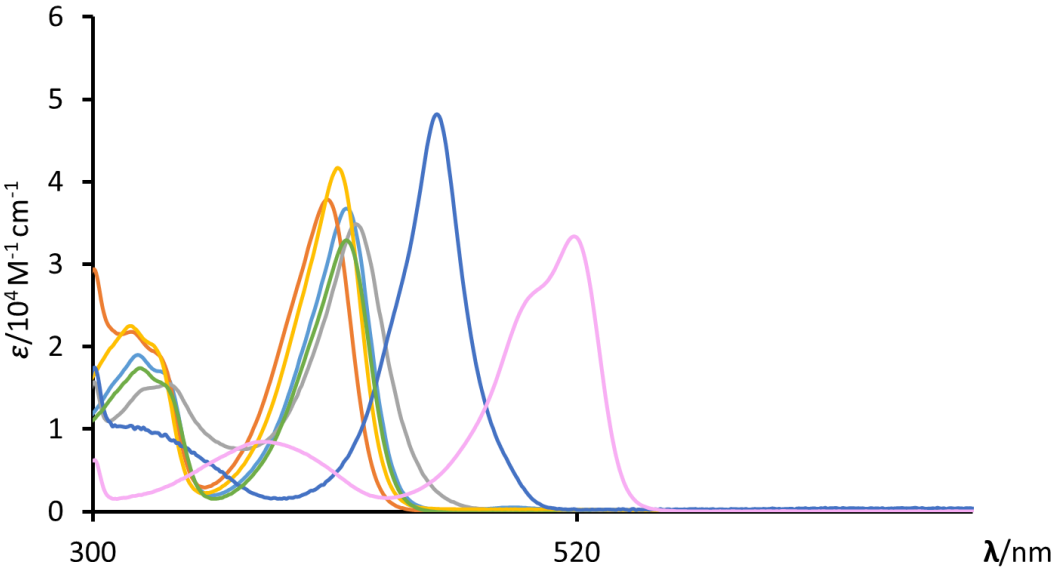

Figure 64. Extinction spectrum for all derivatives; **6a** (yellow), **6b** (light blue), **6c** (green), **7a** (orange), **7b** (grey), **7c** (blue) and **7d** (pink) (CH_2Cl_2, 295 K).

6. Emission spectra.

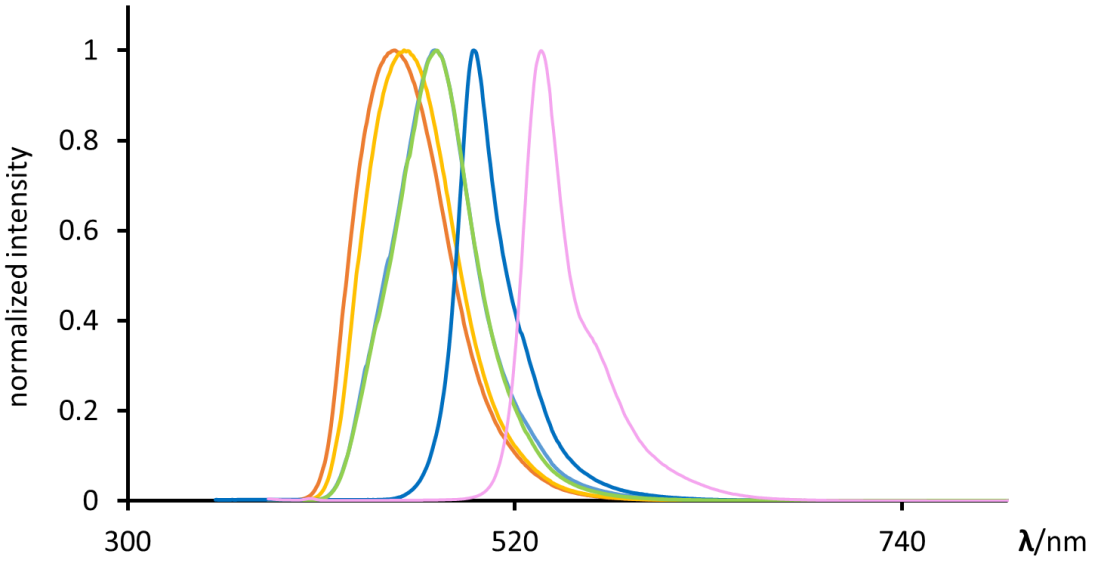

Figure S65. Normalized emission spectrum for all the derivatives; **6a** (yellow), **6b** (light blue), **6c** (green), **7a** (orange), **7c** (blue) and **7d** (pink) (CH_2Cl_2, 295 K).

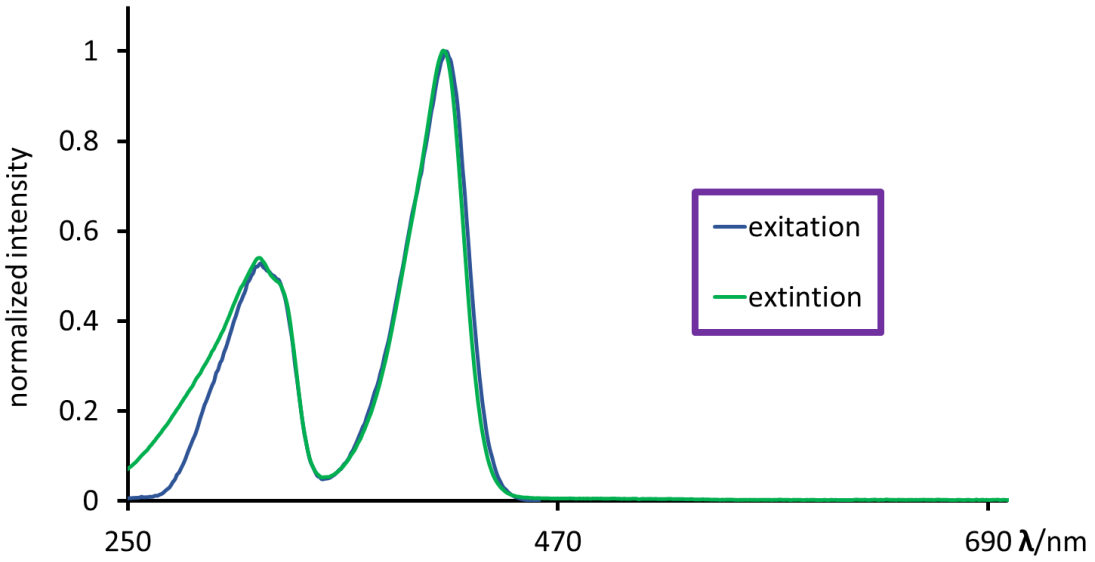

Figure S66. Normalized excitation spectrum displayed with extinction for compound **6a**.

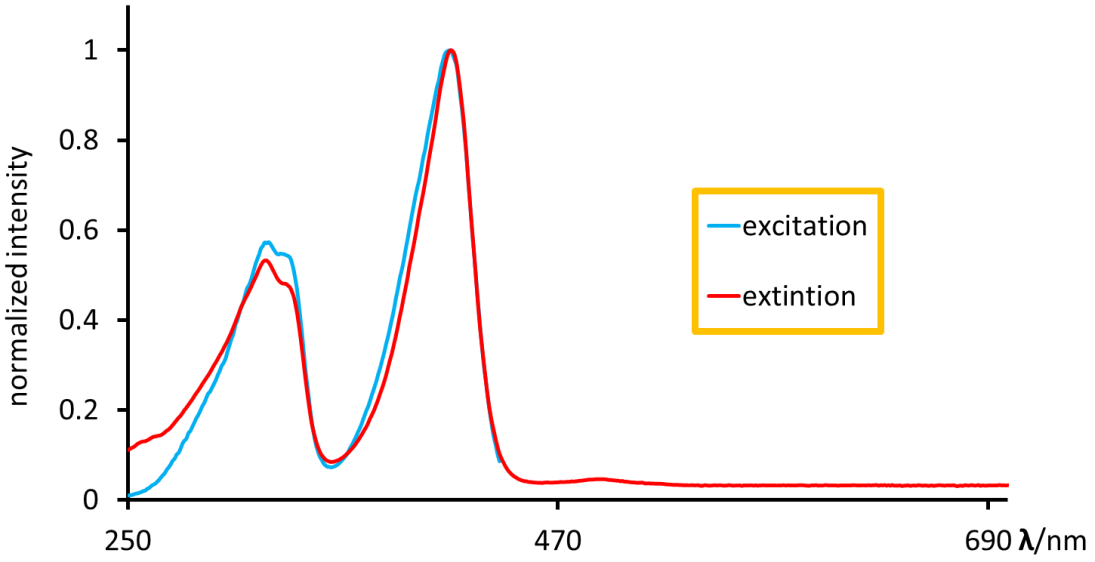

Figure S67. Normalized excitation spectrum displayed with extinction for compound **6b**.

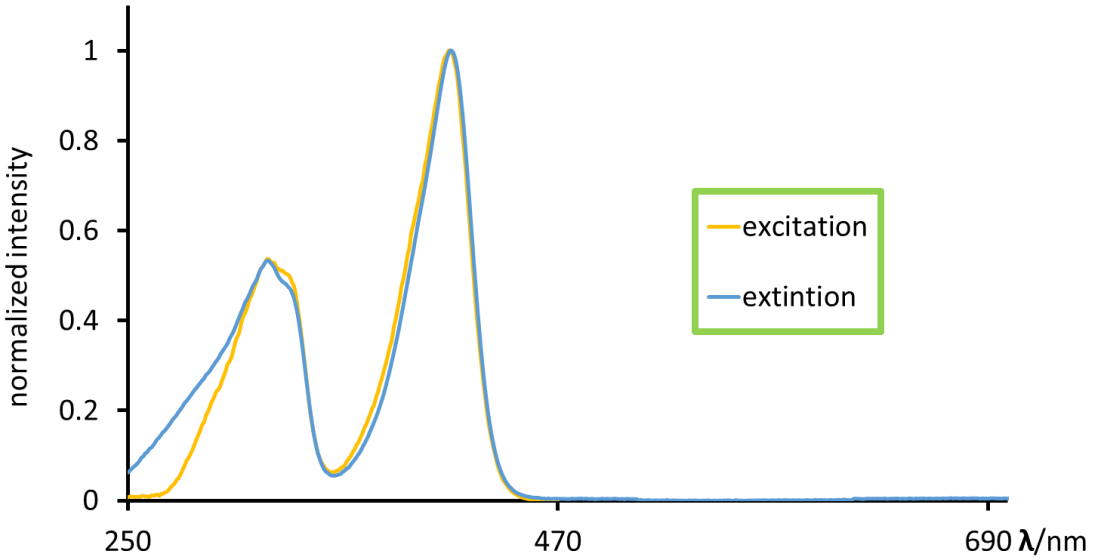

Figure S68. Normalized excitation spectrum displayed with extinction for compound **6c**.

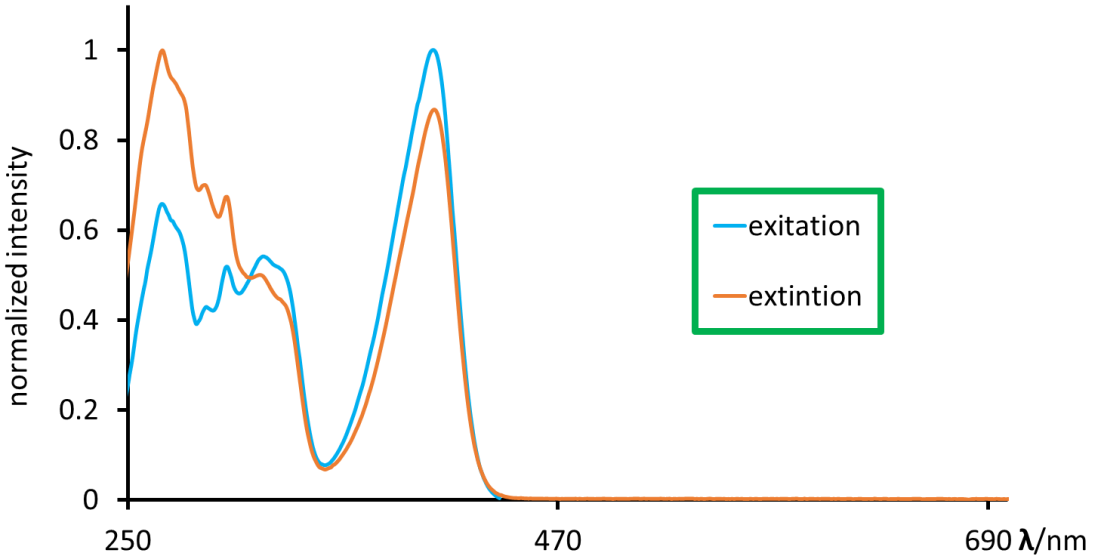

Figure S69. Normalized excitation spectrum displayed with extinction for compound **7a**.

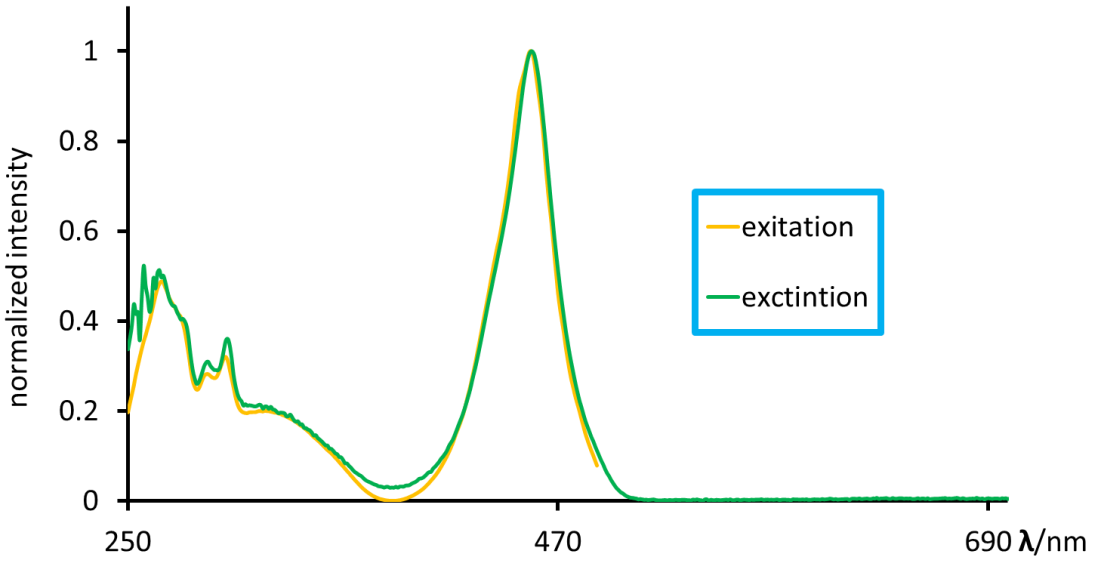

Figure S70. Normalized excitation spectrum displayed with extinction for compound **7c**.

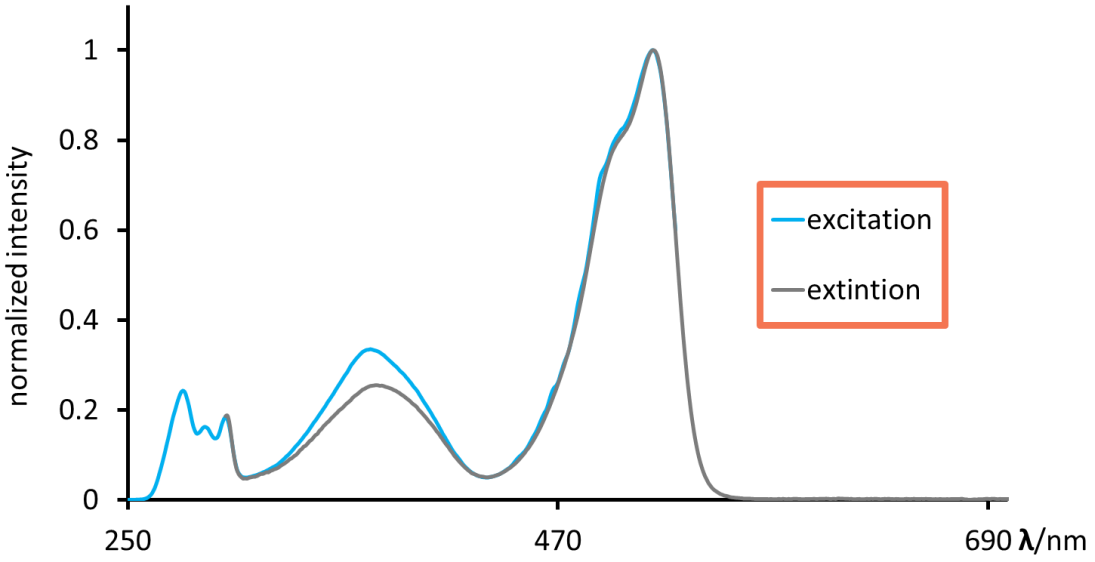

Figure S71. Normalized excitation spectrum displayed with extinction for compound **7d**.

7. Lifetime measurements.

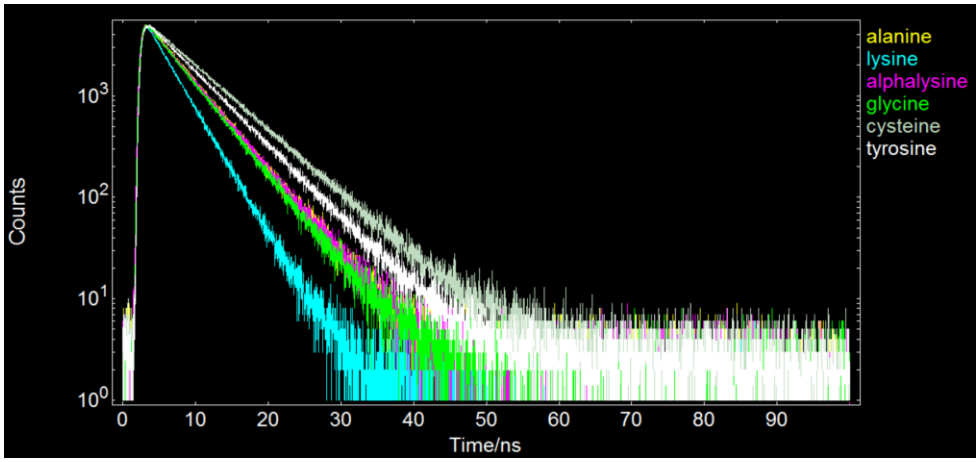

Figure S72. Normalized decay traces displayed for **6a** (green), **6b** (yellow), **6c** (purple) and **7a** (cyan), **7b** (white), **7d** (grey).

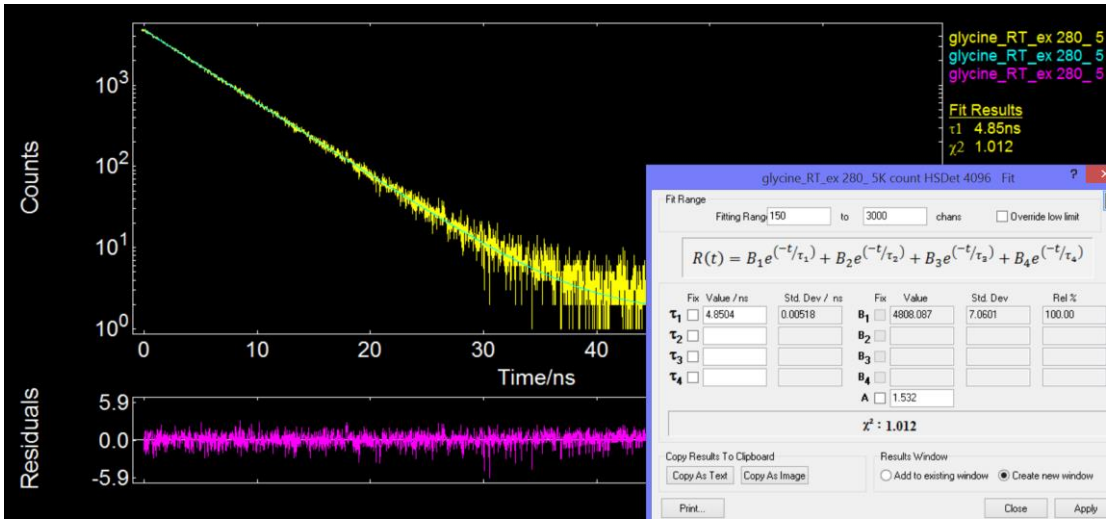

Figure S73. Linear fitting for **6a**.

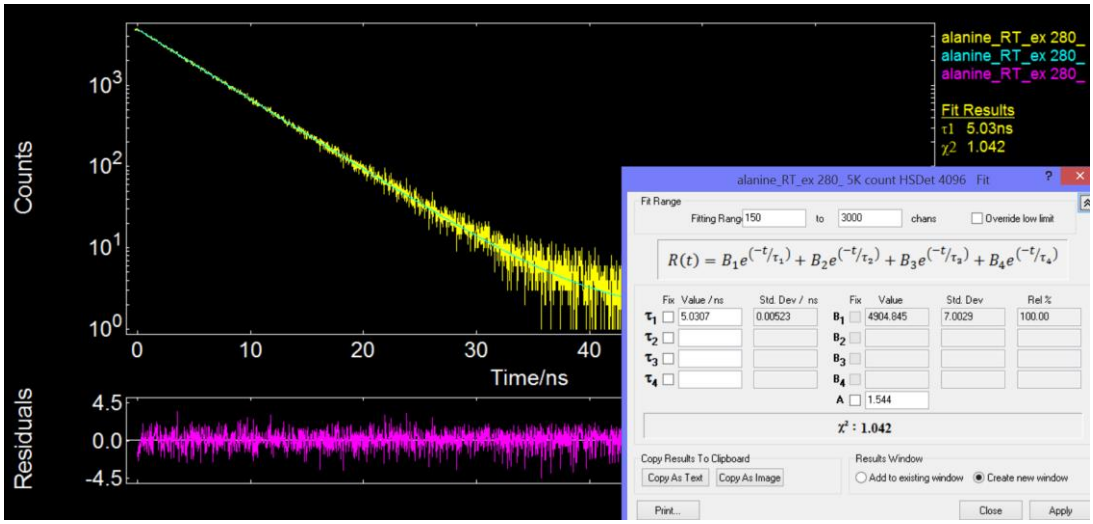

Figure S74 Linear fitting for **6b**.

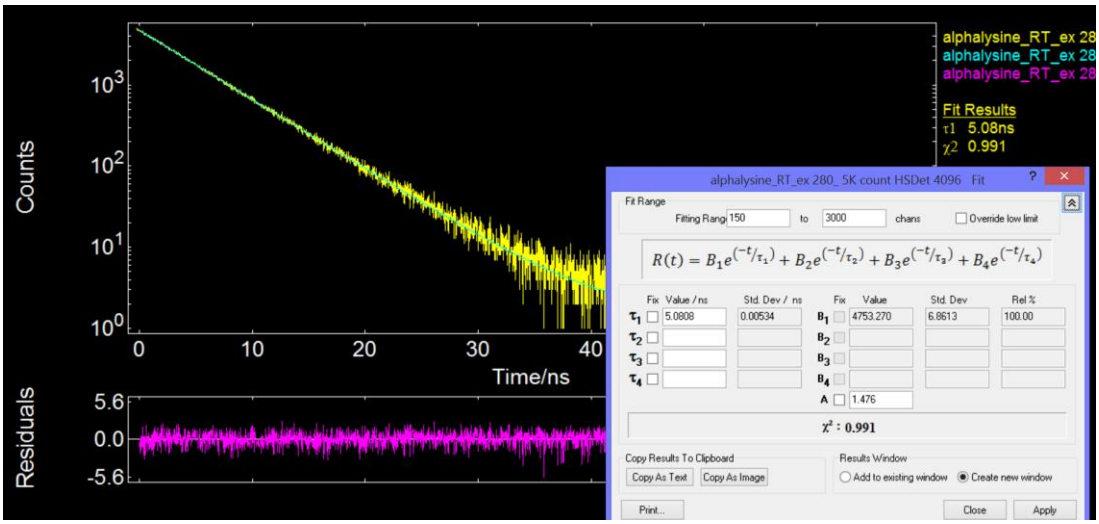

Figure S75 Linear fitting for **6c**.

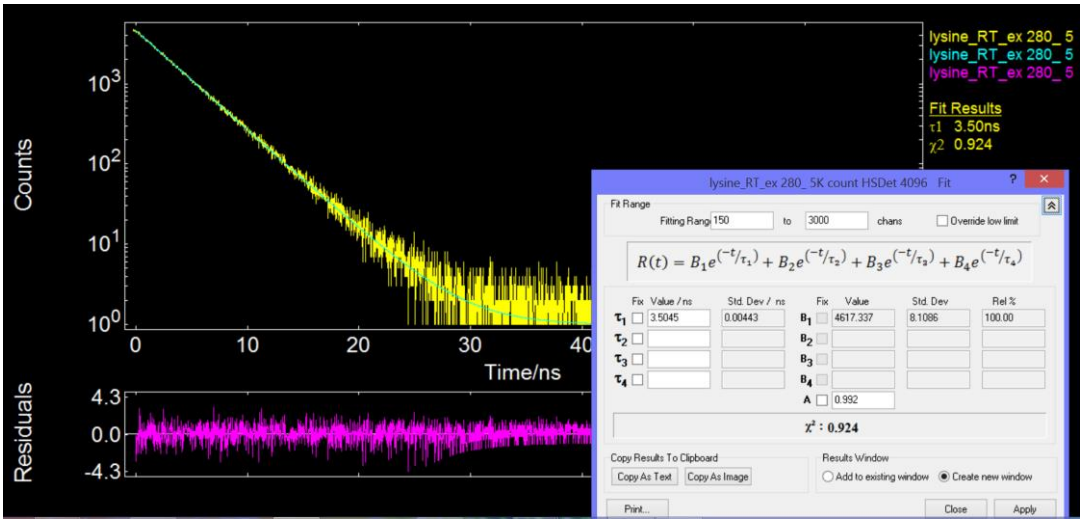

Figure S76. Linear fitting for **7a**.

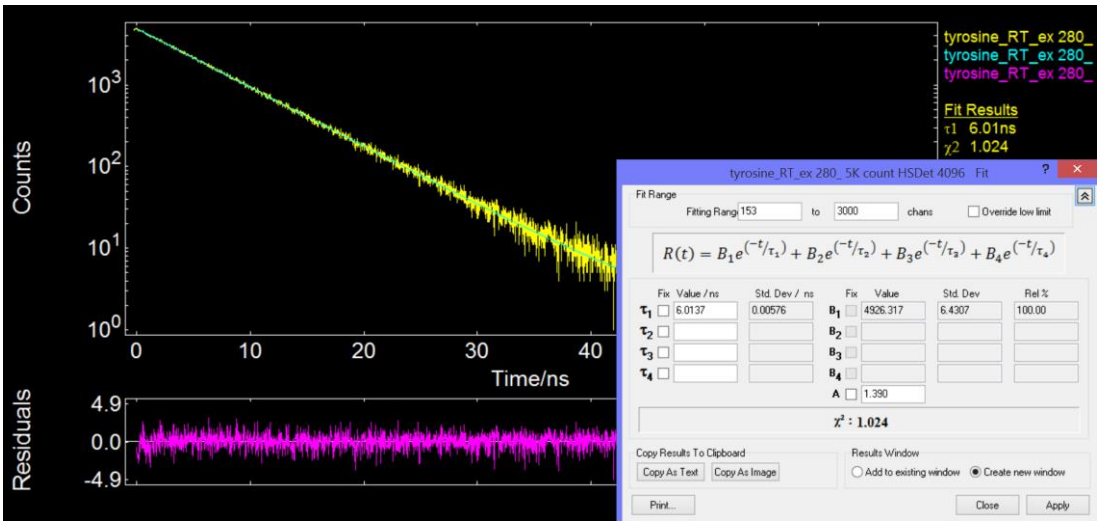

Figure S77. Linear fitting for **7c**.

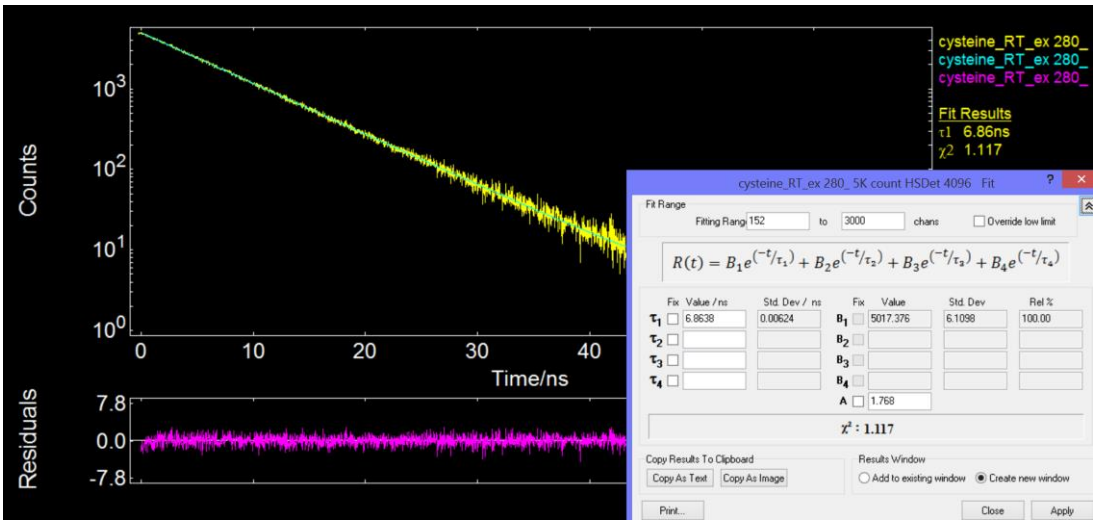

Figure S78. Linear fitting for **7d**.

8. Theoretical calculations.

8.1. Optimisation details.

Table S1. optimization details for **6a**, **6b**, **6c**, **7a**, **7b**, **7c** and **7d**.

Structure	Code[a]	SCF E[b]	ZPV[c]	lowest freq. [d]	G[e]
		a.u.	a.u.	cm^{-1}	a.u.
6a	6_a	-1003.952429	0.241637	21.33	-1003.710792
6b	6_b	-1043.271618	0.269393	17.38	-1043.002225
6c	6_c	-1675.531658	0.498758	11.84	-1675.032900
7a	7_a	-1944.697690	0.586106	7.87	-1944.111584
7b	7_b	-2057.810474	0.580073	9.75	-2057.230401
7c	7_c	-2077.661867	0.566461	5.12	-2077.095407
7d	7_d	-2169.569528	0.482966	11.28	-2169.08655

[a] Optimized geometry available as <code>.pdb file. [b] Electronic energy. [c] Zero-point vibrational energy. [d] Lowest vibrational frequency. [e] Gibbs free energy.

8.2. TD-DFT predicted UV Vis transitions.

Table S2. UV-Vis transitions (oscillator strength > 0.01) calculated with TD-DFT for **6a**.

No.	Energy (cm^{-1})	Wavelength (nm)	Osc. Strength	Major contribs
1	27019.57337	370.1020687	0.4279	HOMO->LUMO (97%)
2	31946.81438	313.0202555	0.0985	H-2->LUMO (70%), H-1->LUMO (27%)
3	33605.09028	297.5739662	0.111	H-3->LUMO (24%), H-2->LUMO (22%), H-1->LUMO (52%)
4	34434.22824	290.4087157	0.2082	H-3->LUMO (74%), H-1->LUMO (20%)
7	43616.04386	229.2734305	0.0011	H-4->L+1 (15%), H-1->L+1 (80%)
13	50935.5253	196.3266294	0.1678	HOMO->L+2 (83%)
15	53718.13808	186.1568617	0.0269	H-3->L+2 (10%), HOMO->L+3 (70%)
16	54815.0521	182.4316427	0.013	H-8->LUMO (42%), H-1->L+2 (53%)
24	59239.8097	168.8054038	0.18	H-3->L+2 (48%), H-1->L+5 (12%), HOMO->L+3 (11%)
25	59506.77922	168.0480801	0.0523	H-1->L+3 (40%), H-1->L+4 (30%)
27	60251.22896	165.9717183	0.0297	H-15->LUMO (19%), H-14->LUMO (10%), H-2->L+2 (10%), H-1->L+4 (27%), HOMO->L+5 (16%)
28	60676.28314	164.8090404	0.1057	H-15->LUMO (17%), H-3->L+3 (10%), H-2->L+2 (18%), H-2->L+3 (13%), H-1->L+3 (11%), HOMO->L+5 (10%)
29	60769.84345	164.555303	0.035	H-15->LUMO (41%), H-1->L+3 (11%), H-1->L+4 (25%)
30	61256.19577	163.2487926	0.1046	H-2->L+3 (54%)
33	63577.45942	157.2884493	0.0265	H-5->L+1 (41%), H-1->L+5 (17%), HOMO->L+6 (17%)
34	63792.80945	156.7574792	0.0812	H-5->L+1 (46%), HOMO->L+6 (12%)
35	64208.99154	155.7414275	0.0683	H-1->L+5 (20%), HOMO->L+6 (56%)
36	64386.43351	155.3122211	0.0182	H-17->LUMO (55%), H-16->LUMO (24%)
38	65380.91512	152.9498322	0.0136	H-17->LUMO (21%), H-16->LUMO (20%), H-3->L+3 (16%)
39	65530.93425	152.5996862	0.1147	HOMO->L+7 (46%)
40	66160.85326	151.146781	0.0591	H-3->L+4 (68%), H-2->L+5 (15%)
41	66663.33667	150.0074929	0.148	H-2->L+5 (50%)
44	67308.58021	148.5694687	0.0142	H-4->L+2 (61%), HOMO->L+8 (10%)
45	67623.13644	147.878382	0.024	H-4->L+2 (16%), H-3->L+5 (10%), HOMO->L+8 (25%)
49	68614.39183	145.742019	0.0228	H-1->L+6 (78%)
50	69181.39959	144.5475237	0.0515	H-18->LUMO (76%)

Table S3. UV-Vis transitions (oscillator strength > 0.01) calculated with TD-DFT for **6b**.

No.	Energy (cm-1)	Wavelength (nm)	Osc. Strength	Major contribs
1	26986.50464	370.5555845	0.4173	HOMO->LUMO (97%)
2	31918.58497	313.2970966	0.1045	H-2->LUMO (68%), H-1->LUMO (28%)
3	33429.26142	299.1391247	0.1492	H-3->LUMO (16%), H-2->LUMO (25%), H-1->LUMO (56%)
4	34372.12355	290.9334358	0.1886	H-3->LUMO (82%), H-1->LUMO (13%)
13	50930.68597	196.345284	0.1753	HOMO->L+2 (85%)
15	53698.78077	186.2239674	0.0284	H-3->L+2 (10%), H-1->L+2 (11%), HOMO->L+3 (68%)
16	54777.9506	182.555205	0.0109	H-9->LUMO (14%), H-8->LUMO (24%), H-1->L+2 (53%)
18	55568.37394	179.958478	0.0106	H-9->LUMO (38%), H-2->L+2 (29%), HOMO->L+4 (15%)
24	58942.99767	169.6554365	0.0644	H-13->LUMO (15%), H-3->L+2 (28%), H-1->L+3 (19%)
25	59303.5275	168.6240334	0.146	H-12->LUMO (18%), H-3->L+2 (24%), H-1->L+3 (13%), H-1->L+4 (10%)
26	59771.32907	167.3042938	0.0195	H-12->LUMO (21%), H-1->L+3 (34%)
27	60291.55668	165.8607034	0.0223	H-15->LUMO (27%), H-14->LUMO (10%), H-2->L+2 (10%), HOMO->L+5 (12%)
28	60594.01459	165.0328018	0.0845	H-15->LUMO (22%), H-3->L+3 (16%), H-2->L+2 (21%), HOMO->L+5 (10%)
29	61025.52121	163.865868	0.032	H-16->LUMO (12%), H-15->LUMO (25%), H-14->LUMO (21%), H-2->L+3 (13%)
30	61057.78338	163.7792833	0.1077	H-14->LUMO (11%), H-2->L+3 (28%), H-1->L+4 (17%), H-1->L+5 (16%)
31	61173.12067	163.4704898	0.0379	H-2->L+3 (27%), H-1->L+4 (25%)
32	63033.03518	158.6469693	0.0331	H-16->LUMO (32%), H-5->L+1 (42%)
33	63513.74162	157.446243	0.01	H-16->LUMO (38%), H-5->L+1 (14%), H-1->L+5 (11%)
34	63595.20362	157.244563	0.0746	H-5->L+1 (29%), H-3->L+3 (13%), H-1->L+5 (13%), HOMO->L+7 (11%)
35	63848.46171	156.6208446	0.0345	HOMO->L+6 (71%)
36	64003.32016	156.2418946	0.0116	H-17->LUMO (15%), H-2->L+4 (46%), H-2->L+5 (11%)
39	65327.68253	153.0744642	0.1517	HOMO->L+7 (46%)
40	65380.91512	152.9498322	0.0346	H-18->LUMO (13%), H-3->L+3 (30%)
42	66286.67575	150.8598808	0.0131	H-11->L+1 (27%), H-10->L+1 (14%), H-9->L+1 (15%), H-8->L+1 (28%)
43	66652.0449	150.0329062	0.1694	H-2->L+5 (48%)
44	66930.30618	149.4091477	0.0443	H-4->L+2 (14%), H-3->L+4 (42%), H-3->L+5 (15%), H-2->L+4 (11%)
47	67422.30438	148.31887	0.0429	H-21->LUMO (14%), H-6->L+1 (14%), H-3->L+5 (18%), HOMO->L+8 (14%)
49	68079.64624	146.8867797	0.0204	H-1->L+6 (61%), HOMO->L+8 (24%)

Table S4. UV-Vis transitions (oscillator strength > 0.01) calculated with TD-DFT for **6c**.

No.	Energy (cm-1)	Wavelength (nm)	Osc. Strength	Major contribs
1	26196.0813	381.7364852	0.4943	HOMO->LUMO (98%)
2	31647.58269	315.9798996	0.099	H-3->LUMO (25%), H-2->LUMO (33%), H-1->LUMO (40%)
3	32873.54542	304.1959689	0.0914	H-3->LUMO (72%), H-1->LUMO (22%)
4	33094.54133	302.1646349	0.1808	H-4->LUMO (11%), H-2->LUMO (58%), H-1->LUMO (27%)
5	33828.50586	295.6086811	0.069	H-4->LUMO (86%)
6	34420.51681	290.5244002	0.096	H-5->LUMO (97%)
11	42215.86537	236.8777689	0.0163	H-7->LUMO (73%), HOMO->L+3 (20%)
19	47773.83194	209.3196127	0.0105	H-5->L+1 (11%), H-3->L+1 (36%), H-2->L+1 (37%)
22	48848.96899	204.7126113	0.0717	H-4->L+3 (23%), H-3->L+2 (37%), H-2->L+2 (21%)
29	50419.33047	198.3366282	0.2147	H-12->LUMO (12%), HOMO->L+5 (77%)
32	51759.82393	193.200039	0.0121	H-12->LUMO (51%), H-11->LUMO (27%)
33	51828.38105	192.9444794	0.011	H-6->L+1 (15%), H-6->L+2 (78%)
37	53187.42527	188.0143652	0.0584	H-6->L+3 (84%)
39	53547.9551	186.7484945	0.0221	H-15->LUMO (15%), H-1->L+5 (10%), HOMO->L+6 (57%)
41	54298.85727	184.1659383	0.1602	H-1->L+4 (75%)
42	54395.6438	183.8382507	0.7327	H-4->L+3 (45%), H-1->L+4 (16%)
43	54572.27922	183.2432169	0.3114	H-4->L+2 (20%), H-3->L+3 (11%), H-2->L+3 (12%), H-1->L+5 (30%)
44	54664.22643	182.9349952	0.2054	H-4->L+2 (10%), H-1->L+5 (43%)
45	55568.37394	179.958478	0.0333	H-8->L+4 (21%), H-2->L+4 (53%)
46	55589.34436	179.8905908	0.0204	H-17->LUMO (45%), H-3->L+5 (12%), H-2->L+5 (12%), HOMO->L+7 (11%)
48	55923.25789	178.8164777	0.0381	H-8->L+4 (28%), H-3->L+4 (52%)

Table S5. UV-Vis transitions (oscillator strength > 0.01) calculated with TD-DFT for **7a**.

No.	Energy (cm-1)	Wavelength (nm)	Osc. Strength	Major contribs
1	27272.83146	366.6652659	0.4578	HOMO->LUMO (96%)
3	32290.40657	309.6895042	0.1113	H-4->LUMO (73%), H-2->LUMO (24%)
4	33601.05751	297.6096808	0.1403	H-6->LUMO (14%), H-4->LUMO (23%), H-2->LUMO (62%)
6	34873.8004	286.7482146	0.1912	H-6->LUMO (84%), H-2->LUMO (13%)
8	37134.57247	269.2908343	0.4683	H-1->L+1 (77%)
11	38012.10368	263.0741009	0.0601	H-5->L+1 (16%), H-1->L+1 (13%), H-1->L+2 (67%)
12	39535.685	252.93605	0.0139	H-3->L+1 (65%), H-1->L+4 (30%)
20	44802.48542	223.2019029	0.0203	H-5->L+1 (20%), H-4->L+1 (66%)
21	44846.84592	222.9811215	0.0424	H-5->L+1 (52%), H-4->L+1 (25%), H-1->L+2 (13%)
22	46004.25152	217.3712139	0.0482	H-3->L+1 (15%), H-3->L+2 (49%), H-1->L+4 (21%)
25	46607.55423	214.5574932	0.0451	H-9->L+3 (15%), H-7->L+1 (44%), H-3->L+2 (13%)
28	46854.35989	213.4273102	0.0211	H-6->L+1 (73%)
29	47001.1528	212.7607389	0.1443	H-7->L+1 (38%), H-3->L+2 (17%), H-1->L+4 (26%)
30	47852.87427	208.9738632	0.1059	H-5->L+2 (75%), H-3->L+4 (21%)
37	50000.72872	199.9970852	0.0678	H-7->L+3 (40%), H-3->L+3 (10%), HOMO->L+5 (14%)
38	50017.66636	199.9293595	0.0916	H-15->LUMO (10%), H-14->LUMO (20%), H-7->L+3 (15%), HOMO->L+5 (35%)
45	51562.21809	193.9404543	0.0266	H-14->LUMO (24%), H-13->LUMO (27%), HOMO->L+5 (21%)
46	51611.41791	193.7555759	0.0271	H-5->L+3 (61%), H-5->L+4 (15%)
49	52079.21948	192.0151665	0.8448	H-5->L+2 (17%), H-3->L+4 (69%)
50	52218.7534	191.5020821	0.0169	H-17->LUMO (36%), H-15->LUMO (24%)

Table S6. UV-Vis transitions (oscillator strength > 0.01) calculated with TD-DFT for **7b**.

No.	Energy (cm-1)	Wavelength (nm)	Osc. Strength	Major contribs
1	26704.21059	374.4727809	0.3997	HOMO->LUMO (97%)
3	30100.61129	332.2191667	0.2543	H-2->LUMO (92%)
4	31620.15983	316.2539359	0.0828	H-4->LUMO (94%)
6	33542.98559	298.1249231	0.0561	H-7->LUMO (31%), H-6->LUMO (42%), H-5->LUMO (23%)
7	34564.0835	289.317667	0.0217	H-6->LUMO (19%), H-5->LUMO (63%)
8	35165.7731	284.3674152	0.1052	H-8->LUMO (14%), H-7->LUMO (46%), H-6->LUMO (32%)
9	36011.8487	277.6863827	0.0617	H-8->LUMO (81%)
11	36883.73404	271.122224	0.3727	H-1->L+1 (76%)
12	37650.7673	265.5988368	0.0973	H-1->L+1 (19%), H-1->L+2 (36%), H-1->L+4 (32%)
13	37902.41228	263.83545	0.0113	HOMO->L+2 (93%)
14	38339.56478	260.8271653	0.0124	H-9->LUMO (89%)
15	39079.17519	255.8907641	0.0183	HOMO->L+3 (96%)
16	39362.2758	254.0503514	0.0131	H-3->L+1 (52%), H-1->L+6 (24%)
22	41143.95453	243.0490728	0.0114	H-2->L+2 (27%), H-2->L+3 (40%)
24	41818.23403	239.1301362	0.0186	H-2->L+2 (46%), H-2->L+3 (30%)
30	44474.21777	224.8493734	0.0431	H-5->L+1 (73%)
31	44739.57418	223.5157617	0.0154	H-6->L+1 (12%), H-4->L+2 (12%), H-3->L+2 (41%)
34	45003.31747	222.2058408	0.01	H-6->L+1 (27%), H-4->L+2 (40%)
36	45521.12542	219.6782243	0.0115	H-8->L+2 (12%), H-7->L+1 (11%), H-6->L+3 (11%), H-4->L+2 (25%)
38	45782.44905	218.4243134	0.0142	H-12->L+5 (17%), H-2->L+5 (39%)
39	45856.65206	218.0708698	0.0287	H-3->L+2 (13%), H-3->L+3 (34%), H-3->L+4 (23%), H-1->L+6 (11%)
42	46372.8469	215.6434351	0.0858	H-7->L+2 (10%), H-6->L+2 (19%), H-5->L+2 (39%)
43	46668.85237	214.2756784	0.1663	H-6->L+2 (18%), H-1->L+6 (29%)
44	47035.02808	212.6075057	0.0196	H-8->L+1 (23%), H-6->L+2 (26%), H-5->L+2 (27%), H-3->L+4 (10%)
46	47218.92249	211.7795043	0.0333	H-8->L+1 (65%)

Table S7. UV-Vis transitions (oscillator strength > 0.01) calculated with TD-DFT for **7c**.

No.	Energy (cm-1)	Wavelength (nm)	Osc. Strength	Major contribs
1	24710.40804	404.687773	0	HOMO->LUMO (100%)
2	25626.65387	390.2187172	0.4612	H-1->LUMO (95%)
3	28039.86472	356.6351014	0.0789	H-3->LUMO (97%)
4	30282.08604	330.2282408	0.1335	H-5->LUMO (94%)
6	31791.14937	314.5529557	0.0313	H-7->LUMO (16%), H-6->LUMO (83%)
8	32993.72203	303.087963	0.031	H-8->LUMO (41%), H-7->LUMO (47%)
9	34402.77261	290.6742463	0.0156	H-8->LUMO (53%), H-7->LUMO (36%)
10	37162.80187	269.086277	0.415	HOMO->L+1 (82%)
11	37417.67307	267.2533907	0.0264	H-10->LUMO (82%), H-9->LUMO (17%)
12	37481.39087	266.799064	0.2261	H-10->LUMO (18%), H-9->LUMO (71%)
13	37870.95666	264.0545918	0.0637	H-4->L+1 (14%), HOMO->L+1 (14%), HOMO->L+4 (68%)
16	39472.77376	253.3391766	0.0118	H-1->L+1 (32%), H-1->L+2 (66%)
17	39686.51068	251.9747851	0.0113	H-2->L+1 (60%), HOMO->L+6 (30%)
20	40433.38008	247.3204066	0.0126	H-1->L+3 (96%)
23	42540.10025	235.0723186	0.0118	H-3->L+2 (45%), H-3->L+3 (20%)
25	44297.58235	225.7459543	0.0122	H-4->L+1 (10%), HOMO->L+5 (78%)
27	44821.03617	223.109523	0.0637	H-4->L+1 (62%), HOMO->L+4 (15%), HOMO->L+5 (14%)
29	45286.41808	220.8167575	0.0745	H-12->L+5 (12%), H-3->L+2 (16%), H-3->L+3 (21%)
32	46067.96932	217.0705622	0.0237	H-2->L+2 (44%), H-2->L+4 (35%)
33	46315.58153	215.9100603	0.0109	H-2->L+2 (50%), H-2->L+4 (29%)
34	46941.46777	213.0312595	0.1229	H-12->L+5 (12%), H-5->L+2 (18%), H-3->L+2 (11%), H-3->L+3 (11%)
35	47012.44456	212.7096367	0.1715	H-2->L+1 (14%), H-2->L+4 (19%), HOMO->L+6 (37%)
38	47509.28209	210.4851844	0.0565	H-5->L+2 (48%)
40	47645.58978	209.8830143	0.0181	H-4->L+2 (67%)
41	47948.85425	208.5555569	0.1066	H-7->L+2 (10%), H-4->L+4 (55%)
43	48027.89658	208.2123247	0.0125	H-7->L+2 (38%), H-6->L+2 (10%), H-4->L+2 (12%), H-4->L+4 (10%)
47	48836.06412	204.7667063	0.0107	H-7->L+3 (12%), H-4->L+3 (75%)
48	49096.5812	203.6801699	0.0816	H-7->L+3 (20%), H-6->L+2 (28%), H-4->L+3 (15%)
49	49194.98084	203.2727695	0.0213	H-7->L+2 (20%), H-7->L+3 (28%), H-6->L+2 (18%)

Table S8. UV-Vis transitions (oscillator strength > 0.01) calculated with TD-DFT for **7d**.

No.	Energy (cm-1)	Wavelength (nm)	Osc. Strength	Major contribs
1	21480.96411	465.5284535	0	HOMO->LUMO (100%)
2	23804.64742	420.0860372	0.4381	H-1->LUMO (93%)
3	25878.29885	386.424164	0.14	H-3->LUMO (97%)
5	28203.59527	354.5647249	0.1506	H-5->LUMO (92%)
7	29879.61538	334.6763295	0.0672	H-6->LUMO (98%)
12	37194.25749	268.8587076	0.4596	HOMO->L+1 (84%)
13	38002.42503	263.141102	0.0595	H-4->L+1 (16%), HOMO->L+1 (12%), HOMO->L+2 (70%)
15	39558.26852	252.7916507	0.013	H-2->L+1 (64%), HOMO->L+4 (33%)
16	39927.67045	250.4528786	0.09	H-12->LUMO (81%)
24	44861.3639	222.9089607	0.0603	H-4->L+1 (73%), HOMO->L+2 (19%)
28	46070.38898	217.0591614	0.051	H-2->L+1 (15%), H-2->L+2 (52%), HOMO->L+4 (23%)
30	46899.52694	213.2217669	0.2235	H-2->L+1 (13%), H-2->L+2 (38%), HOMO->L+4 (36%)
34	47620.5866	209.9932133	0.0105	H-20->LUMO (58%), H-1->L+5 (17%), H-1->L+6 (17%)
35	47786.73681	209.2630857	0.0591	H-10->L+3 (10%), H-4->L+2 (43%), H-3->L+2 (23%), H-2->L+4 (13%)
36	47872.23158	208.8893638	0.0452	H-10->L+3 (25%), H-4->L+2 (29%), H-3->L+2 (13%), H-3->L+3 (10%)
41	49177.23665	203.3461146	0.0133	H-3->L+5 (48%), H-3->L+6 (21%)
44	49485.34044	202.0800486	0.0376	H-18->LUMO (49%), H-17->LUMO (11%)
45	49834.5785	200.6638824	0.0876	H-18->LUMO (20%), H-17->LUMO (15%), H-1->L+6 (19%)
46	50209.62631	199.1649955	0.0274	H-23->LUMO (60%), H-22->LUMO (10%)
48	50655.65091	197.4113415	0.014	H-25->LUMO (32%), H-24->LUMO (29%), H-23->LUMO (18%)

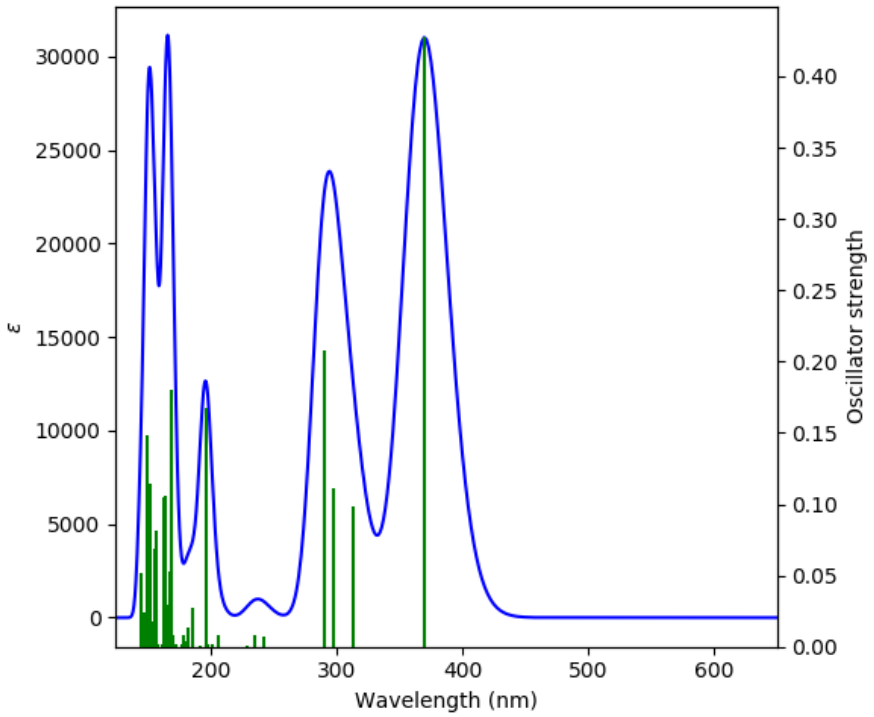

Figure S79. TD-DFT predicted absorption spectra for **6a** (solvent dichloromethane).

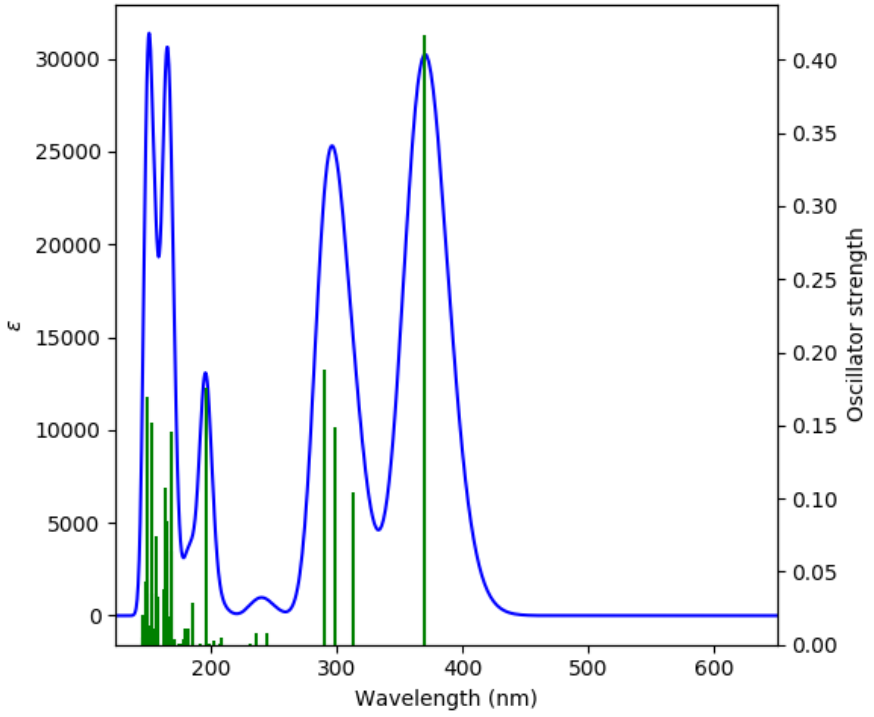

Figure S80. TD-DFT predicted absorption spectra for **6b** (solvent dichloromethane).

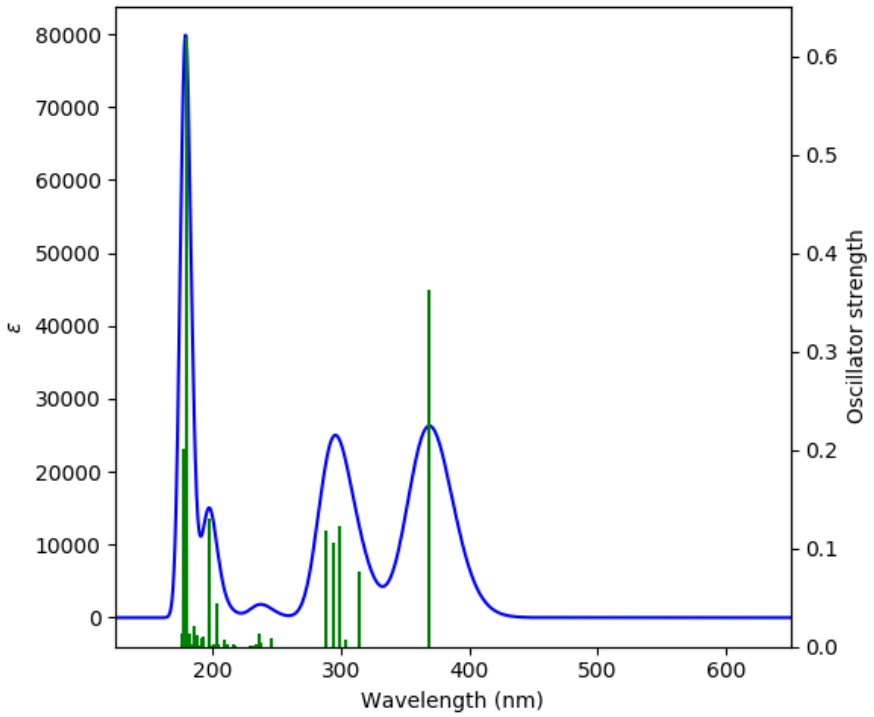

Figure S81. TD-DFT predicted absorption spectra for **6c** (solvent dichloromethane).

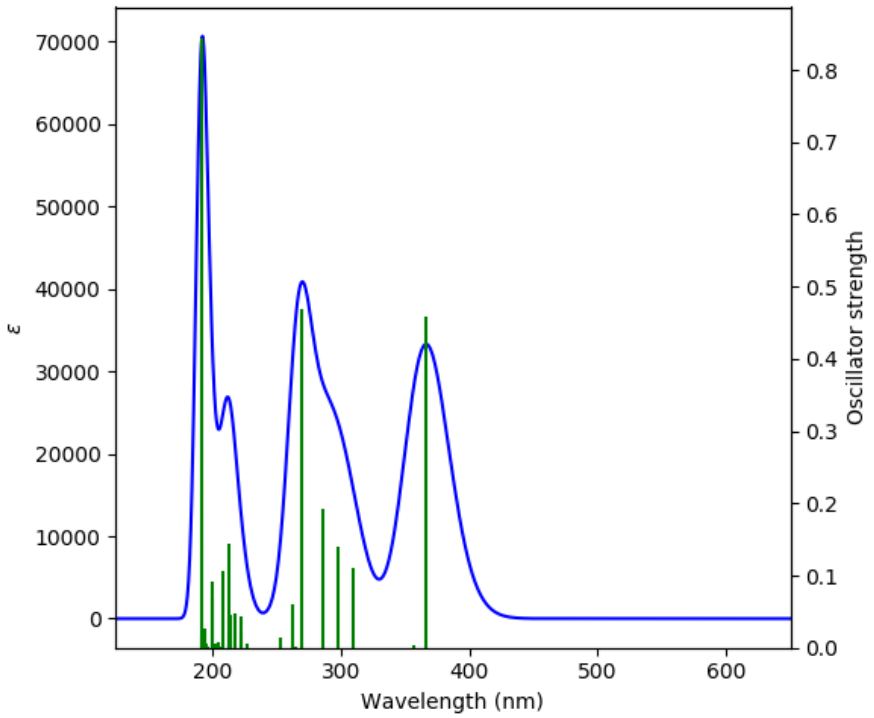

Figure S82. TD-DFT predicted absorption spectra for **7a** (solvent dichloromethane).

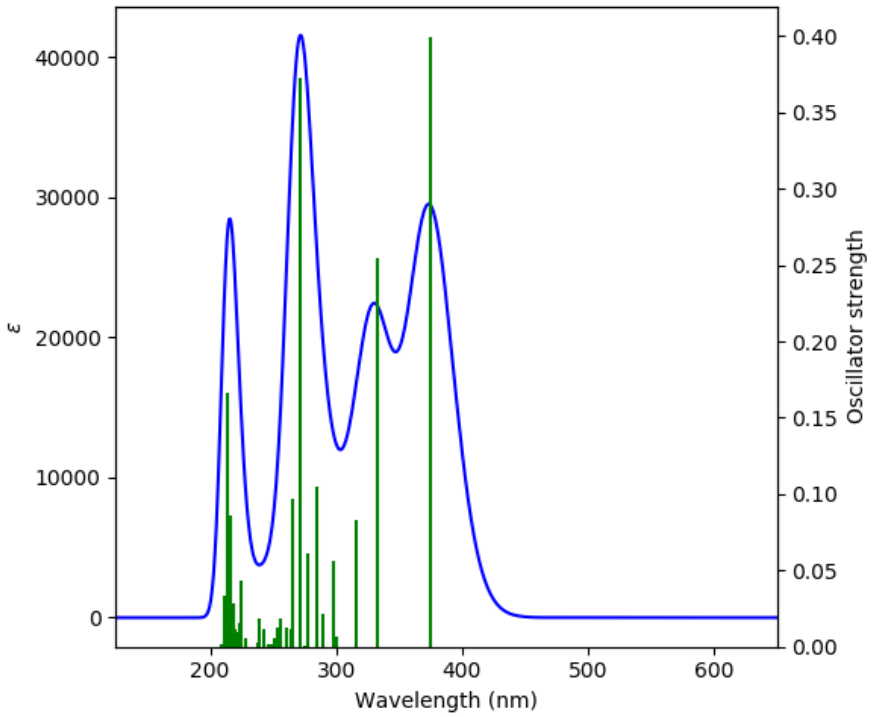

Figure S83. TD-DFT predicted absorption spectra for **7b** (solvent dichloromethane).

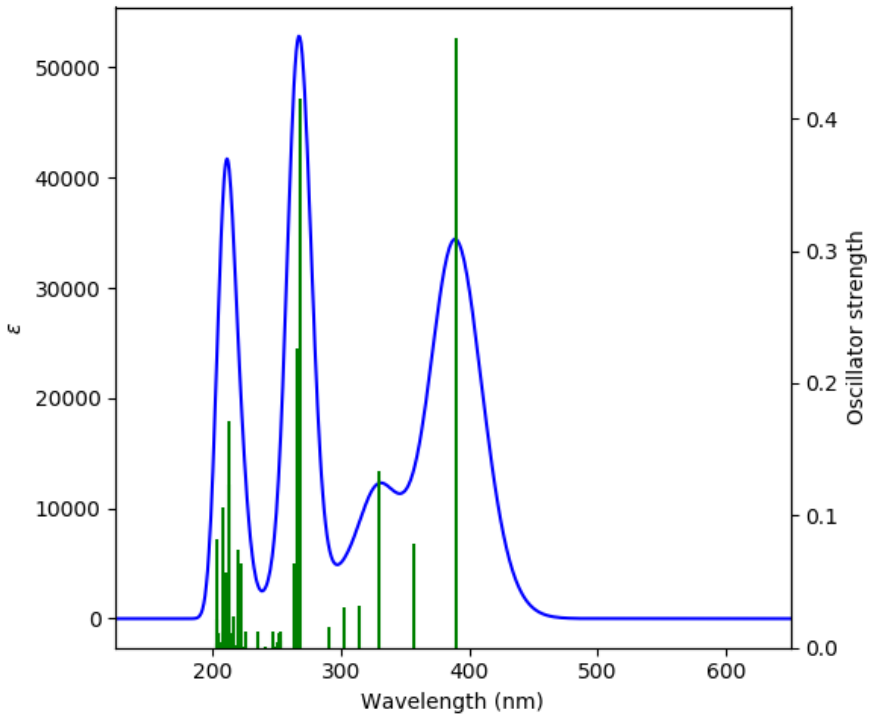

Figure S84. TD-DFT predicted absorption spectra for **7c** (solvent dichloromethane).

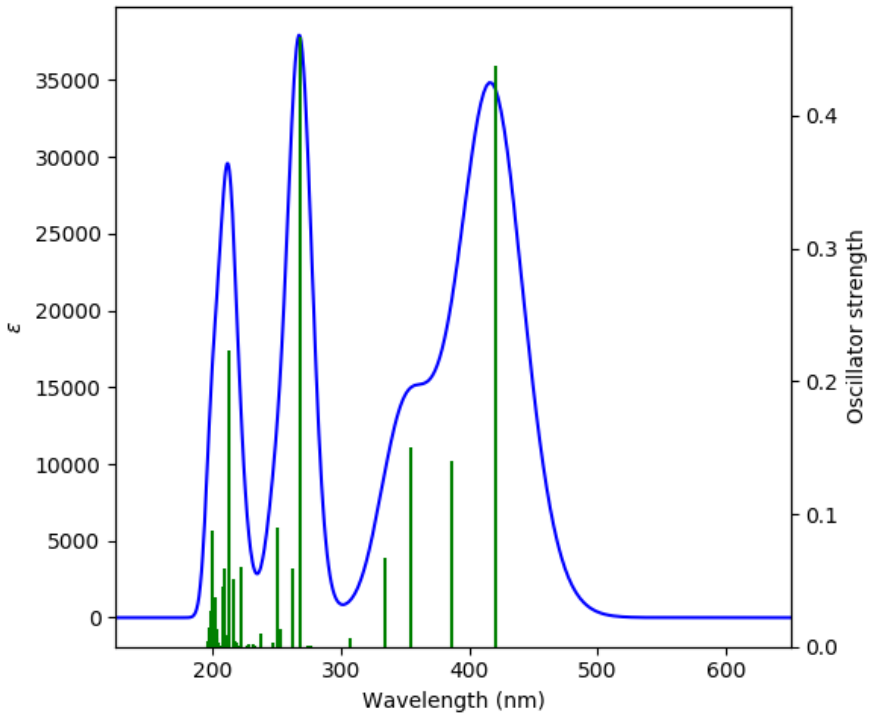

Figure S85. TD-DFT predicted absorption spectra for **7d** (solvent dichloromethane).

9. Crystallographic data.

Table S9. crystallographic details for **6a**.

Identification[a]	1997970
Empirical formula	$C_{12}H_{12}BF_2N_3O_2$
Formula weight	279.06
Temperature/K	293(2)
Crystal system	orthorhombic
Space group	$Pna2_1$
a/Å	7.1383(6)
b/Å	20.8629(14)
c/Å	8.3699(6)
α/°	90
β/°	90
γ/°	90
Volume/Å^3	1246.49(16)
Z	4
ρ_{calc}g/cm^3	1.487
μ/mm^{-1}	0.122
F(000)	576.0
Crystal size/mm^3	0.2433 × 0.1222 × 0.0791
Radiation	MoKα (λ = 0.71073)
2Θ range for data collection/°	6.032 to 59.968
Index ranges	-7 ≤ h ≤ 9, -26 ≤ k ≤ 25, -11 ≤ l ≤ 10
Reflections collected	8372
Independent reflections	2790 [R_{int} = 0.1317, R_{sigma} = 0.1469]
Data/restraints/parameters	2790/1/183
Goodness-of-fit on F^2	1.003
Final R indexes [I>=2σ (I)]	R_1 = 0.0754, wR_2 = 0.1419
Final R indexes [all data]	R_1 = 0.1284, wR_2 = 0.1707
Largest diff. peak/hole / e Å^{-3}	0.27/-0.36
Flack parameter	-3.7(10)

[a] CCDC deposition number.